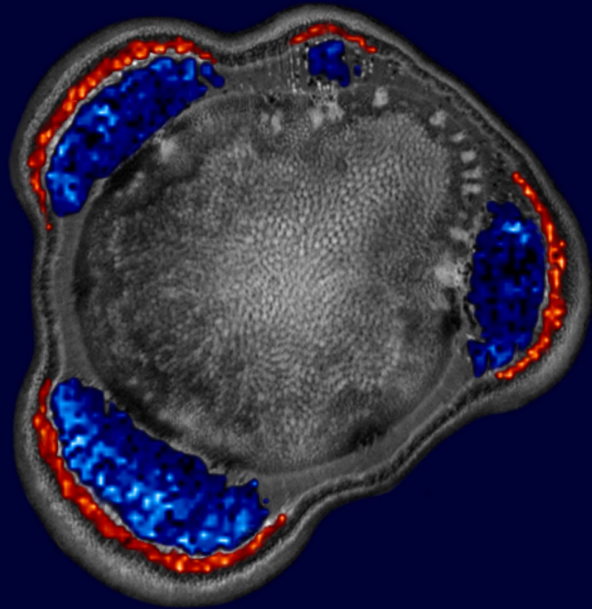


Light on phloem transport (an MRI approach)



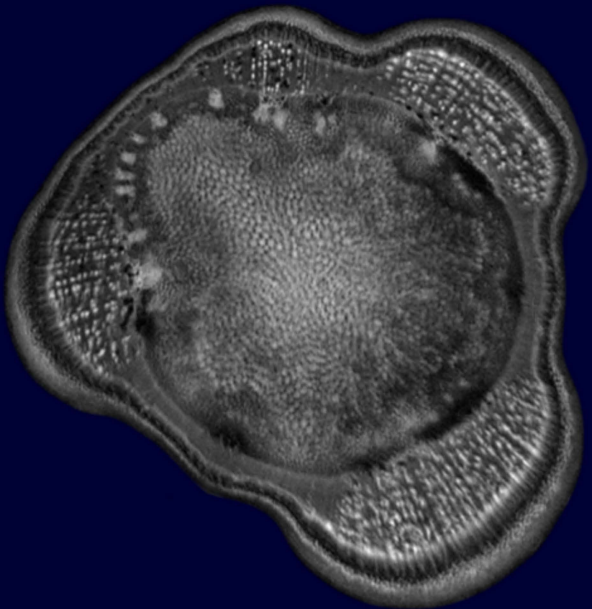
Alena Průšová

Light on phloem transport (an MRI approach)

Alena Průšová



2016



Light on phloem transport

(an MRI approach)

Alena Průšová

Thesis committee

Promotor

Prof. Dr H. van Amerongen
Professor of Biophysics
Wageningen University

Co-promotor

Dr H. Van As
Associate professor, Laboratory of Biophysics
Wageningen University

Other members

Prof. Dr J. Molenaar, Wageningen University
Dr T.W.J. Scheenen, Radboud University Nijmegen
Dr J. Harbinson, Wageningen University
Dr C.G. van der Linden, Wageningen University

This research was conducted under the auspices of the Graduate School of Experimental Plant Sciences.

Light on phloem transport (an MRI approach)

Alena Průšová

Thesis

submitted in fulfilment of the requirements
for the degree of doctor
at Wageningen University
by the authority of the Rector Magnificus
Prof. Dr A.P.J. Mol,
in the presence of the
Thesis Committee appointed by the Academic Board
to be defended in public
on Thursday 20 October 2016
at 11 a.m. in the Aula.

Alena Průšová

Light on phloem transport (an MRI approach)

130 pages.

PhD thesis, Wageningen University, Wageningen, NL (2016)

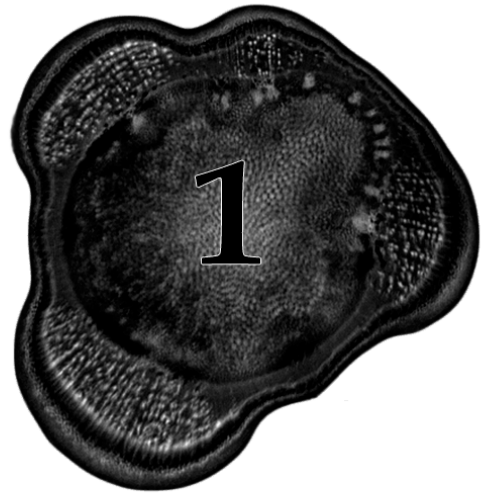
With references, with summary in English

ISBN 978-94-6257-915-6

DOI 10.18174/389397

Contents

1.	Introduction	7
2.	Source strength manipulation in tomato changes phloem volume flow, but not flow velocity.	23
3.	Effect of photoperiod on xylem and phloem sap transport in tomato.	47
4.	Does the NMR transverse relaxation time in phloem region reflect phloem carbon status?	71
5.	MRI characterisation of phloem transport in potato plant.	89
6.	General Discussion	103
	Summary	117
	Acknowledgements	119
	Curriculum Vitae	121
	Publications	123
	Educational Statement	125



Introduction

The storage of light energy in chemical form via photosynthesis is the key process underlying life as we know it. However, for plants to use the photo-assimilates efficiently they have to be transported from leaves (the source) where the photo-assimilates are produced to the areas of growth or storage (the sinks). This fine-tuned long-distance transport of photo-assimilates is accommodated in the phloem part of the vascular tissue (Fig. 1.1). The phloem pathway is located parallel with xylem part of the vascular tissue which transports water and nutrients from roots up to the aerial parts of the plant (Fig. 1.1). Xylem sap flow is driven by transpiration and is therefore operating under negative pressure. During transpiration, plants lose precious water to accommodate the assimilation of CO₂ which is eventually (in the form of photo-assimilates) exported by phloem. In this way, both xylem and phloem interact to ensure that a plant's essential life processes are maintained. Of these two long-distance transports, phloem is arguably the less well understood, and holds the potential to either limit or increase the productivity of the whole plant system, as it is the conduit for photo-assimilates in the plant. The focus of this thesis is to shed light on this process of long-distance photo-assimilates transport.

1.1. Phloem transport

The phloem pathway distributes photo-assimilated from source to (plant) sinks (Fig. 1.1). 'Source' here refers to the photosynthetically active part of the plant (which supplies photo-assimilates) like a mature leaf. However, source can also refer to an organ which releases sugars at specific periods of a plant's life. Such a source can be for example roots, storage tissue in stems or tubers. The distributed photo-assimilates are non-reducing carbohydrates like sucrose, sugar alcohols or carbohydrates of raffinose type. In some plant families reducing hexose is also translocated (van Bel & Hess, 2008). However, among the distributed carbohydrates, sucrose represents the largest fraction across all herbaceous plants (van Bel & Hess, 2008).

The photo-assimilates are translocated in a continuum of specialised cells called sieve elements (SE) which comprise sieve tubes. To allow the phloem sap to move unimpeded through the sieve elements, the SE lack most of the organelles like for example nuclei. Therefore the SE are functionally supported by companion cells (CC) which are associated via plasmodesmata (Oparka & Turgeon, 1999). The theory describing phloem transport (the so-called 'pressure flow hypothesis' (Knoblauch & Peters, 2010)) was postulated almost one hundred years ago by

Ernst Münch. Even though the hypothesis has often been challenged over the decades, like for example by the electro-osmotic theory (Spanner, 1970) or that phloem flow is propelled by peristaltic waves (Thaine, 1969), it is still the most widely-accepted theory (Knoblauch & Peters, 2013). According to the pressure flow hypothesis, phloem flow is driven by an actively-maintained pressure difference between source and sink. At the source site, the osmotic pressure increases when osmotically-active photo-assimilates are loaded into the phloem sieve tubes. This increased osmotic pressure attracts water from the surrounding tissues, creating a turgor pressure in the transport phloem. At the sink site, the photo-assimilates are (actively) removed from the phloem sap and the osmotic pressure decreases. The result of this active loading and unloading of photo-assimilates is the osmotically generated pressure gradient which drives the phloem sap flow. Although the pressure flow hypothesis is widely accepted it has not yet been experimentally proven as the data on the presence of a pressure differential between source and sink are lacking (Knoblauch & Peters, 2010) and therefore the true phloem pressure differences is a matter of continuous discussion (Mullendore *et al.*, 2010).

Since the pressure flow hypothesis was first proposed it has undergone several modifications. For example, it has been recognised that the loading and unloading of photo-assimilates into and from the phloem pathway take place along the whole stretch of transport phloem and occurs by a variety of combinations of direct symplasmic diffusion, apoplastic transport, or polymer trap mechanisms (De Schepper *et al.*, 2013). Our view of the sieve tubes has also changed since the time of Münch who envisaged them as simple semi-permeable pipes. It has since been discovered that along the transport phloem, some photo-assimilates passively diffuse outwards with a part of these lost photo-assimilate being subsequently actively reloaded (via sucrose transporters embedded in SE plasma membrane) into the sieve tubes, a process known as leakage-retrieval (van Bel, 2003). It has also been concluded that sieve tubes must operate under enormously high turgor (positive) pressure (Turgeon & Wolf, 2009). This may be possible for shorter plants, but when extrapolated to trees, tremendous pressures would have to be achieved to transport phloem sap along the whole transport phloem pathway. To help account for this, the relay mechanism was suggested in which the sieve tubes are shorter than the tree axial lengths and the individual sieve tubes are overlapping with apoplastic loading steps between them (Lang, 1979). This is an elegant, albeit somewhat criticised theory (Turgeon, 2010). More recently, it has been suggested that the pressure gradient between source and sink should be redefined as low or

negligible, in such a way that the SE of transport phloem would regulate their own turgor pressure rather than the turgor pressure gradient between them (Thompson, 2006).

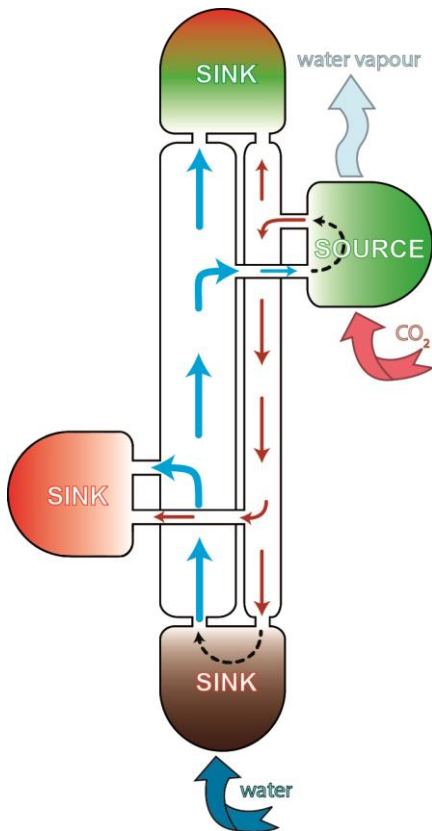


Figure 1.1: Scheme of the main water and photo-assimilates distribution pathways between source and sink(s). Xylem vascular tissue is here denoted as the wider channel with blue arrows. The xylem transports water and minerals from the roots, which are denoted as the bottom sink in brown colour, up to the aerial parts of the plant. Xylem transport is driven by the transpiration of water from the leaves, which are denoted as a source in green colour. In the leaves, CO₂ diffuses in and is subsequently photo-assimilated and the resulting sugars are exported by phloem. Phloem part of the vascular tissue is here denoted as the narrower channel with red arrows. Phloem transports photo-assimilates from source to the sink(s) like growing tips, vascular cambium, terminal sinks like fruits (here denoted as red sink) or roots (in brown).

Even today, after almost a hundred years since the pressure flow hypothesis was first postulated, many research questions remain unanswered and hypotheses experimentally unverified. Phloem flow is known to be notoriously difficult to measure for several reasons. The phloem vascular tissue consists of living cells and therefore if the phloem pathway is perturbed a defence mechanism immediately blocks the perturbed part (Knoblauch & Peters, 2010). On top of this, the phloem pathway, unlike xylem, operates under positive pressure and therefore an insertion of any probe or sensor disturbs the pressure and the measured data become biased. Therefore, minimally-invasive measurement techniques are required to study the long-distance photo-assimilates distribution and dynamics.

This task is becoming more feasible because of current developments in phloem flow measuring and imaging techniques. Radioactive-label (^{11}C or ^{14}C) tracking is one such technique which can measure phloem flow non-invasively. This technique was originally pioneered by Minchin in the mid-1970's and has continued to be used in subsequent years (Minchin & Thorpe, 2003). Although somewhat neglected in the past decade, radioactive-tracking techniques have undergone something of a renaissance due to the advent of positron emission tomography (PET) techniques being used in plant research (Hubeau & Steppe, 2015). One drawback of CO_2 -based techniques is that they require CO_2 uptake, a process which does not necessarily cover the full 24 hour period in many plant species. Another method is fluorescent dye tracking (Jensen *et al.*, 2011; Froelich *et al.*, 2011), although this cannot be truly termed “non-invasive” as the tracking agent must be physically injected into the phloem vascular tissue. The only truly non-invasive technique with the ability to measure over 24 hours and for extended time-frames is magnetic resonance imaging (MRI) (Kockenberger *et al.*, 1997; Windt *et al.*, 2006; Van As, 2007; Van As *et al.*, 2009; Borisjuk *et al.*, 2012). A representative MRI image of a tomato plant stem is depicted in Figure 1.2. Phloem imaging techniques have also been used to gain insight into the structure of phloem, as opposed to flow measurement techniques, which aim to quantify the (rates of) flow. Of these, confocal laser scanning microscopy, transmission or scanning electron microscopy are worth mentioning (Knoblauch & Oparka, 2012). (Note: MRI is also an imaging technique, although its resolution is much lower). These and other novel techniques are providing input and calibration parameters for phloem flow models which have the potential to unlock further insights into how phloem works (Hölttä *et al.*, 2006; De Schepper & Steppe, 2010).

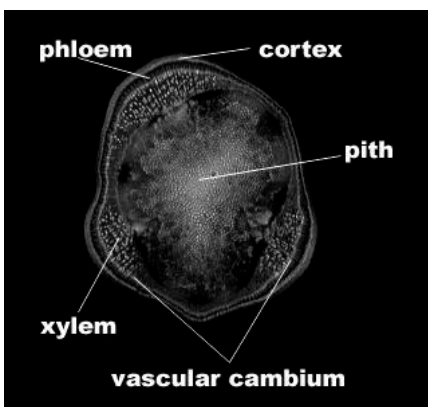


Figure 1.2: Representative cross-sectional MRI image of tomato stem with enhanced contrast. Different types of tissue like cortex, phloem, vascular cambium, xylem and pith can be distinguished.

1.2. Main experimental methods

In order to access the most realistic data on phloem flow a non-invasive technique had to be used in this study, and therefore the central experimental method was Magnetic Resonance Imaging (MRI). MRI can be used to measure both phloem and xylem flow. However, to obtain a more complete view of phloem transport and plant behaviour a combination of techniques is preferable. Therefore, besides MRI, plant sensors like a linear motion potentiometer (DDS) for stem diameter changes (De Swaef *et al.*, 2015), tensiometer for soil water potential or heat balance sap flow sensor for xylem sap flow (Baker & Vanbavel, 1987; Vandegehuchte & Steppe, 2013) were applied simultaneously with MRI.

Magnetic Resonance Imaging

Magnetic resonance imaging (MRI) has become an indispensable technique in everyday medical practice. However, in the last two decades MRI has also become an increasingly common technique to study plant water status as well as xylem and phloem long distance transport in plants (Kockenberger *et al.*, 1997; Peuke *et al.*, 2001, 2015; Scheenen *et al.*, 2002; Windt *et al.*, 2006; Van As, 2007; Borisjuk *et al.*, 2012; Windt & Blumler, 2015). The principal advantage of MRI over other techniques for phloem and xylem flow measurement is that MRI is completely non-invasive. The non-invasiveness lies in the fact that MRI does not require the insertion of tracer compounds like radioactive or fluorescence dye tracking techniques do. The MRI signal originates from the protons of water molecules that are naturally present in plants. A complete description of the principles of MRI is beyond the scope of this introduction; however, the interested reader is directed to any of a number of excellent books on the subject, like for example 'Principles of Nuclear Magnetic Resonance Microscopy' (Callaghan, 1991) or 'Magnetic Resonance Imaging: Physical Principles and Sequence Design' (Haacke *et al.*, 1999). MRI can provide a wealth of information about the properties of the water being imaged. For example, MRI can provide information about water content or relaxation times for every pixel of the imaged part of the plant or when used in flow mode it can provide quantitative information about the flowing water on a per pixel basis.

NMR Relaxation

In general, the nuclear magnetic resonance (NMR) signal, the underlying principle of MRI, originates from nuclei with a non-zero nuclear spin quantum number (I).

The protons (^1H with $I = \frac{1}{2}$) of water molecules are the most important nuclei for MRI measurements. When such nuclei are subjected to an external magnetic field (B_0), previously randomly-oriented spins align either parallel or antiparallel with B_0 . This results in a net macroscopic magnetic moment in the direction of B_0 (which is by definition along the z-axis). The macroscopic magnetic moment is called the magnetisation vector (M_0) and is proportional to the total amount of (water) protons present in the sample. To be able to detect this magnetisation, it has to be rotated into the transverse (xy) plane by applying an orthogonal 90° -radiofrequency (RF) pulse to create a phase coherence. Immediately following this RF pulse, the initial magnetisation level can be detected. Therefore an MRI image obtained (in principle) in such a way is called a proton density image. After a certain time (called the relaxation time), the disturbed thermal equilibrium is restored and magnetisation returns to the z-axis. The process of NMR relaxation can be characterised by two components, the T_1 (spin-lattice or longitudinal) and T_2 (spin-spin or transversal) relaxation time. The T_1 represents the restoration of the magnetisation vector along the z-axis and the T_2 characterises the decay of the magnetisation vector in the xy-plane. In general, the relaxation times of nuclei are determined by their rotational correlation time (τ_c) which in turn is determined by the interaction or rigidity of the molecules bearing the NMR active nucleus. The interactions can be inter- or intramolecular like for example dipolar interactions, hydrogen bonds, hydrophobic interactions, electrostatic interactions or dispersion forces (Israelachvili, 1997). That said, the relaxation time is sensitive to the physical environment the nuclei find themselves in and therefore the relaxation can be used as a probe for studying the environment. For example, water protons close to macromolecules or to solid surfaces (which represent relaxation sinks) have generally shorter T_2 ($\ll 2$ s) in comparison to bulk water (~ 2 s). Exchange of water protons between water molecules and other molecules such as carbohydrates and proteins also influences the relaxation time. Furthermore, the T_2 of water protons is influenced by many other factors like for example the size of organelles, membrane permeability or proximity to a membrane (van der Weerd *et al.*, 2002). A more comprehensive introduction to the theory of NMR relaxation can be found in dedicated literature on the subject (Bakmutov, 2005) or (Van As, 2007) and (Van As & van Duynhoven, 2013).

In addition to the aforementioned processes, the transverse magnetisation is perturbed by local magnetic field inhomogeneities. These can be caused by either imperfections in the external magnetic field or by the presence of paramagnetic

particles or areas with different magnetic susceptibility (like for instance air pockets in plant tissue). This leads to a loss of phase coherence of the individual spins and a faster decay of the magnetisation vector in the xy-plane. The resulting apparent relaxation time is called T_2^* . However, the loss of the phase coherence caused by the B_0 field inhomogeneities can be reversed by the application of a 180° RF pulse following the initial 90° RF pulse. The resulting signal is called a spin echo and ideally its amplitude is attenuated by the intrinsic transversal relaxation processes only. After recording a complete echo train, the echo envelope is fitted (for example by using Levenberg-Marquardt non-linear least square algorithm) with a sum of exponential curves ('components') $\sum_i A_i \cdot e^{-t/T_{2,i}}$ where A_i is an amplitude of the $T_{2,i}$ relaxation time. In this way the T_2 relaxation time can be estimated. In imaging mode this results in the creation of a T_2 map (Edzes *et al.*, 1998) (Fig. 1.3).

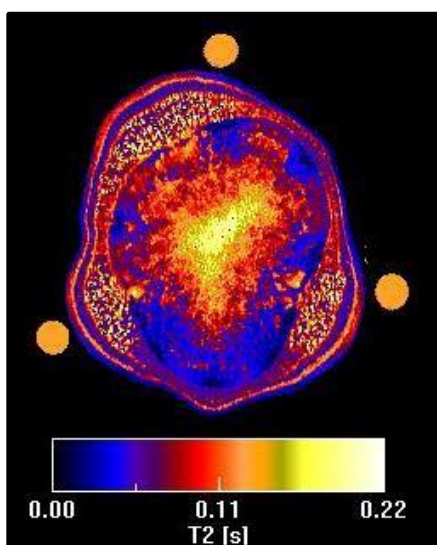


Figure 1.3: Representative cross-sectional T_2 map of a tomato stem. The T_2 values were obtained after fitting the echo train with a 1 component exponential function. The dots around the stem represent reference tubes filled with stationary doped water. Unlike in figures 1.2 and 1.5, the colour scale used is non-linear to accentuate differences between adjacent tissues. It can be clearly seen that the T_2 in the phloem region is lower in comparison to the cortex and xylem tissue (*cf.* Fig. 1.2).

MRI flowmetry

The displacement of water protons can be measured with the pulsed field gradient (PFG) experiment by which we can measure the ensemble average propagator $P(R, \Delta)$ that describes the probability of a ^1H moving over a distance R during a (flow) labelling time (Δ). In the PFG experiment a pair of short field gradient pulses separated by the labelling time is applied. During the labelling time the so-called q-

space evolves and attenuates the resulting signal. A detailed description of the PFG method can be found in the excellent book: *Translational Dynamics & Magnetic Resonance* (Callaghan, 2011).

In this work we applied the PFG turbo spin echo PFG-TSE method (Scheenen *et al.*, 2000). This sequence allows measuring both the k-space (the imaging part) as well as the q-space (the displacement part usually with 32 different PFG steps). For every step in the q-space the whole k-space has to be acquired, and therefore the flow imaging (depending on several factors) can be relatively long (for example for a phloem flow measurement it can be ca. 60 min). The parameter Δ (in combination with the amplitude of the PFG pulse) determines the span of flow velocities which can be measured correctly and for phloem flow measurement this flow encoding time can be as long as 150 ms. Such a long flow encoding time is required in order to distinguish very slowly moving phloem water from stationary, randomly diffusing, water. After acquiring such a measurement the propagator for every pixel and along the gradient direction is obtained. A representative pixel propagator of such a PFG-TSE measurement is depicted in Figure 1.4. As can be seen, the propagator is asymmetric; at positive displacements (in this example) it forms an approximately Gaussian-shaped function, whereas for negative displacements it appears as a distorted Gaussian function. The purely-Gaussian region (here, at positive displacements) represents stationary and hence randomly-diffusing water. In other words, in the absence of flow, the propagator would form a Gaussian-shaped function symmetrically distributed around zero. However, if in the pixels of interest a net displacement occurs in one direction, a distortion in the propagator function is caused which can be detected. This fact can be used to discriminate between stationary and flowing water occurring within one pixel. This is achieved by fitting the symmetric half of the propagator with a Gaussian curve and subsequently subtracting the reflection of the fitted values in the flow direction of the propagator. As a result, an estimate of the amount of stationary water as well as the propagator of the water which exhibits net displacement is obtained. Whether the asymmetric part of the propagator appears as a positive or a negative displacement depends on the flow direction with respect of the direction of the PFGs. The aforementioned approach could be summarised as follows: acquiring the propagator, subtracting non-flow direction and further quantification by comparing the signal amplitude of the measured pixel with a pixel filled with stationary water in a reference object (which provides a 100% value for a pixel filled with water). The propagator represents the probability of the displacement,

and therefore if the displacement (R) is divided by the flow labelling time (Δ) a velocity distribution is obtained. Using this approach, every pixel provides information about the average flow velocity (calculated from the velocity profile), the flow conducting area, the volume flow and the amount of stationary water. These results can be depicted in a respective parameter map, like for example a phloem flow velocity map as shown in Figure 1.5.

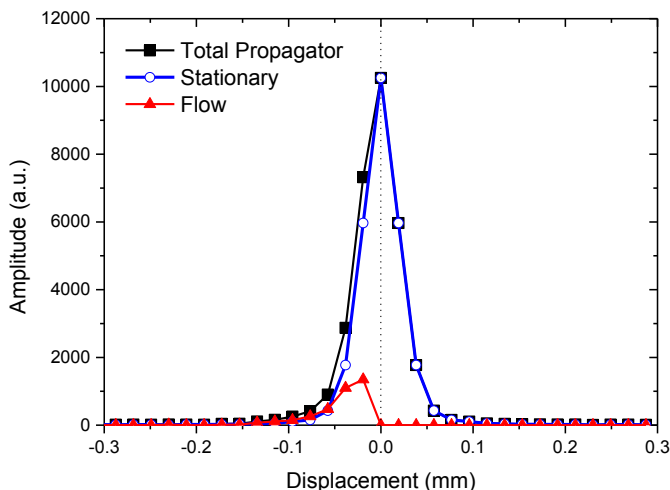


Figure 1.4: Representative total propagator (in black) for one pixel within the phloem vascular tissue of a tomato stem. After subtracting the non-flow component of the propagator from the flow component, the propagator for stationary water (in blue) and flowing water (in red) is obtained.

The detailed formulation of this approach is fully described in the work of Scheenen and Windt (Scheenen *et al.*, 2000, 2001, 2002, 2007; Windt *et al.*, 2006; Van As, 2007). This PFG-TSE flow measurement (when the whole q -space is acquired) should not be mistaken with MRI velocimetry, when essentially only two points in the q -space are recorded and from their slope the average flow velocity can be calculated. However, if the velocity profile, flow conducting area and the amount of stationary water per pixel are also of interest (and not only the average flow velocity), the use of an approach such as PFG-TSE is needed (Scheenen *et al.*, 2000). Therefore, to distinguish this approach from MRI velocimetry, we use the term MRI flowmetry.

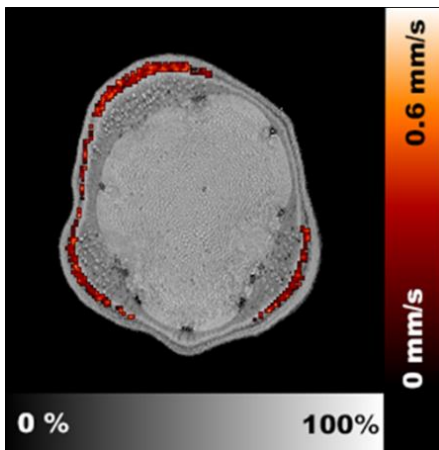


Figure 1.5: Representative cross-section proton density image of a tomato stem, presented as a water content map with a grey scale on the bottom. It is possible to distinguish several tissue types in the proton density image. However, these different tissue types are less obvious than those obtained from the contrast enhanced image (*cf.* Fig. 1.2). The proton density image is overlaid with a representative phloem flow velocity map with a red velocity scale on the right hand side.

1.3. Outline of the thesis

This thesis attempts to answer the long-standing question of whether phloem transport can be a limiting factor for photosynthesis efficiency (and ultimately, causing a bottleneck towards achieving higher yields). This remains the central research question underlying every chapter, although different aspects of this question are examined in the various experimental chapters. In **Chapter 2**, we will approach the question of how tomato plants cope with increased source strength. This will be examined by measuring phloem flow characteristics with MRI flowmetry during various controlled changes in the light intensity. With this experiment we will test the hypothesis regarding the constant nature of phloem flow velocity, which has previously been suggested in other studies. We investigate whether the expected increase in the amount of photo-assimilates under higher light intensities is transported by an increased phloem flow velocity or by another mechanism. In chapter 2 we study a simplified system, i.e., a tomato plant in which all trusses and flowers were pruned. In **Chapter 3**, we examine how fruit-bearing tomato plants behave while exposed to short photoperiods (another form of source strength manipulation). This problem will be approached by measuring flow characteristics with MRI flowmetry and simultaneous monitoring of other plant processes like xylem flow rates (monitored with heat balance sensor), net photosynthesis (monitored with gas exchange) and stem diameter change (monitored with linear motion potentiometer - DDS). With this integrated approach we will attempt to uncover any interplay between these various plant

processes. In **Chapter 4**, we will approach the question whether T_2 relaxation time in the phloem region reflects phloem carbon status. For this purpose we analyse the T_2 dataset which was acquired during the experiment presented in chapter 2, i.e., from a tomato plant exposed to different light intensities. In order to select only phloem tissue, the phloem flow mask acquired during the phloem flow measurement will be used, after which the average T_2 relaxation time in that region will be assessed with a phasor approach. In the same way, a dataset obtained from a measurement under different photoperiods will be analysed. In the last experimental chapter, **Chapter 5**, we will examine whether the potato plant might represent a better test subject than that of tomato for investigations into the dynamics of phloem flow. A potato plant with developing tubers would appear to be an ideal test subject for MRI flowmetry as this plant species possesses a strong sink below the MRI measurement site.

1.4. References

- Baker JM, Vanbavel CHM. 1987.** Measurement of Mass-Flow of Water in the Stems of Herbaceous Plants. *Plant Cell and Environment* **10**: 777–782.
- Bakhtmutov VI. 2005.** *Practical NMR relaxation for chemists*. Chichester: Wiley & Sons Ltd.
- Borisjuk L, Rolletschek H, Neuberger T. 2012.** Surveying the plant's world by magnetic resonance imaging. *The Plant Journal: for cell and molecular biology* **70**: 129–46.
- Callaghan PT. 1991.** *Principles of Nuclear Magnetic Resonance Microscopy*.
- Callaghan PT. 2011.** *Translational Dynamics & Magnetic Resonance*. New York: Oxford University Press.
- De Schepper V, Steppe K. 2010.** Development and verification of a water and sugar transport model using measured stem diameter variations. *Journal of Experimental Botany* **61**: 2083–99.
- De Schepper V, De Swaef T, Bauweraerts I, Steppe K. 2013.** Phloem transport: a review of mechanisms and controls. *Journal of Experimental Botany* **64**: 4839–50.
- De Swaef T, De Schepper V, Vandegehuchte MW, Steppe K. 2015.** Stem diameter variations as a versatile research tool in ecophysiology. *Tree Physiology* **35**: 1047–1061.
- Edzes HT, van Dusschoten D, Van As H. 1998.** Quantitative T2 imaging of plant tissues by means of multi-echo MRI microscopy. *Magnetic Resonance Imaging* **16**: 185–196.
- Froelich DR, Mullendore DL, Jensen KH, Ross-Elliott TJ, Anstead JA, Thompson GA, Pélissier HC, Knoblauch M. 2011.** Phloem ultrastructure and pressure flow: Sieve-Element-Occlusion-Related agglomerations do not affect translocation. *The Plant cell* **23**: 4428–45.
- Haacke EM, Brown RW, Venkatesan R, Thompson MR. 1999.** *Magnetic Resonance Imaging: Physical Principles and Sequence Design*. New York: Wiley-Liss.
- Hölttä T, Vesala T, Sevanto S, Perämäki M, Nikinmaa E. 2006.** Modeling xylem and phloem water flows in trees according to cohesion theory and Münch hypothesis. *Trees - Structure and Function* **20**: 67–78.
- Hubeau M, Steppe K. 2015.** Plant-PET Scans: In Vivo Mapping of Xylem and Phloem Functioning. *Trends in Plant Science* **20**: 676–685.
- Israelachvili JN. 1997.** *Intermolecular and Surface Forces*. London: Academic Press Ltd.
- Jensen KH, Lee J, Bohr T, Bruus H, Holbrook NM, Zwieniecki MA. 2011.** Optimality of the Münch mechanism for translocation of sugars in plants. *Journal of the Royal Society, Interface / the Royal Society* **8**: 1155–65.
- Knoblauch M, Oparka K. 2012.** The structure of the phloem - still more questions than answers. *The Plant Journal*. **70**: 147–56.
- Knoblauch M, Peters WS. 2010.** Münch, morphology, microfluidics - our structural problem with the phloem. *Plant, Cell & Environment* **33**: 1439–52.

- Knoblauch M, Peters WS. 2013.** Long-distance translocation of photosynthates: a primer. *Photosynthesis Research* **117**: 189–96.
- Kockenberger W, Ki WI, Pope JM, Xia Y, Jeffrey KR, Komor E, Callaghan PT. 1997.** Planta A non-invasive measurement of phloem and xylem water flow in castor. *Planta* **201**: 53–63.
- Lang A. 1979.** Relay mechanism for phloem translocation. *Annals of Botany* **44**: 141 – 145.
- Minchin PEH, Thorpe MR. 2003.** Using the short-lived isotope ^{11}C in mechanistic studies of photosynthate transport. *Functional Plant Biology* **30**: 831–841.
- Mullendore DL, Windt CW, Van As H, Knoblauch M. 2010.** Sieve tube geometry in relation to phloem flow. *The Plant Cell* **22**: 579–93.
- Oparka KJ, Turgeon R. 1999.** Sieve elements and companion cells-traffic control centers of the phloem. *The Plant Cell* **11**: 739–50.
- Peuke AD, Gessler A, Trumbore S, Windt CW, Homan N, Gerkema E, Van As H. 2015.** Phloem flow and sugar transport in *Ricinus communis* L. is inhibited under anoxic conditions of shoot or roots. *Plant, Cell & Environment* **38**: 433–447.
- Peuke AD, Rokitta M, Zimmermann U, Schreiber L, Haase A. 2001.** Simultaneous measurement of water flow velocity and solute transport in xylem and phloem of adult plants of *Ricinus communis* over a daily time course by nuclear magnetic resonance spectrometry. *Plant, Cell and Environment* **24**: 491–503.
- Scheenen TW, van Dusschoten D, de Jager PA, Van As H. 2000.** Microscopic displacement imaging with pulsed field gradient turbo spin-echo NMR. *Journal of Magnetic Resonance*. **142**: 207–15.
- Scheenen T, Heemskerk A, de Jager A, Vergeldt F, Van As H. 2002.** Functional imaging of plants: a nuclear magnetic resonance study of a cucumber plant. *Biophysical Journal* **82**: 481–492.
- Scheenen TWJ, Vergeldt FJ, Heemskerk AM, Van As H. 2007.** Intact Plant Magnetic Resonance Imaging to Study Dynamics in Long-Distance Sap Flow and Flow-Conducting Surface Area. *Plant Physiology* **144**: 1157–1165.
- Scheenen TW, Vergeldt FJ, Windt CW, de Jager P A, Van As H. 2001.** Microscopic imaging of slow flow and diffusion: a pulsed field gradient stimulated echo sequence combined with turbo spin echo imaging. *Journal of Magnetic Resonance*. **151**: 94–100.
- Spanner DC. 1970.** Electro-osmotic theory of phloem transport in light of recent measurements on heracleum phloem. *Journal of Experimental Botany* **21**: 325.
- Thaine R. 1969.** Movement of Sugars through Plants by Cytoplasmic Pumping. *Nature* **222**: 873–875.
- Thompson M V. 2006.** Phloem: the long and the short of it. *Trends in Plant Science* **11**: 26–32.
- Turgeon R. 2010.** The puzzle of phloem pressure. *Plant Physiology* **154**: 578–81.
- Turgeon R, Wolf S. 2009.** Phloem transport: cellular pathways and molecular trafficking. *Annual Review of Plant Biology* **60**: 207–21.

Vandeghehuchte MW, Steppe K. 2013. Sap-flux density measurement methods: working principles and applicability. *Functional Plant Biology*: 213–223.

Van As H. 2007. Intact plant MRI for the study of cell water relations, membrane permeability, cell-to-cell and long distance water transport. *Journal of Experimental Botany* **58**: 743–756.

Van As H, van Duynhoven J. 2013. MRI of plants and foods. *Journal of Magnetic Resonance* **229**: 25–34.

Van As H, Scheenen T, Vergeldt FJ. 2009. MRI of intact plants. *Photosynthesis Research* **102**: 213–22.

van Bel AJE. 2003. The phloem, a miracle of ingenuity. *Plant, Cell and Environment* **26**: 125–149.

van Bel AJE, Hess PH. 2008. Hexoses as phloem transport sugars: the end of a dogma? *Journal of Experimental Botany* **59**: 261–72.

van der Weerd L, Claessens MMAE, Efdé C, Van As H. 2002. Nuclear magnetic resonance imaging of membrane permeability changes in plants during osmotic stress. *Plant, Cell & Environment* **25**: 1539–1549.

Windt CW, Blumler P. 2015. A portable NMR sensor to measure dynamic changes in the amount of water in living stems or fruit and its potential to measure sap flow. *Tree Physiology*: 366–375.

Windt CW, Vergeldt FJ, de Jager PA, van As H. 2006. MRI of long-distance water transport: a comparison of the phloem and xylem flow characteristics and dynamics in poplar, castor bean, tomato and tobacco. *Plant, Cell & Environment* **29**: 1715–29.



**Source strength manipulation in tomato
changes phloem volume flow, but not flow
velocity.**

Alena Prusova, Frank J. Vergeldt, Carel W. Windt, Edo Gerkema, Rob B. M.
Koehorst, John G.M. Philippi, Henk Van As

2.1. Summary

To test the hypothesis that phloem flow is regulated to a constant velocity we measured phloem flow in the main stem of tomato over several consecutive days while simultaneously manipulating source strength.

Phloem and xylem flow were measured in the main stem of adult tomato plants using magnetic resonance imaging (MRI) flowmetry. Source manipulation was achieved by changing the light intensity.

Under high light conditions a larger volume of phloem sap was transported towards the roots than under low light. The average phloem flow velocity exhibited a diurnal pattern with higher velocity of $0.24 \pm 0.03 \text{ mm} \cdot \text{s}^{-1}$ during the day and lower velocity of $0.20 \pm 0.01 \text{ mm} \cdot \text{s}^{-1}$ at night. Under all light conditions the average phloem flow velocity remained within those boundaries and therefore it remained virtually unchanged.

Light-induced changes in source strength had a substantial effect on the volume of phloem sap which was transported, but did not notably affect its velocity. An increase in the flow conducting area indicated that the additional volume of flow was accommodated in sieve tubes that were not functional at lower source strengths.

2.2. Introduction

Phloem transport

Effective usage of photo-assimilates is one of the major determinants of plant growth. To be available, the photo-assimilates have to be transported from photosynthetically-active tissue (the source) to energy-demanding tissue (the sink) (van Bel, 2003; Lemoine *et al.*, 2013). This transport is accommodated in phloem vascular tissue and is driven by an osmotically-generated moderate pressure gradient (Münch, 1930; Thompson, 2006; Knoblauch & Oparka, 2012; De Schepper *et al.*, 2013). Both source and sink activity regulate this dynamic system (Björkman & Holmgren, 1963; Wolswinkel, 1984; Wardlaw, 1993; Marcelis, 1996; Farrar, 1996; Murchie *et al.*, 2009; Turgeon, 2010). This relationship between source and sink(s) is known as the source : sink ratio where the relative sink strength dictates the distribution of photo-assimilates (Heuvelink & Muiskool, 1995; Fatichi *et al.*,

2014). Previous studies which tried to understand how the source : sink ratio influences photo-assimilates allocation found that changes in the source : sink ratio (mostly by defoliation or fruit pruning) can significantly influence the yield and plant performance (Minchin & Thorpe, 1996; Heuvelink, 1997; Matsuda *et al.*, 2011). Measurement of the rate of photo-assimilates translocation, i.e., the phloem flow is, however, experimentally elusive because the fragile pressure gradient in the phloem transport pathway is very easily disturbed. Thus, reliable data on phloem velocities and flow remain scarce (Knoblauch & Peters, 2010).

There are only a few techniques which are suitable to measure phloem flow velocities, like for example radioactive-label (^{11}C or ^{14}C) tracking (Minchin & Thorpe, 2003). This method is however limited to the study of translocation during the light period (when stomata are open and tracer CO_2 diffuses in). Another method is fluorescent dye tracking (Jensen *et al.*, 2011; Froelich *et al.*, 2011) a method which can be used during both the light and dark period, but in this case a fluorescent tracer has to be injected in the transport phloem and therefore this method is invasive. So far, the only non-invasive and long-term applicable technique is magnetic resonance imaging (MRI) (Kockenberger *et al.*, 1997; Windt *et al.*, 2006; Van As, 2007; Van As *et al.*, 2009; Borisjuk *et al.*, 2012).

Phloem flow velocity

It has been predicted that carbon assimilation by day and the depletion of leaf carbon reserves by night can influence the source : sink ratio of the plant because of observed diurnal changes in phloem sucrose concentrations (Sharkey & Pate, 1976; Mitchell & Madore, 1992). In turn this could cause diurnal phloem flow velocity changes. A clear diurnal pattern in phloem flow has not yet been reported. Some indication about diurnal changes in phloem velocity in castor bean was reported by Peuke *et al.* (2001). However, the technique used was unable to measure phloem velocity, only phloem flow. The authors concluded that phloem flow velocity was probably constant over the day/night period. A day-night pattern in phloem flow velocity was previously reported by Windt *et al.* (2006) who found 'insignificant but consistent' changes in phloem flow velocity with a simultaneous decrease in flow conducting area during the night in comparison to day in tomato. The authors hypothesised that phloem flow velocity is regulated to be more or less constant and relatively slow. This

might help the plant to maintain a predictable signalling (Turnbull & Lopez-Cobollo, 2013) and potentially prevent the dislocation of parietal sieve-tube organelles due to shear forces (Windt *et al.*, 2006). Published phloem flow velocities in general report only marginal differences; some of these (measured in herbaceous plants) are summarised in Table 1. In contrast to herbaceous plants, trees exhibit much larger differences (Liesche *et al.*, 2015).

The majority of the literature on phloem velocity focuses on flow under steady-state conditions. Although useful, these studies provide little or no insight into how alterations in the source: sink ratio affect phloem transport. One of the few studies measuring phloem velocity during simultaneous plant manipulation was performed on developing cucumber seedlings. This study reported basipetal phloem flow velocity increasing incrementally as the plants develops, reaching a maximum at adulthood (Savage *et al.*, 2013) which indicated that phloem flow velocity is not necessarily always constant. Another study measuring phloem flow velocity used anoxia to manipulate both sink and source strength in castor bean (Peuke *et al.*, 2015). Under anoxia the phloem velocity remained approximately constant, although the phloem volume flow decreased and an increase in sucrose concentration was observed. Despite the fact that source and sink anoxia is an extreme condition, this study suggested that phloem flow velocity is maintained to be constant.

Treatments which enhance a plant's source strength (such as increasing, but still optimal, light intensities) not only avoid unduly stressing the plant, but may also be directly relevant for production which often uses such techniques to increase yield. Light has a direct effect on photosynthesis and thus the amount of photo-assimilates (sucrose) produced (Björkman & Holmgren, 1963), but also affects the companion cell (CC) anatomy. In *A. thaliana*, acclimation to high light conditions is manifested by an increase of CC cell wall invagination, potentially allowing higher sucrose phloem loading (Amiard *et al.*, 2007). Similar to *A. thaliana*, tomato is also an apoplasmic loader (van Bel, 2003). Then, if a greater amount of photo-assimilates are loaded into transport phloem under increased source strength conditions – how would a tomato plant cope with it? Would an adult plant growing under optimal conditions still regulate phloem flow velocity to maintain a constant value?

Table 1: Overview of reported phloem flow velocities.

Technique	Plant species	Velocity (mm · s ⁻¹)	Reference
¹¹ C	castor bean	0.39-0.41	(Grimmer & Komor, 1999)
¹⁴ C	castor bean	0.23	(Hall <i>et al.</i> , 1971)
¹⁴ C	sugar beet	0.14-0.42	(Mortimer, 1965)
¹⁴ C	sugar cane	0.17-0.22	(Hartt, 1967)
¹⁴ C	soybean	0.13-0.35	(Fisher, 1978)
FLASH -MRI ^a	castor bean	0.58	(Kockenberger <i>et al.</i> , 1997)
FLASH -MRI	castor bean	0.25	(Peuke <i>et al.</i> , 2001)
PFG-STE- TSE-MRI ^b	castor bean	0.30 ± 0.02	(Peuke <i>et al.</i> , 2006)
PFG-STE- TSE-MRI	castor bean	0.25	(Windt <i>et al.</i> , 2006)
PFG-STE- TSE-MRI	tomato plant	0.44	(Windt <i>et al.</i> , 2006)
PFG-STE- TSE-MRI	cucumber plant	0.199	(Mullendore <i>et al.</i> , 2010)
Fluo. dye tracking	cucumber plant	0.16 ± 0.02	(Savage <i>et al.</i> , 2013)
PFG-TSE- MRI ^c	castor bean	0.27 ± 0.06	(Peuke <i>et al.</i> , 2015)

^a Fast low angle shot MRI; ^b Pulsed field gradient stimulated echo turbo spin echo (PFG-STE-TSE) MRI; ^c Pulsed field gradient turbo spin echo (PFG-TSE) MRI

Research question

In this study, we examined the effect of light intensity on phloem flow over an extended time period to help unravel whether light-induced source strength manipulation in tomato affects phloem sap flow, in terms of volume flow, average velocity, or both. We hypothesise that phloem sap flow velocity is regulated to remain constant and that an increase in phloem sap volume flow can only be achieved by an increase in the flow conducting area. In order to test this hypothesis, we measured basipetal phloem flow in

the transport phloem of an adult tomato plant by means of MRI while gradually increasing and decreasing source strength by subjecting the plant to slow, step wise changes in light intensity.

2.3. Materials and Methods

We conducted two experiments, one of which involved increasing the light intensity ('light-up') and the other which involved decreasing it ('light-down'). Both experiments were conducted on three-month-old tomato plants (*Solanum lycopersicum* cv. 'GT'). The lower leaves and all trusses with immature fruits and flowers were removed two days before the experiment to clear the main stem of obstacles and to remove strong sinks upstream from the imaging site, located ca. 25 cm above the soil surface. Each experiment was performed on a different plant.

Plant material and microclimate conditions

Plants were grown in a greenhouse during the winter months in 15-L pots with standard compost potting mixture under the following conditions: ca. 70 % relative humidity and 16h days. Inside the MRI scanner the following conditions were applied: day 24 °C, 16 h photoperiod of 230, 400, 600 or 780 $\mu\text{mol} \cdot \text{m}^{-2} \cdot \text{s}^{-1}$ PAR; night 20°C, 8 h. Relative humidity fluctuated around 60%. Plants were watered daily. During experiment 'light-up', the light intensity was increased from the lowest to the higher intensity, and during experiment 'light-down' the light intensity was decreased from the highest to the lower intensity and then increased back to the second highest intensity. In both experiments, each light-regime lasted 3 days. Plants were inserted in the MRI scanner one day prior to the measurements to recover from handling and to acclimatise to the new environment. The plants remained inside the MRI scanner for the entire duration of the experiment.

In the 'light-down' experiment, the soil water potential and stem diameter were also monitored. The soil water potential was monitored with a tensiometer (CV5-U, Banbach Tensio-technique, Geisenheim, Germany), and was maintained at a value of around -33kPa, i.e., the plant was well-watered. The stem diameter was monitored with a linear motion potentiometer (DDS, Ecomatik, Dachau/Munich, Germany) which was fixed to the main stem. The DDS measured relative changes in the stem diameter. DDS and tensiometer were logged on a homebuilt data-logger.

MRI measurements

Phloem and xylem sap flow measurements were conducted in a MRI scanner, consisting of a vertically-orientated superconducting magnet with a 50 cm vertical free bore (Magnex, Oxford, UK). For induction and detection of the signal, a bird cage RF coil of 4 cm diameter was used inside a 1 T/m gradient set (Bruker, Karlsruhe, Germany) and controlled by the Avance console (Bruker, Karlsruhe, Germany); for details see Homan et al. (2007).

In MRI flowmetry, the phloem flow (the volume transported per unit of time) is defined as the product of flow velocity and flow conducting area, parameters which traditionally could not be separately measured until the advent of MRI techniques to disentangle the two (Scheenen *et al.*, 2000; Windt *et al.*, 2006). Here we used a pulsed field gradient-turbo spin echo (PFG-TSE) sequence (Scheenen *et al.*, 2000) to measure sap displacement. For every pixel we obtained a displacement spectrum, the propagator (Scheenen *et al.*, 2000). This propagator was analysed with an approach described elsewhere (Scheenen *et al.*, 2000; Windt *et al.*, 2006; Van As, 2007) and resulted in the following parameters per pixel: volume flow, amount of stationary water, flow conducting area (FCA) and average flow velocity. Flow measurements were carried out using the following imaging parameters: imaging matrix = 128x128 pixels, field of view = 30x30 mm², slice thickness = 3 mm, echo time = 5 ms, and spectral width = 50 kHz. For the xylem measurements the specific parameters were: turbo factor = 8, number of averages = 2, repetition time = 2500 ms, displacement labelling time = 20 ms, gradient duration = 4 ms, 32 gradient steps, maximum gradient strengths = 400 mT · m⁻¹, and acquisition time = 42 min. For the phloem measurements the parameters were: turbo factor = 8, averages = 4, repetition time = 2000 ms, labelling time = 150 ms, gradient duration = 3 ms, 32 gradient steps, maximum gradient strengths = 200 mT · m⁻¹, and acquisition time = 68 min. We alternated between both xylem and phloem measurement. Data analysis was performed with IDL (Research Systems, USA) using in-house processing, fitting, and quantification routines.

LED lighting system

The light source inside the MRI scanner was a dedicated, cooled, telescopic LED module which consisted of four 4-LED assemblies positioned on each quadrant. Each assembly consisted of 4 LEDs Bridgelux BXRA-C2000 (68 V,

1.75 A). The LED module was built to function inside a strong magnetic field with adjustable light intensity (0 – 100%). The light control used a micro-computer unit operating 4 current sources (70 VDC, 2 A) in pulse width modulation (PWD) mode. The total power output of 476 W and PWD frequency of 980 Hz corresponds to maximum of $2750 \mu\text{mol} \cdot \text{m}^{-2} \cdot \text{s}^{-1}$ PAR and colour temperature of 5600 K at 40 cm distance.

2.4. Results

We conducted two types of experiments, one of which involved increasing the light intensity ('light-up') and the other which involved decreasing it ('light-down'). Both experiments were conducted on adult tomato plants. Here we present two representative results of one light-up and one light-down experiment of phloem and xylem flow measured with MRI. A representative cross-sectional image of the main stem of one of the tomato plants used and the corresponding water content map overlaid with phloem velocity map are presented in Fig. 2.1.

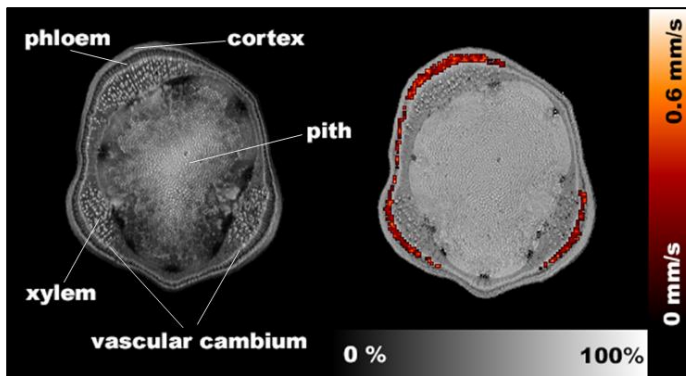


Figure 2.1: From left, representative cross-sectional image with enhanced (T_2 based) contrast of tomato main stem which can serve as an anatomical reference. On the right, a water content map overlaid with a phloem flow velocity map calculated from four MRI flow measurements.

Diurnal dynamics of phloem velocity and flow conducting area

The results in both experiments ('light-up' (Fig. 2.2) and 'light-down' (Fig. 2.3)) showed diurnal dynamics of average phloem flow velocity, flow conducting area (FCA) and phloem volume flow, with higher volume flow

during the day compared to night. The average phloem flow velocity was independent of the light intensity that was applied, i.e., although the velocity alternated between a value of $0.24 \pm 0.03 \text{ mm} \cdot \text{s}^{-1}$ during the day and $0.20 \pm 0.01 \text{ mm} \cdot \text{s}^{-1}$ during the night (both values give the average over all day or night periods, with standard error), the phloem velocity remained virtually constant during all light intensities. The FCA also alternated between a higher value during the day and a lower value at the night, but contrary to the average phloem flow velocity, the value of the FCA during the individual days was positively correlated with the light intensity, i.e., the FCA was higher at higher light intensities and vice versa.

Effect of light regime on phloem volume flow

The results showed a positive correlation between phloem volume flow and light intensity. In both experiments, an increase in the phloem volume flow was associated with an increase in FCA, but (albeit diurnally-alternating) the average phloem flow velocity remained constant. Phloem volume flow also decreased when the light intensity was decreased. In both experiments, the FCA was at least twice as high at the second highest light intensity as at the lowest light intensity (Fig. 2.2 and 2.3). During the highest light intensity in the 'light-up' experiment the FCA levelled off and decreased. This may have been caused by the (unwanted) development of a truss with three small fruits, creating a strong sink upstream of the imaging slice and thus decreasing the relative root sink strength. We also saw that the FCA gradually increased during the period of highest light intensity in the 'light-down' experiment. This is likely to have been caused by an adaptation to the sudden high light condition, reflecting starch/sucrose-for-export partitioning changes and more photo-assimilates available for growth. This agrees well with the highest increase in the stem diameter during that period (Fig. 2.4).

In both experiments we saw changes in the FCA. The FCA is calculated from the PFG-TSE MRI measurement (Scheenen *et al.*, 2000). It is known that the FCA estimate can be biased by exchange between flowing and stagnant water pools (Tallarek *et al.*, 1999; Homan *et al.*, 2010). The effect of exchange becomes more pronounced at longer flow labelling times (such as for example 150 ms, the labelling time in the phloem measurement used in this study). In plants, the phloem leakage-retrieval mechanism (van Bel, 1996) results in exchange. To rule out the possibility that the observed increase in

FCA is due to exchange, we conducted an additional experiment under high light conditions with varying displacement labelling times (Figure S2.1 in online supporting information). The resulting FCA values were independent of the labelling time, indicating that FCA is not affected by exchange between SEs and CCs, i.e., potentially accelerated exchange due to the leakage-retrieval mechanism does not significantly affect our observation.

In this study we assumed that none of the light intensities that were used in the experiment caused photo-inhibition. To verify this, we conducted pulsed amplitude modulated (PAM) fluorescence measurements on the leaves of the tomato plant used in the 'light-down' experiment immediately after the end of the MRI experiment as well as on a control plant. The PAM measurement demonstrated that none of the light intensities induced (irreversible) photo-inhibition (Table S1 in appendix).

Effect of the light regime on xylem flow

Our results showed diurnal dynamics of xylem. Xylem transport is driven by evapotranspiration and therefore the maximal values of xylem flow were observed during the day when stomata are open and the plant is transpiring (Fig. 2.2 and 2.3). The minimum values were observed during the night when stomata are closed, but due to a hydraulic linkage between xylem and phloem tissue the xylem stream remains active during the night, driven by the demand of water for Münch's counter-flow, i.e., water for phloem flow, growth, respiratory loss, evapotranspiratory loss and possible guttation (Tanner & Beevers, 2001; Hölttä *et al.*, 2006; Windt *et al.*, 2006).

The leaf area of the plant used in the 'light-up' experiment was 0.824 m² and in the 'light-down' experiment 1.688 m². This difference was reflected in the fact that the maximal values of xylem volume flow were approximately twice as high in the 'light-down' experiment as in the 'light-up' experiment. In both experiments the xylem volume flow decreased during the second half of the day. In contrast to the 16h photoperiod used in this study, this phenomenon of decreased xylem flow during the second half of the day was not observed during the shorter photoperiod of 10 hours (Fig. S2.2 in appendix). Therefore, the decrease in xylem volume flow could reflect photosynthesis feedback regulation resulting in its inhibition (Quereix *et al.*, 2001; Kelly *et al.*, 2013). This phenomenon was more obvious in experiment 'light-up' because of a better temporal resolution in the experiment.

Under the same light conditions the range of xylem flow does not appear to remain fixed from one day to the next (Fig. 2.2 and 2.3). This was likely caused by a changing microclimate.

Experimental set-up

Acclimation to higher light intensity is a process which can take anything from a number of days to weeks (Amiard *et al.*, 2007; Adams III *et al.*, 2014), and therefore the plants used in our experiment were likely not fully steady-state after three days of individual light intensity. This can be seen particularly in Fig. 2.3, where the phloem volume flow (and FCA) continued to increase during the first days of the experiment under highest light intensity, reflecting adaptation to the sudden high light conditions. One simple amendment to future experiments would be to allow a longer period of acclimation prior to the commencement of MRI measurements under higher light conditions.

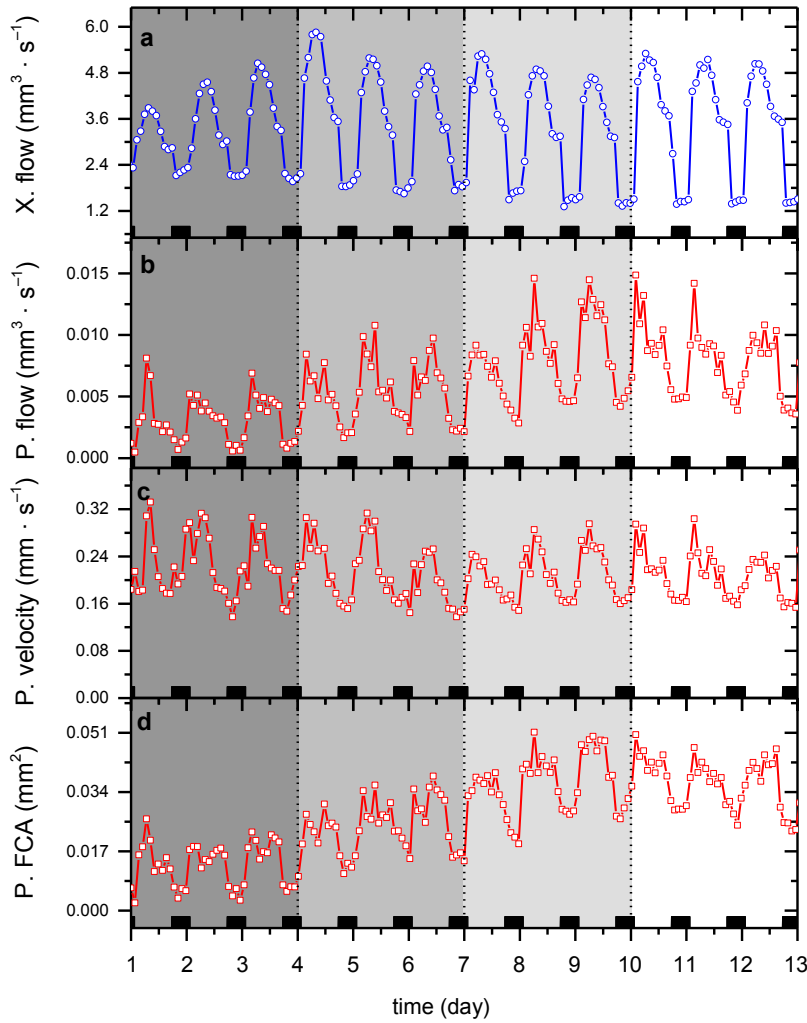


Figure 2.2: Experiment 'light-up'. From the top of the plot: (a) volume flow of xylem sap, (b) volume flow of phloem sap, (c) average phloem flow velocity, and (d) phloem flow conducting area, all as a function of time. Black rectangles represent night-time. The different hues of grey correspond to different light intensities from the darkest to the brightest: 230, 400, 600, and 780 $\mu\text{mol} \cdot \text{m}^{-2} \cdot \text{s}^{-1}$.

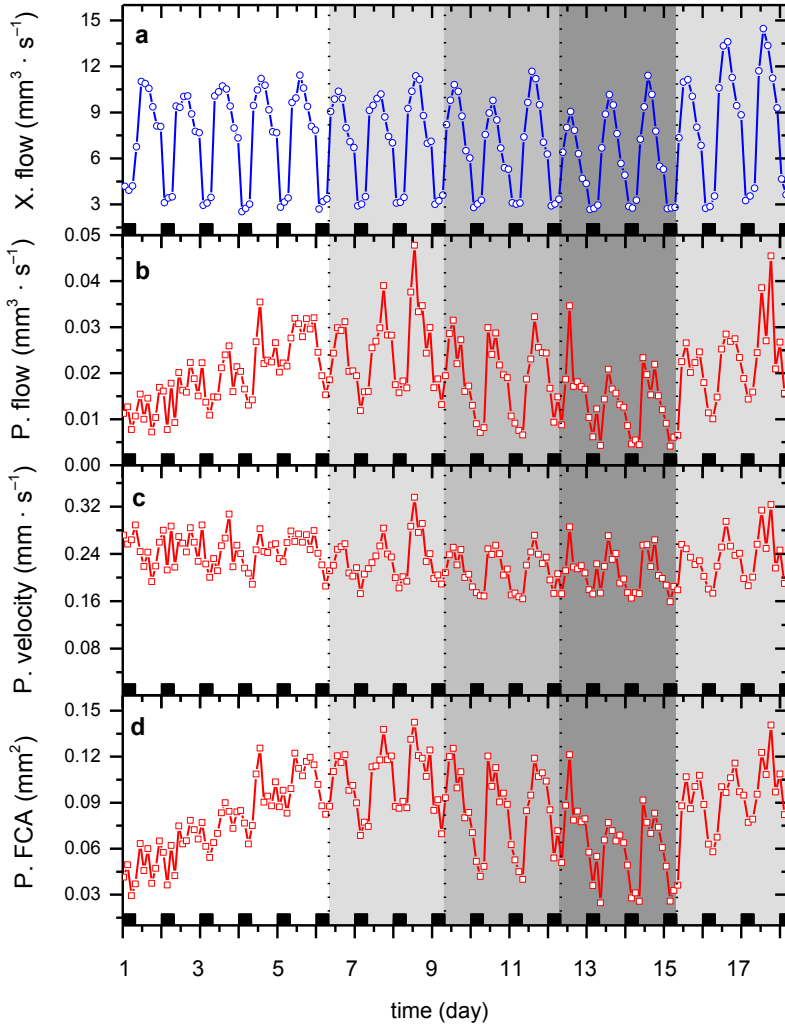


Figure 2.3: Experiment ‘light-down’. From the top of the plot: (a) volume flow of xylem sap, (b) volume flow of phloem sap, (c) average phloem flow velocity, and (d) phloem flow conducting area, all as a function of time. Black rectangles represent night-time. The different hues of grey correspond to different light intensities from the brightest to the darkest: 780, 600, 400, 230, and back to 600 $\mu\text{mol} \cdot \text{m}^{-2} \cdot \text{s}^{-1}$.

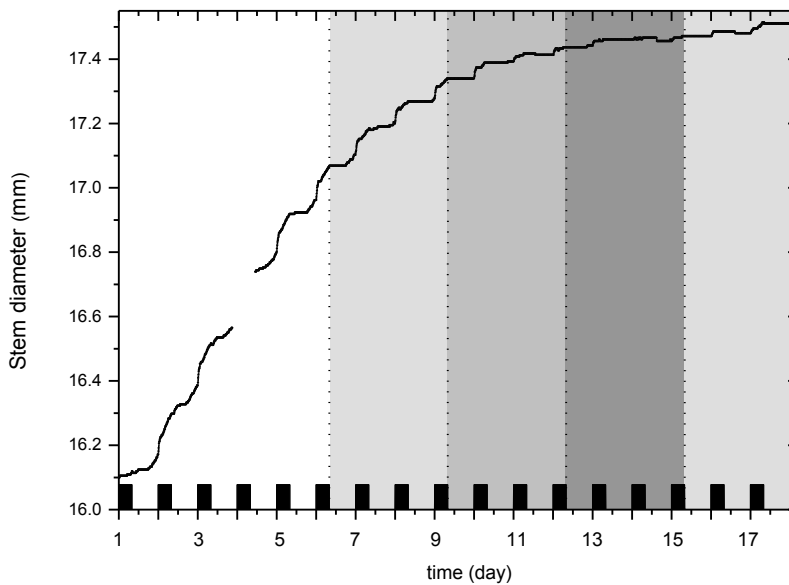


Figure 2.4: Experiment ‘light-down’ stem diameter as a function of time. Black rectangles represent night-time. The different hues of grey correspond to different light intensities during the day from the brightest to the darkest: 780, 600, 400, 230, and back to 600 $\mu\text{mol} \cdot \text{m}^{-2} \cdot \text{s}^{-1}$.

2.5. Discussion

Diurnal pattern of phloem flow velocity

Although some authors have speculated that phloem flow velocity should exhibit a diurnal fluctuation, no such diurnal pattern in phloem flow velocity has yet been reported. In both the ‘light-up’ and ‘light-down’ experiments we observed a lower average phloem flow velocity during the night than during the day (Fig. 2.2 and 2.3). However, it is not just the availability of light that varies between day and night. The origin of sucrose in phloem sap, the principal osmotically-active compound, also differs between these periods. During the day, sucrose is loaded to the phloem stream as a direct product of ongoing photosynthesis while during the night, sucrose is supplied by a cleavage of carbon storage pools (Osorio *et al.*, 2014). It is also known that gene expression of sucrose transporters exhibits a circadian rhythm in tomato (Hackel *et al.*, 2006). This would promote higher sucrose export from the leaves during the day when compared to the night.

When these facts are considered together, it is clear that a diurnal pattern in average phloem flow velocity occurs.

Windt et al (2006) reported ‘insignificant but consistent’ changes in phloem flow velocity in tomato. We believe the authors did not observe a more clearly defined diurnal pattern of phloem velocity variation because they grew their plants at a lower light intensity and at a shorter photoperiod in their experimental set-up.

Is phloem flow regulated to a constant velocity?

We set out in these experiments to test whether phloem flow velocity is regulated to maintain a constant value under increased source strength. Over the course of both experiments we found that the average day/night phloem flow velocity indeed remained constant, independent of the light intensity, which indicates a strict control of phloem flow velocity. This observation is striking because phloem flow velocity is thought to be governed by hydraulic conductivity, inversely proportional to the phloem viscosity (Thompson & Holbrook, 2003; Thompson, 2006). It is known that increasing sucrose concentration leads to an exponential increase in viscosity (Quintas *et al.*, 2006). It has been shown that the sucrose concentration in transport phloem can vary significantly (Peuke *et al.*, 2001, 2015; Najla *et al.*, 2010). In tomato the concentration has been reported as being between 58–350 mmol · l⁻¹ (Ho *et al.*, 1987). Nevertheless, we did not observe a decrease in phloem velocity during the day (which most likely translates to a higher sucrose concentration in phloem (Kallarackal *et al.*, 2012)). However, a similar observation was reported by Peuke *et al.* (2015) who observed a substantial increase in phloem sucrose concentration while the phloem flow velocity remained approximately constant (in combination with a decrease in phloem volume flow and FCA).

Additional sieve tubes activated under higher source strength

Our results (Fig. 2.2 and 2.3) revealed an increase of up to 300% phloem volume flow under higher light intensity (i.e., higher source strength). Interestingly, this increase in flow under higher light intensity was accompanied by an increase in phloem flow conducting area, not in phloem flow velocity. Phloem FCA could possibly be affected by various processes, such as plant growth (*cf.* Fig. 2.2 and 2.3: plants with different leaf area and clearly different FCA), sieve elements (SE) elasticity, exchange of phloem sap

between SE and CC or activation of additional vessels. We can discount growth as a possible influencing factor given the relatively short time frame over which our experiment was conducted and a decrease in FCA was also observed in reverse order of light intensities (Fig. 2.3). SE elasticity is also unlikely to have a major effect on the change in FCA because the SE elastic modulus is rather low (Hölttä *et al.*, 2006) and it cannot explain an increase by a factor of two or higher in FCA. As we concluded earlier, exchange made no significant contribution either (Materials & Methods, S1 in online supporting materials). We therefore have to conclude that the increased amount of phloem sap was transported in sieve tubes which, apparently, previously were not functional. This phenomenon of activation of additional sieve tubes would seem to occur diurnally to accommodate the higher volume flow rates that are translocated during the day as compared to the night. On top of this diurnal FCA fluctuation, additional sieve tubes are also activated under higher light conditions. It thus would appear that the activation of inactive sieve tubes to accommodate larger volumes of flow may be a common occurrence in tomato: the plant apparently is able to regulate sieve tube conductivity as required.

Conclusions

Under higher light conditions, we observed greater amounts of phloem sap being transported towards the roots. Light intensity appears to have no effect on average phloem flow velocity. Under all light intensities, phloem flow velocity alternated diurnally between $0.24 \pm 0.03 \text{ mm} \cdot \text{s}^{-1}$ during the day and $0.20 \pm 0.01 \text{ mm} \cdot \text{s}^{-1}$ at night.

The increased phloem volume flow, at higher source strength, was accompanied with higher flow conducting area. We conclude that the higher phloem flow is accommodated in sieve tubes which were not conducting under lower source strength. The activation of those sieve tubes is a direct response to higher source strength which occurs both diurnally as well as in optimal conditions. Our results suggest that tomato plants are able to activate individual sieve tubes when needed. This indicates that phloem flow is regulated locally on a per-sieve tube basis. However, if phloem transport is regulated to be maintained at constant velocity (as emerged from this study), phloem is ultimately a bottle neck to higher productivity due to the finite number of sieve tubes available for photo-assimilates transport.

2.6. Acknowledgements

This research is financed in part by the BioSolar Cells open innovation consortium, supported by the Dutch Ministry of Economic Affairs, Agriculture and Innovation. Herbert van Amerongen and Peter M. Bourke are acknowledged for critical reading of the manuscript.

2.7. References

- Adams III WW, Cohu CM, Amiard V, Demmig-Adams B. 2014.** Associations between the acclimation of phloem-cell wall ingrowths in minor veins and maximal photosynthesis rate. *Frontiers in Plant Science* **5**: 24.
- Amiard V, Demmig-Adams B, Mueh KE, Turgeon R, Combs AF, Adams WW. 2007.** Role of light and jasmonic acid signaling in regulating foliar phloem cell wall ingrowth development. *New Phytologist* **173**: 722–731.
- Björkman O, Holmgren P. 1963.** Adaptability of the photosynthetic apparatus to light intensity in ecotypes from exposed and shaded habitats. *Physiologia Plantarum* **16**: 889–903.
- Borisjuk L, Rolletschek H, Neuberger T. 2012.** Surveying the plant's world by magnetic resonance imaging. *The Plant Journal*. **70**: 129–46.
- De Schepper V, De Swaef T, Bauweraerts I, Steppe K. 2013.** Phloem transport: a review of mechanisms and controls. *Journal of Experimental Botany* **64**: 4839–50.
- Farrar JF. 1996.** Sinks-integral parts of a whole plant. *Journal of Experimental Botany* **47 Spec No**: 1273–9.
- Faticchi S, Leuzinger S, Körner C. 2014.** Moving beyond photosynthesis: From carbon source to sink-driven vegetation modeling. *New Phytologist* **201**: 1086–1095.
- Fisher DB. 1978.** An Evaluation of the Munch Hypothesis for Phloem Transport in Soybean. *Planta* **28**: 25–28.
- Froelich DR, Mullendore DL, Jensen KH, Ross-Elliott TJ, Anstead JA, Thompson GA, Péliissier HC, Knoblauch M. 2011.** Phloem ultrastructure and pressure flow: sieve-element-occlusion-related agglomerations do not affect translocation. *The Plant Cell* **23**: 4428–45.
- Grimmer C, Komor E. 1999.** Assimilate export by leaves of *ricinus communis* L. growing under normal and elevated carbon dioxide concentrations: the same rate during the day, a different rate at night. *Planta* **209**: 275–81.
- Hackel A, Schauer N, Carrari F, Fernie AR, Grimm B, Kühn C. 2006.** Sucrose transporter LeSUT1 and LeSUT2 inhibition affects tomato fruit development in different ways. *The Plant Journal* **45**: 180–192.

- Hall SM, Baker DA, Milburn JA. 1971.** Phloem transport of ^{14}C -labelled assimilates in *Ricinus*. *Planta* **100**: 200–207.
- Hartt CE. 1967.** Effect of moisture supply upon translocation and storage of C in sugarcane. *Plant Physiology* **42**: 338–46.
- Heuvelink E. 1997.** Effect of fruit load on dry matter partitioning in tomato. *Scientia Horticulturae* **69**: 51–59.
- Heuvelink E, Muiskool RP. 1995.** Influence of sink-source interaction on dry matter production in tomato. *Annals of botany* **75**: 381–389.
- Ho LC, Grange RI, Picken AJ. 1987.** An Analysis of the Accumulation of Water and Dry-Matter in Tomato Fruit. *Plant Cell & Environment* **10**: 157–162.
- Hölttä T, Vesala T, Sevanto S, Perämäki M, Nikinmaa E. 2006.** Modeling xylem and phloem water flows in trees according to cohesion theory and Münch hypothesis. *Trees - Structure and Function* **20**: 67–78.
- Homan NM, Venne B, Van As H. 2010.** Flow characteristics and exchange in complex biological systems as observed by pulsed-field-gradient magnetic-resonance imaging. *Physical Review E - Statistical, Nonlinear, and Soft Matter Physics* **82**: 1–9.
- Homan NM, Windt CW, Vergeldt FJ, Gerkema E, Van As H. 2007.** 0.7 and 3 T MRI and Sap Flow in Intact Trees: Xylem and Phloem in Action. *Applied Magnetic Resonance* **32**: 157–170.
- Jensen KH, Lee J, Bohr T, Bruus H, Holbrook NM, Zwieniecki MA. 2011.** Optimality of the Münch mechanism for translocation of sugars in plants. *Journal of the Royal Society, Interface / the Royal Society* **8**: 1155–65.
- Kallarackal J, Bauer SN, Nowak H, Hajirezaei M-R, Komor E. 2012.** Diurnal changes in assimilate concentrations and fluxes in the phloem of castor bean (*Ricinus communis* L.) and tansy (*Tanacetum vulgare* L.). *Planta* **236**: 209–23.
- Kelly G, Moshelion M, David-Schwartz R, Halperin O, Wallach R, Attia Z, Belausov E, Granot D. 2013.** Hexokinase mediates stomatal closure. *The Plant Journal*. **75**: 977–88.
- Knoblauch M, Oparka K. 2012.** The structure of the phloem - still more questions than answers. *The Plant Journal*. **70**: 147–56.
- Knoblauch M, Peters WS. 2010.** Münch, morphology, microfluidics - our structural problem with the phloem. *Plant, Cell & Environment* **33**: 1439–52.
- Kockenberger W, Ki WI, Pope JM, Xia Y, Jeffrey KR, Komor E, Callaghan PT. 1997.** Planta A non-invasive measurement of phloem and xylem water flow in castor. *Planta* **201**: 53–63.
- Lemoine R, La Camera S, Atanassova R, Dédaldéchamp F, Allario T, Pourtau N, Bonnemain J-L, Laloi M, Coutos-Thévenot P, Maurousset L, et al. 2013.** Source-to-sink transport of sugar and regulation by environmental factors. *Frontiers in Plant Science* **4**: 272.

- Liesche J, Windt C, Bohr T, Schulz a., Jensen KH. 2015. Slower phloem transport in gymnosperm trees can be attributed to higher sieve element resistance. *Tree Physiology* **35**: 376–386.
- Marcelis LFM. 1996. Sink strength as a determinant of dry matter partitioning in the whole plant. *Journal of Experimental Botany* **47**, 1281–1291.
- Matsuda R, Suzuki K, Nakano A, Higashide T, Takaichi M. 2011. Responses of leaf photosynthesis and plant growth to altered source–sink balance in a Japanese and a Dutch tomato cultivar. *Scientia Horticulturae* **127**: 520–527.
- Minchin PEH, Thorpe MR. 1996. What determines carbon partitioning between competing sinks? *Journal of Experimental Botany* **47**, 1293–6.
- Minchin PEH, Thorpe MR. 2003. Using the short-lived isotope ^{14}C in mechanistic studies of photosynthate transport. *Functional Plant Biology* **30**: 831–841.
- Mitchell DE, Madore MA. 1992. Patterns of Assimilate Production and Translocation in Muskmelon (*Cucumis melo* L.): I. Diurnal Patterns. *Plant Physiology* **99**: 966–971.
- Mortimer DC. 1965. Translocation and the control of photosynthesis in sugar beet. *Canadian Journal of Botany* **43**: 269–280.
- Mullendore DL, Windt CW, Van As H, Knoblauch M. 2010. Sieve tube geometry in relation to phloem flow. *The Plant Cell* **22**: 579–93.
- Münch E. 1930. *Die Stoffbewegungen in der Pflanze*. Jena: Verlag von Gustav Fischer.
- Murchie EH, Pinto M, Horton P. 2009. Agriculture and the new challenges for photosynthesis research. *New Phytologist* **181**: 532–52.
- Najla S, Vercambre G, Génard M. 2010. Improvement of the enhanced phloem exudation technique to estimate phloem concentration and turgor pressure in tomato. *Plant Science* **179**: 316–324.
- Osorio S, Ruan Y-L, Fernie AR. 2014. An update on source-to-sink carbon partitioning in tomato. *Frontiers in Plant Science* **5**: 1–11.
- Peuke AD, Gessler A, Trumbore S, Windt CW, Homan N, Gerkema E, Van As H. 2015. Phloem flow and sugar transport in *Ricinus communis* L. is inhibited under anoxic conditions of shoot or roots. *Plant, Cell & Environment* **38**: 433–447.
- Peuke AD, Rokitta M, Zimmermann U, Schreiber L, Haase A. 2001. Simultaneous measurement of water flow velocity and solute transport in xylem and phloem of adult plants of *Ricinus communis* over a daily time course by nuclear magnetic resonance spectrometry. *Plant, Cell & Environment* **24**: 491–503.

- Peuke AD, Windt C, Van As H. 2006.** Effects of cold-girdling on flows in the transport phloem in *Ricinus communis*: is mass flow inhibited? *Plant Cell & Environment* **29**: 15–25.
- Quereix A, Dewar RC, Gaudillere JP, Dayau S, Valancogne C. 2001.** Sink feedback regulation of photosynthesis in vines: measurements and a model. *Journal of Experimental Botany* **52**: 2313–2322.
- Quintas M, Brandão TRS, Silva CLM, Cunha RL. 2006.** Rheology of supersaturated sucrose solutions. *Journal of Food Engineering* **77**: 844–852.
- Savage JA, Zwieniecki MA, Holbrook NM. 2013.** Phloem transport velocity varies over time and among vascular bundles during early cucumber seedling development. *Plant Physiology* **163**: 1409–18.
- Scheenen TW, van Dusschoten D, de Jager PA, Van As H. 2000.** Microscopic displacement imaging with pulsed field gradient turbo spin-echo NMR. *Journal of Magnetic Resonance*. **142**: 207–15.
- Sharkey PJ, Pate JS. 1976.** Translocation from leaves to fruits of a legume, studied by a phloem bleeding technique: Diurnal changes and effects of continuous darkness. *Planta* **128**: 63–72.
- Tallarek U, Vergeldt FJ, As H Van. 1999.** Stagnant Mobile Phase Mass Transfer in Chromatographic Media: Intraparticle Diffusion and Exchange Kinetics. *The Journal of Physical Chemistry B* **103**: 7654–7664.
- Tanner W, Beevers H. 2001.** Transpiration, a prerequisite for long-distance transport of minerals in plants? *Proceedings of the National Academy of Sciences of the United States of America* **98**: 9443–9447.
- Thompson M V. 2006.** Phloem: the long and the short of it. *Trends in Plant Science* **11**: 26–32.
- Thompson M V., Holbrook NM. 2003.** Scaling phloem transport: water potential equilibrium and osmoregulatory flow. *Plant, Cell & Environment* **26**: 1561–1577.
- Turgeon R. 2010.** The role of phloem loading reconsidered. *Plant Physiology* **152**: 1817–23.
- Turnbull CGN, Lopez-Cobollo RM. 2013.** Tansley review Heavy traffic in the fast lane: long-distance signalling by macromolecules. *New Phytologist* **198**: 33–51.
- Van As H. 2007.** Intact plant MRI for the study of cell water relations, membrane permeability, cell-to-cell and long distance water transport. *Journal of Experimental Botany* **58**: 743–756.
- Van As H, Scheenen T, Vergeldt FJ. 2009.** MRI of intact plants. *Photosynthesis Research* **102**: 213–22.
- van Bel AJE. 1996.** Interaction between sieve element and companion cell and the consequences for photoassimilate distribution. Two structural hardware frames with associated physiological software packages in dicotyledons? *Journal of Experimental Botany*. **47**, 1129–1140.

van Bel AJE. 2003. The phloem, a miracle of ingenuity. *Plant, Cell & Environment* **26**: 125–149.

Wardlaw IF. 1993. Sink strength: Its expression in the plant. *Plant Cell & Environment* **16**: 1029–1031.

Windt CW, Vergeldt FJ, de Jager PA, Van As H. 2006. MRI of long-distance water transport: a comparison of the phloem and xylem flow characteristics and dynamics in poplar, castor bean, tomato and tobacco. *Plant, Cell & Environment* **29**: 1715–29.

Wolswinkel P. 1984. Phloem unloading and 'sink strength': The parallel between the site of attachment of *Cuscuta* and developing legume seeds. *Plant Growth Regulation* **2**: 309–317.

2.8. Supporting information

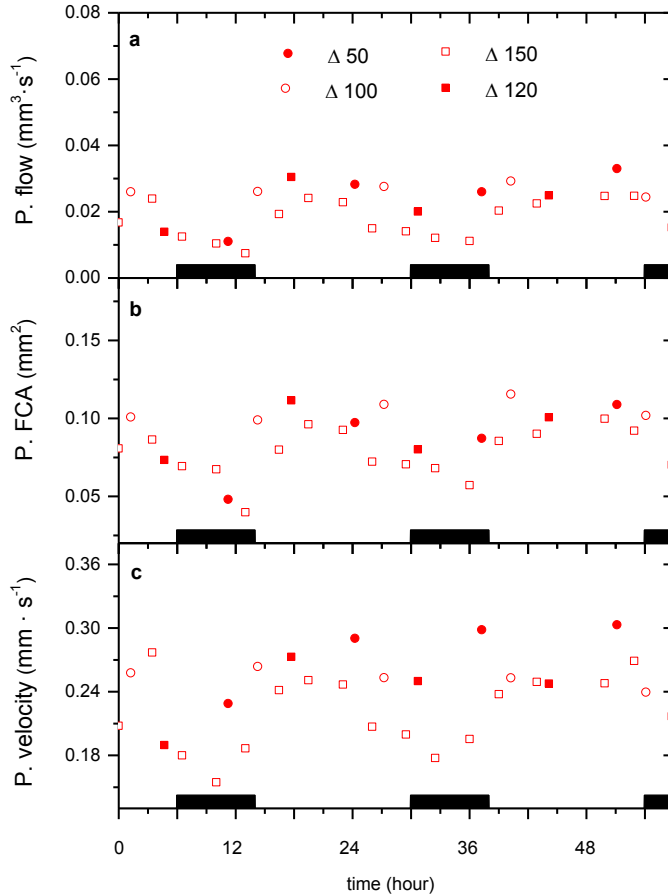


Figure S2.1: From the top of the plot: (a) phloem volume flow, (b) phloem flow conducting area (FCA), and (c) average phloem flow velocity as a function of displacement labelling times, i.e., 50, 100, 120, and 150 ms measured under light intensity of $600 \mu\text{mol} \cdot \text{m}^{-2} \cdot \text{s}^{-1}$. Black rectangles represent night-time. The FCA of all labelling times is virtually the same, albeit with some slight discrepancies caused by the calculating procedure (since labelling times other than 150 ms are not ideal for this phloem flow measurement). For different labelling times we adjusted the amplitude of the pulsed field gradients to keep the b-value constant for all measurements. However, this increases the q-value for shorter labelling times and therefore produces a higher sensitivity to noise. Nevertheless, these results confirm that leakage-retrieval has a marginal effect on measured FCA because the FCA is independent of the displacement labelling time. This experiment was conducted on a separate tomato plant which grew under the same conditions as the plants used in

this study. During the measurement, the light intensity inside of the MRI bore was $600 \mu\text{mol} \cdot \text{m}^{-2} \cdot \text{s}^{-1}$.

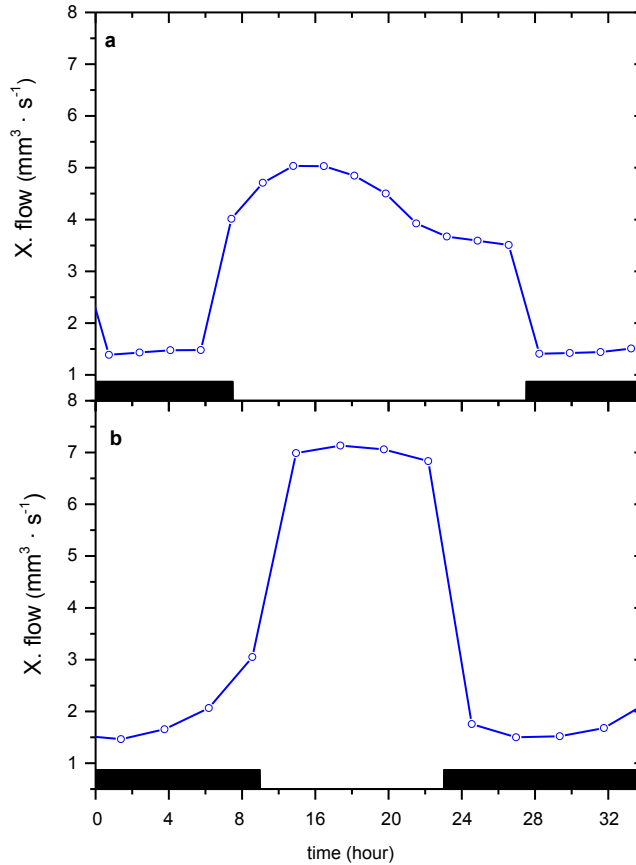


Figure S2.2: Representative xylem volume flow in a tomato plant exposed to (a) 16 hour day and (b) 10 hour day as a function of time. Black rectangles represent nighttime. Both xylem flow day profiles were measured on separate tomato plants grown under the same conditions as the plants used in this study. During both measurements, the light intensity inside of the MRI bore was $600 \mu\text{mol} \cdot \text{m}^{-2} \cdot \text{s}^{-1}$. Both presented xylem day profiles were recorded after 5 days of acclimation to the day lengths. The results depicted in this graph show that decreased xylem volume flow during the second half of the day was not observed under the shorter photoperiod of 10h.

Table S1: Photochemical yields of photosystem II for lower and upper leaves of plant after MRI experiment and control plant: the maximal yield after dark-adaptation (Φ_{\max}), the effective yield during exposure to $780 \mu\text{mol} \cdot \text{m}^{-2} \cdot \text{s}^{-1}$ (Φ_{eff}) and the yield after 30 minutes of dark-relaxation (Φ_{rel}).

Photochemical Yield (%)	Plant after MRI experiment		Control plant	
	Lower leaves	Upper leaves	Lower leaves	Upper leaves
Φ_{\max}	80 ± 1	81 ± 1	81 ± 1	81 ± 1
Φ_{eff}	6 ± 1	21 ± 1	20 ± 1	27 ± 1
Φ_{rel}	68 ± 1	80 ± 1	79 ± 1	80 ± 1

The results reveal that photosynthetic cells of leaves from the upper parts of the tomato plants, exposed to highest light intensities (in MRI, or greenhouse), have a maximal photochemical yield (Φ_{\max} in Table 1; also known as the Fv/Fm parameter) of approximately 80%. This is indicative of a vital photosynthetic apparatus. During exposure of the leaves to $780 \mu\text{mol} \cdot \text{m}^{-2} \cdot \text{s}^{-1}$ of white light the effective photochemical yield (Φ_{eff} in Table 1) decreases to 20–30%, due to the dissipation of excess energy via a protection mechanism called non-photochemical quenching (NPQ). After the light has been switched off and dark-relaxation takes place, photosystems recover and photochemical efficiency increases again to 80% within 30 minutes (Φ_{rel} in Table 1). However, for leaves of the lower parts of the plant, recovery after exposure to $780 \mu\text{mol} \cdot \text{m}^{-2} \cdot \text{s}^{-1}$ of white light is not complete within 30 minutes ($\Phi_{\text{rel}} = 70\%$). This is most likely due to the fact that leaves from the lower parts of the plant were acclimated to relatively low light intensities as a result of shadowing by upper leaves, and therefore showed more photo-inhibition in a PAM experiment. We can conclude that the plant was in perfect condition and not experiencing any light-stress at intensities of up to $780 \mu\text{mol} \cdot \text{m}^{-2} \cdot \text{s}^{-1}$.



Effect of photoperiod on xylem and phloem sap transport in tomato

Alena Prusova, Bart A.E. Van de Wal, Veerle De Schepper, Frank J. Vergeldt,
Edo Gerkema, Kathy Steppe, Henk Van As

3.1. Summary

The dynamic nature of phloem flow, one of the major determinants of plant growth, has yet to be fully understood. In this study we shed light on phloem transport under different photoperiods using simultaneous monitoring of phloem and xylem flow with magnetic resonance imaging (MRI), xylem sap flow rate with a heat balance sap flow sensor, as well as monitoring stem diameter changes and leaf photosynthesis. The resulting unique dataset revealed that phloem volume flow exhibited a diurnal pattern under both short (8 h) and normal (16 h) photoperiod. During short photoperiods, the night-time phloem volume flow decreased as a result of a lower number of active sieve tubes while maintaining a constant average phloem flow velocity. This decrease in night-time phloem volume flow correlated well with a simultaneous decrease in leaf dark respiration and stem growth retardation. Furthermore, our integrated approach gave us for the first time a detailed overview of both phloem and xylem flow dynamics and their interaction under a range of environmental conditions (short photoperiod, but also drought and continuous light), providing interesting insights on the plant's reaction to such challenging circumstances.

3.2. Introduction

A plant's growth and development rely on long distance transport and distribution of water and nutrients. This long distance transport is accommodated in vascular tissue, which consists of two parallel pathways: xylem and phloem. Xylem transport takes place in xylem vessels or tracheids, and is responsible for the transport of water and nutrients from the roots into the aerial parts of the plant. Phloem transport is accommodated in sieve tubes and distributes photo-assimilates from source to sink tissues (van Bel *et al.*, 2002; van Bel, 2003a; De Schepper *et al.*, 2013). Phloem transport is one of the major determinants of plant growth and therefore its thorough understanding may help in optimising plant growth conditions in order to increase crop yield. However, our current understanding of phloem transport is far from complete (Thompson, 2006; Hubeau & Steppe, 2015).

Although hypotheses about xylem and phloem transport mechanisms exist for almost a century (i.e., cohesion tension theory and Munch pressure flow), the measurement of both, but particularly phloem transport, has remained experimentally elusive (Minchin & Thorpe, 2003; Borisjuk *et al.*, 2012; De Schepper

et al., 2013; Hubeau & Steppe, 2015). The major drawback of most reported techniques lies in their invasiveness, which can precipitate an immediate defence reaction in the phloem transport pathway or may lead to embolism within xylem conduits. To avoid systematic errors due to such manipulations, it is advisable to use the least invasive techniques. Some examples of techniques suitable to measure phloem or xylem flow are radioactive-label (^{11}C or ^{14}C) tracking (Minchin & Thorpe, 2003), some heat based techniques (Vandeghehuchte & Steppe, 2013), fluorescent dye tracking (Jensen *et al.*, 2011; Froelich *et al.*, 2011) or non-invasive magnetic resonance imaging (MRI) flowmetry (Kockenberger *et al.*, 1997; Van As, 2007). Both heat-based techniques and MRI do not directly detect transport of photo-assimilates, but mainly water (Hubeau & Steppe, 2015). However, the simultaneous measurement of phloem water transport velocity (measured with MRI) and transport velocity of a fluorescent dye (5(6)-carboxyfluorescein which could be seen as a proxy for sucrose) showed comparable velocities (Windt CW, Savage J, Knoblauch M, Holbrook M, Van As H, Unpublished results).

That said, no comprehensive technique for phloem flow measurement has been developed and therefore we propose that an integrated approach is needed to reveal more about phloem transport (Van As & van Duynhoven, 2013). Such an integrated approach implies a simultaneous measurement of both phloem transport and other relevant parameters like for example xylem flow, photosynthesis and stem diameter variations. An integrated approach also strives to use non-invasive techniques like for example MRI, sap flow sensors using external heating, branch bags or cuvettes connected to an infrared gas analyser, and stem diameter variation sensors. Such simultaneous data acquisition of a single plant has the potential to provide unique insights, and could for example shed light on phloem-xylem interaction which remains an understudied field (Hubeau & Steppe, 2015).

Recently it has been reported that in tomato, basipetal phloem volume flow exhibits a diurnal pattern with higher values during the day compared to the night (Chapter 2). Some evidence for diurnal pattern of phloem volume flow had already been reported in earlier studies on tomato (Windt *et al.*, 2006) and castor bean (Peuke *et al.*, 2001) although not as clearly nor as prolonged as demonstrated in Chapter 2. The diurnal phloem volume flow pattern was observed in a simplified system, i.e., an adult tomato plant with pruned trusses. This raises the question whether basipetal phloem volume flow still performs diurnal pattern under more

common conditions, i.e., with the presence of strong sinks like tomato fruit trusses? If so, is this basipetal phloem volume flow alternation caused by an excess of photo-assimilates due to normal photoperiods (16 h), and would this diurnal pattern disappear under shorter photoperiods? In order to answer these questions, we measured basipetal phloem volume flow in an adult tomato plant (bearing unripe fruits) with MRI under normal (16 h) and short (8 h) photoperiod. To obtain a comprehensive view, we simultaneously measured xylem volume flow with MRI and with heat balance sap flow sensors, as well as stem diameter variations, leaf photosynthesis and transpiration on the same plant, and monitored air relative humidity and temperature.

3.3. Materials and Methods

The experiments were conducted on a three-month-old potted tomato plant (*Solanum lycopersicum* cv. 'GT'). Tomato plants are both an important crop (world production of 164 M tones in 2013 (FAOSTAT)) and are well suited for MRI measurements. MRI measurements were conducted on the tomato main stem, about 25 cm from the soil surface. Therefore the lower leaves were removed two days prior to the start of the experiment (to obtain 25 cm of bare stem). The plant was inserted in the MRI scanner two days prior to the start of the measurements to acclimatise. We conducted a replicate of the experiment on another plant of the same age.

Plant material and microclimate conditions

Plants were grown in a greenhouse during the summer months in 15-L pots with standard compost potting mixture under the following conditions: day ca. 70 % relative humidity and 16h days. In the MRI scanner the following conditions were applied: day 24 °C, 600 $\mu\text{mol PAR m}^{-2} \text{s}^{-1}$, and night 20 °C. In the MRI scanner the plants were watered daily (at 3 a.m., 9 a.m., 3 p.m., and 9 p.m.) with in total 400 mL/day (day 1–4) and 300 mL/day (from day 5 onwards). The photoperiod was adjusted according to Table 1. The plant remained inside the MRI scanner for the entire duration of the experiment. Air temperature was measured below all leaves. Light intensity was measured in the uppermost part of the plant. The total leaf area of the plant used in the experiment was 0.722 m², and leaf area of the plant used for the replicate was 0.994 m².

Table 1. : Photoperiod length (in hours)

Day of experiment	1	2	3	4	5	6	7
Photoperiod (h)	16	16	8	8	8	16	16

MRI measurements

Phloem and xylem (sap) flow was measured with a MRI scanner, consisting of a vertically-orientated superconducting magnet with a 50 cm vertical free bore (Magnex, Oxford, UK). The light source inside the MRI scanner was a dedicated LED module built to function inside a strong magnetic field with an adjustable light intensity up to $2750 \mu\text{mol PAR} \cdot \text{m}^{-2} \cdot \text{s}^{-1}$ at 40 cm distance. For induction and detection of the MRI signal, a bird cage RF coil of 4 cm diameter was used inside of a 1 T/m gradient set (Bruker, Karlsruhe, Germany) controlled with Avance console (Bruker, Karlsruhe, Germany); for details see Homan *et al.*, (2007).

A pulsed field gradient turbo spin echo (PFG-TSE) sequence (Scheenen *et al.*, 2000) was used to measure sap displacement. For every pixel we obtained a displacement spectrum, the propagator (Scheenen *et al.*, 2000). This propagator was analysed with an approach described elsewhere (Scheenen *et al.*, 2000; Windt *et al.*, 2006; Van As, 2007) and resulted in the following parameters per pixel: volume flow, amount of stationary water, flow conducting area (FCA) and average flow velocity. Flow measurements were carried out using the following imaging parameters: imaging matrix = 128×128 pixels, field of view = $22 \times 22 \text{ mm}^2$, slice thickness = 3 mm, echo time = 5 ms and spectral width = 50 kHz. For the xylem measurements the specific parameters were: turbo factor = 16, number of averages = 2, repetition time = 2500 ms, displacement labelling time = 20 ms, gradient duration = 4 ms, maximum gradient strengths = $400 \text{ mT} \cdot \text{m}^{-1}$, 48 gradient steps and acquisition time = 32 min. For the phloem measurements the parameters were: turbo factor = 8, averages = 4, repetition time = 2000 ms, labelling time = 150 ms, gradient duration = 3 ms, maximum gradient strengths = $200 \text{ mT} \cdot \text{m}^{-1}$, 32 gradient steps and acquisition time = 68 min. We alternated between both xylem and phloem measurement. Data analysis was performed with IDL (ITT Visual Information Solutions, Bolder, Colorado, USA) using in-house processing, fitting, and quantification routines.

Measurement of net photosynthesis and transpiration

The net rate of photosynthesis was continuously measured with an infrared gas analyser (IRGA) (LI7000, Licor, Lincoln, Nebraska USA). One branch bag per tomato plant was installed on a first order branch. Branch bags of approximately 8 L contained a leaf area of 400 cm² (an average from both experiments) and were made of low density polyethylene to avoid CO₂ diffusion. Air from the temperature- and humidity-controlled laboratory room was blown into the branch bag at a rate of 3.5 L min⁻¹. Before entering the branch bag, the air passed through a plastic barrel of 100 L to level out fluctuations in CO₂ concentration and to eliminate pressure fluctuations induced by the pump. A programmable logic unit (S7-200, Siemens, Brussels, Belgium) controlled the gas multiplex system, which was used to sample the branch bag during sample periods of 10 minutes and logging frequency of 1 minute. During each sample period, the incoming and outgoing air of the branch bag were continuously measured, but only the stable readings during the last three minutes were averaged and used for calculations. After every two sample periods, a zero measurement was carried out to detect possible drifts in the zero point reading of the IRGA. The net photosynthesis during the light period is then equal to the amount of CO₂ depleted, while dark respiration can be determined as the amount of CO₂ produced during the dark period.

Measurement of xylem sap flow with heat balance

Sap flow rates were measured with sap flow sensors based on the heat balance principle (SGA10, Dynamax Inc., Houston, USA). Two sensors per tomato plant were installed according to the installation manual (van Bavel & van Bavel, 1990) on the main stem at different heights: at 9 cm and 83 cm. Sheath conductance of the gauge was calculated using the overall minimum value observed during the dark periods. The value for the thermal conductance of herbaceous stems of 0.54 W · m⁻¹ · °C⁻¹ was taken from Steinberg *et al.*, (1989).

Measurement of stem diameter variations

One linear motion potentiometer (DDS, Ecomatik, Dachau/Munich, Germany) was installed 55 cm above the soil surface on the main stem using a custom-made, temperature-independent (Steppe & Lemeur, 2004) stainless steel holder. The sensor measured the diameter change of the stem relative to the diameter at the beginning of the measurement campaign.

Data acquisition

All signals from the online sensors were logged at 10 s intervals and 5 min means were stored using a data logger (CR1000, Campbell scientific, Logan, Utah, USA), except for the IRGA measurements for which 1 min means were stored.

3.4. Results

The applied combination of plant sensors produced a very complementary dataset, describing the plant's responses to the manipulation of environmental factors affecting its productivity. During the two days before and after the short photoperiod treatment, the plant showed normal behaviour, i.e., xylem sap flow and transpiration reached maximum values during the day and minimal values at night (Fig. 3.1 a, b, c and S1 in supplementary data), and the stem diameter showed a growing trend superimposed on a typical day/night shrinking/swelling pattern (Fig. 3.1 f). The basipetal phloem volume flow exhibited a diurnal dynamic with higher values during the day and lower values at night (Fig. 3.1). The trends in xylem sap volume flow measured with magnetic resonance imaging (MRI) and xylem sap flow rates measured with heat balance (HB) agreed well (Fig. 3.1 a, b). However, HB has the advantage of higher temporal resolution compared to MRI, and can therefore provide a more detailed picture of the xylem sap flow pattern. The xylem pattern during the normal day showed a decrease in the second half of the light period.

Effect of short photoperiod

During day 3 of the experiment, the plant experienced a late 'dawn' followed by an early 'dusk'. Towards the end of the first prolonged night, and during the following two nights, the xylem volume flow and transpiration began to increase at the expected time of the 'dawn' (Fig. 3.1 a, b, c). This increase in transpiration and xylem flow at expected 'dawn' demonstrates the circadian control of stomatal aperture (Haydon *et al.*, 2011). Surprisingly, a similar effect was also observed in phloem volume flow where at the expected 'dawn', the basipetal phloem volume flow increased and then decreased again. During the normal (16 h) days, the phloem velocity and phloem FCA performed diurnal pattern between higher average values of $0.26 \pm 0.03 \text{ mm} \cdot \text{s}^{-1}$ and $0.039 \pm 0.004 \text{ mm}^2$ during the day and lower average values of $0.21 \pm 0.01 \text{ mm} \cdot \text{s}^{-1}$ and $0.033 \pm 0.002 \text{ mm}^2$ at night (Fig. 3.2 a, b). During the short photoperiod, the phloem flow velocity diurnal pattern was significantly affected although its values remained within well-defined boundaries.

In comparison to the normal days, the average night velocity decreased by 5 % and the average day velocity decreased by 10 %. Unlike the phloem flow velocity, the FCA diurnal pattern remained visible although its values overall decreased. The average night FCA decreased by 60 % and the average day FCA decreased by 5 %. Following the short photoperiod treatment both phloem flow velocity and FCA returned to values similar to those 'normal' day-values already observed during the first two days of the experiment.

During the first prolonged night (Fig. 3.3 day 3), dark respiration decreased towards the end of the dark period. This decrease was even more pronounced during the second prolonged night (Fig. 3.3 day 4) when the plant experienced late 'dawn' after an early 'dusk'. This trend continued during the following night (Fig. 3.3 day 5). During the first 'normal' night after the treatment, the dark respiration returned to normal values observed at night after normal 16 h days. This decrease in dark respiration during the short photoperiod treatment correlated remarkably well with the decrease in night phloem volume flow (Fig. 3.3) and reduced stem growth rate (Fig. 3.1). During the short photoperiod treatment, the mean daily growth rate was 80 % lower in comparison to normal 16 h days where the mean growth rate was $48 \mu\text{m} \cdot \text{day}^{-1}$, and the latter value was reached again after the short photoperiod treatment. The replicate of the experiment showed very comparable results during the short photoperiod treatment (Fig. S3.1 and S3.2 in supporting information).

Additional observations

After the end of the short photoperiod treatment, the plant remained in MRI and we continued measuring. The plant was watered at 6-hour intervals with 100, 50, 100, and then 50 mL of water per day. This watering regime in combination with the relatively high PAR value of $600 \mu\text{mol} \cdot \text{m}^{-2} \cdot \text{s}^{-1}$ caused mild drought to develop (the plant transpired more water than it received). The effect of drought was visible on the stem diameter which started to exhibit daytime shrinkage at day 9 towards the end of the light period (Fig. 3.4 f). The effect of drought was also manifested in a decreased xylem flow towards the end of the light period. This decrease in xylem flow, in combination with the timing of the watering, resulted in a dip in the xylem flow profile due to drought-related stomatal closure (Fig. 3.4 a, b). These observations, combined with the fact that both stem diameter and xylem water flow responded to irrigation events, are a clear indication of drought (De Swaef & Steppe, 2010; De Swaef *et al.*, 2012). In phloem volume flow, drought was

manifested in an overall decrease in phloem volume flow which was first visible in FCA during day 8 and then after two more days in phloem flow velocity (Fig. 3.2). The mild drought also caused an overall decrease in maximum net photosynthesis. During day 10 we pruned all trusses on the plant to see the effect of strong sinks removal. This had a pronounced effect on basipetal phloem volume flow. The pruning resulted in an increase in basipetal phloem volume flow as well as in larger stem growth (two days following pruning the growth rate was $68 \mu\text{m} \cdot \text{day}^{-1}$) (Fig. 3.4). The increase in basipetal phloem volume flow was manifested in higher FCA but not phloem flow velocity (Fig. 3.2). In the replicate of the experiment we intended to perform exactly the same sequence of treatments, however, due to a malfunction of the lighting system, the plant experienced 72 hours of continuous light after the truss pruning (Fig. 3.5). Under continuous light the xylem flow was lower in comparison to the xylem flow under diurnal regime, yet higher than night values, such that a higher daily total was achieved. However, during the 72 hours of continuous light we observed that xylem flow gradually decreased. Both xylem flow and transpiration responded to irrigation events, which also indicate the build-up of drought during continuous lighting. On the other hand, photosynthesis and phloem volume flow responded less to irrigation events. Under continuous light, despite the response to irrigation events, the stem diameter continued to grow. However, the stem grew only at 80 % lower rate than before the short photoperiod treatment (Fig. 3.5), likely caused by drought and an inability to reach full turgidity (Steppe *et al.*, 2015).

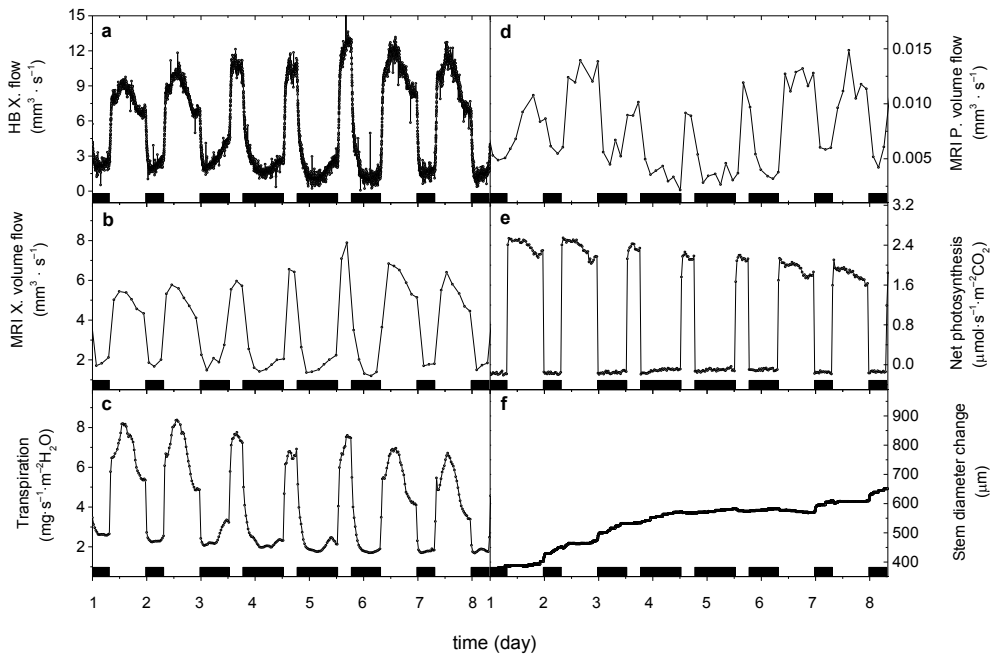


Figure 3.1: The effect of short photoperiod on (a) flow of xylem sap measured with HB, (b) and xylem volume flow measured with MRI, (c) transpiration, (d) volume flow of phloem sap measured with MRI, (e) net photosynthesis, and (f) stem diameter change, all as a function of time in days. Black rectangles represent night-time.

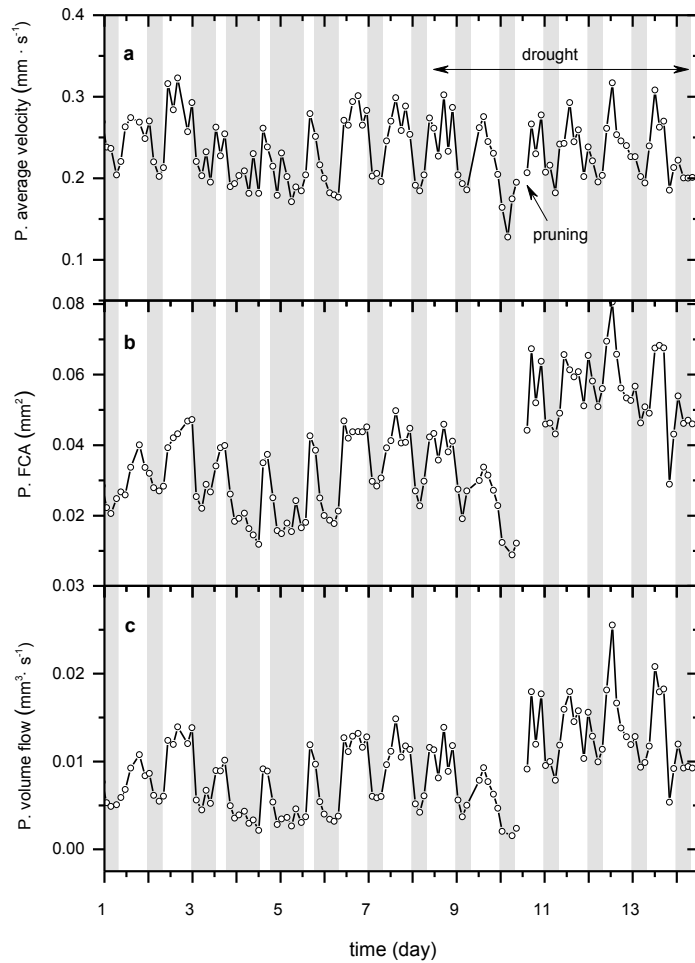


Figure 3.2: The effect of short photoperiod on (a) phloem flow average velocity, (b) phloem flow conducting area (FCA), and (c) phloem volume flow. The short photoperiod treatment is followed by developed mild drought and further combined with simultaneous effect of fruit pruning. All measured with MRI and all as a function of time in days. Grey bars represent night-time.

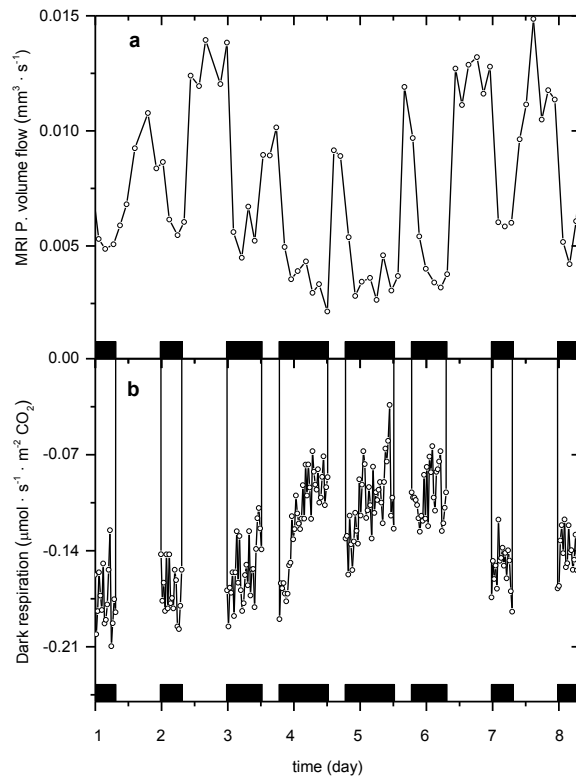


Figure 3.3: Correlation between (a) phloem volume flow and (b) dark respiration. Black rectangles represent night-time. Long nights were manifested by a decrease of both dark respiration and basipetal phloem volume flow.

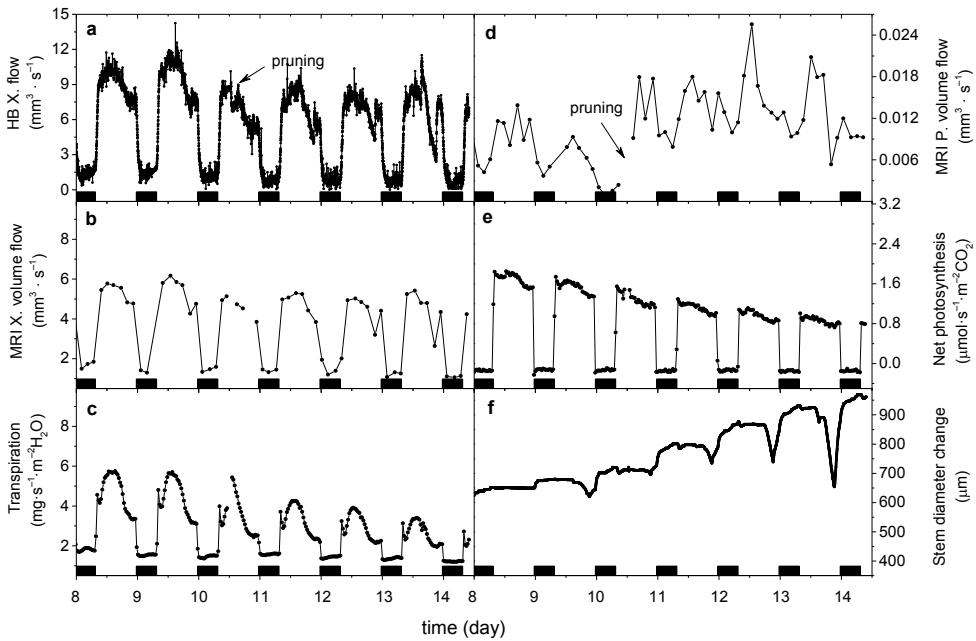


Figure 3.4: The effect of mild drought (from day 8 till the end) and pruning on (a) flow of xylem sap measured with HB, (b) and xylem volume flow measured with MRI, (c) transpiration, (d) volume flow of phloem sap measured with MRI, the arrow indicates the fruit pruning, (e) net photosynthesis, and (f) stem diameter change, all as a function of time in days. Black rectangles represent night-time. The drought manifests itself by dips in xylem flow during the day and larger shrinkages in stem diameter.

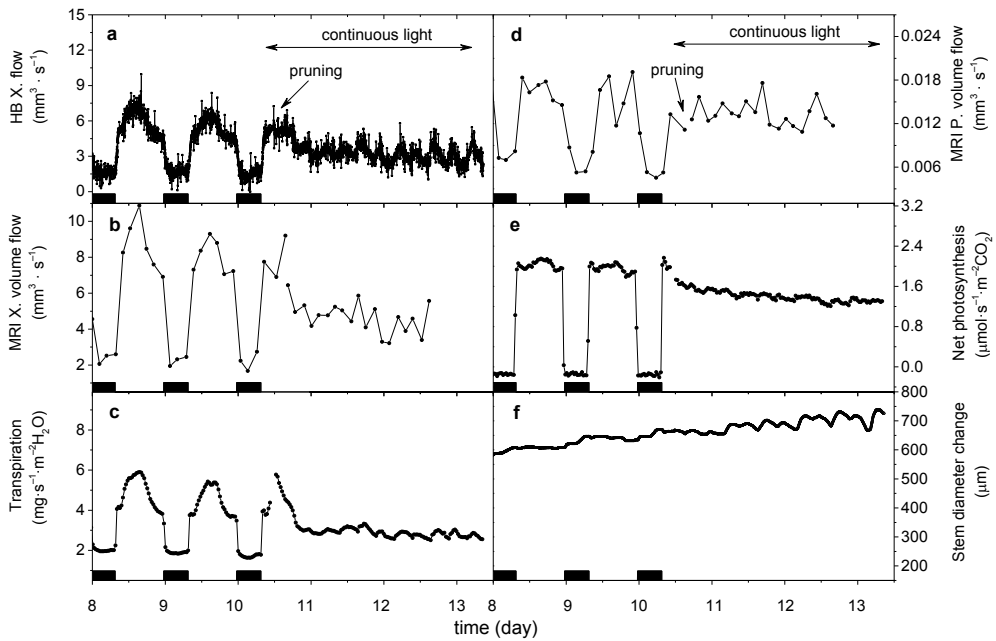


Figure 3.5: The effect of developing drought and (from day 10) pruning with simultaneous continuous light on (a) flow of xylem sap measured with HB, (b) and xylem volume flow measured with MRI, (c) transpiration, (d) volume flow of phloem sap measured with MRI, (e) net photosynthesis, and (f) stem diameter change, all as a function of time in days. Black rectangles represent night-time.

3.5. Discussion

Phloem volume flow diurnal pattern persists under both normal and altered source-sink ratio

During normal days, phloem volume flow showed a diurnal pattern between higher values during the day when compared to night (Fig. 3.1). This diurnal pattern in phloem flow was a result of the diurnal pattern of both phloem flow velocity and phloem flow conducting area as described in Chapter 2 (Fig. 3.2). Unlike that study, we used a tomato plant which carried unripe trusses (representing a strong sink), and yet we observed the diurnal pattern of basipetal phloem volume flow. The diurnal pattern of phloem volume flow persisted also during the short photoperiod which is essentially a source manipulation since the total amount of photo-assimilates produced by the source was lower. However, during the prolonged dark period the average phloem velocity increased at the expected 'dawn' which might indicate a circadian control of phloem velocity (as opposed to being directly activated by light and/or photosynthesis) (McClung, 2006).

These observations indicate that basipetal phloem volume flow pattern is a normal behaviour for tomato plants growing under higher light conditions (at ca. $600 \mu\text{mol} \cdot \text{m}^{-2} \cdot \text{s}^{-1}$). This diurnal phloem volume flow pattern with higher flow during the day is striking because it is in contradiction to modelled phloem flows which predict higher phloem flow at night (Hölttä *et al.*, 2006; De Schepper & Steppe, 2010). However, those models were developed for trees, not for herbaceous plants like tomato. The difference between the models and our observation could be due to a different mechanism in phloem loading between woody and herbaceous species (De Schepper *et al.*, 2013). On the other hand, our observation agrees with the model developed for carbon status in tomato where higher sucrose concentration in the phloem is predicted during the light period (De Swaef *et al.*, 2013).

Phloem volume flow at night correlates with dark respiration

During short photoperiods, the diurnal pattern of basipetal phloem volume flow persisted, although overall the total amount of transported phloem sap decreased, particularly at night. This overall decrease reflected the lower absolute amount of photo-assimilated carbon during the short photoperiod when compared to the

normal day. However, the basipetal phloem volume flow during the short day was less affected (on average 23 % lower than during normal days) than the basipetal volume flow at night (on average 43 % lower than at night following normal days). The lower basipetal phloem flow at night indicated less available carbohydrates for respiration and growth at night (Zeeman *et al.*, 2007). This was reflected in a decrease in dark respiration during nights following short photoperiod (Fig. 3.3) as well as in lower stem growth (Fig. 3.1) (Gibon *et al.*, 2004).

To avoid carbon starvation during 16 h long nights, the photo-assimilate partitioning between transport and transitory starch synthesis during the preceding photoperiod was most likely altered (Lemoine *et al.*, 2013). However, to compensate for such a short photoperiod, the long term carbon reserves were probably also utilised during the prolonged nights (van Bel, 2003b). The correlation between dark respiration and night phloem volume flow suggests that the transitory starch degradation and the allocation of photo-assimilates at night is only part of a highly complex and coordinated system of plant growth and survival.

Xylem and phloem are hydraulically linked; this tight relation is reflected for example in the replenishment of water for the phloem stream by the xylem stream (a fraction of the Munch's counter-flow) (Hölttä *et al.*, 2006; Windt *et al.*, 2006; De Schepper & Steppe, 2010). When we compared the xylem/phloem average volume flow ratio for individual nights, this ratio decreased by 35 % during the nights following short photoperiod. This decrease could indicate less negative water potential in phloem (due to lower sucrose concentration) and therefore less water attracted from the xylem stream.

Confirmation of phloem velocity regulation via (de)activation of sieve tubes

During the short photoperiod, the overall decrease in basipetal phloem volume flow affected both phloem flow velocity and phloem FCA. Of the two, FCA seemed to be more affected than velocity, with its night value being 60 % lower than its normal night value (Fig. 3.2) (in contrast, the FCA day value decreased less dramatically (only 5 % lower)). We observed that phloem flow velocity was less affected: its day and night values decreased only marginally (10 and 5 %, respectively) when compared to the normal days, and the overall phloem flow velocity remained within well-defined boundaries.

During the onset of drought conditions, we further observed that phloem FCA was affected earlier and to a greater extent than phloem flow velocity (Fig. 3.2 day 9 and 10). This difference in response to manipulation between phloem flow velocity and phloem FCA was even more remarkable after pruning the trusses (Fig. 3.2 day 10). Phloem FCA increased by 50 % in comparison to the values before pruning. On the other hand the phloem flow velocity remained constant (apart from the standard diurnal pattern). The pruning of fruits increases the relative root sink strength (Wardlaw, 1993) and, despite the mild drought, it increased the amount of available carbohydrates for stem and roots. Hence pruning resulted in an increase of basipetal phloem volume flow as well as in larger stem growth (Fig. 3.4). Although the drought conditions were not particularly well-controlled, we could speculate that the increase in basipetal phloem flow was partly caused by promoted root growth (Zgallai *et al.*, 2006).

Our observations support the hypothesis of Windt *et al.* (2006) and (Chapter 2) that phloem volume flow is regulated to maintain a constant phloem velocity and any requirement for accommodating higher or lower amounts of translocated phloem sap is realised by regulating the number of active phloem sieve tubes (Chapter 2). An increased number of conducting sieve tubes would decrease hydraulic resistance, and a lower number would increase the resistance (Hall & Minchin, 2013), and therefore it could be a mechanism to maintain constant phloem flow velocity and compensate for viscosity fluctuations caused by fluctuating sucrose concentration. Since we did not measure gene expression of sucrose transporters (which also have a diurnal character (Hackel *et al.*, 2006)) we can only speculate that the sieve tubes are activated or deactivated by an elevated or decreased sucrose concentration, respectively.

Feedback regulation

During the normal 16 h days we observed lower values in the second half of the light period (namely after 11 hours of light) in xylem flow, transportation and net photosynthesis. This is not to be confused with the phenomenon of ‘mid-day depression’, where plants exposed to full sunlight partially close their stomata during the hottest period of the day which could lead to a dip in the xylem flow profile (Roessler & Monson, 1985). Under constant vapour pressure deficit (VPD), xylem flow is predominantly regulated by stomatal conductance (Damour *et al.*, 2010). The factors which influence the opening of stomata include light, plant water status, abscisic acid and CO₂ concentration (Tardieu *et al.*, 2015). In our

experiment, the light intensity remained constant during the entire day and the CO₂ levels remained relatively constant too. On the other hand, the plant water status was changing and mild drought developed during the experiment. However, this afternoon decrease was also observed in the beginning of the experiment, when the plant was still well-watered. Therefore, at least at the beginning of the experiment and under constant temperature and relative humidity one would expect the xylem flow profile to display an approximately rectangular shape (Steppe & Lemeur, 2004). Since this afternoon decrease was also observed in net photosynthesis (Fig. 3.1) we suspect that this phenomenon might be caused by a filling of the carbon storage pools (the transitory starch stored in chloroplasts), reflecting photosynthesis feedback regulation resulting in its inhibition (Kelly *et al.*, 2013), although further experiments might be needed to confirm this. In contrast to the normal 16 h photoperiod, the xylem afternoon decrease was not observed during the shorter photoperiod treatment (Fig. 3.1, Fig. S3.1 in supporting information). This observation also supports our hypothesis, since this would mean that during the short days, photosynthesis feedback regulation did not occur due the shorter time-period of photosynthesis, i.e., 8 hours, whereas the feedback regulation in long days was only observed after 11 hours.

Further discussion

During the whole experiment, the stem diameter showed growth and a typical day/night shrinking/swelling pattern (Fig. 3.1 f) (De Swaef & Steppe, 2010). During mild drought the stem diameter responded to irrigation events (De Swaef *et al.*, 2012), and showed drought dips, which coincided with the progression of the drought. Those dips earlier in the experiment indicated that the plant was using water storage pools to sustain full transpiration. As drought developed, the water storage pools were depleted (and were less refilled at night) and therefore the deficiency of water was also observed in xylem flow in the form of dips at the end of the light period (Fig. 3.4 day 11–14). Despite the water limitation, the stem diameter still increased. This observation is striking in comparison to the lower growth rate during the short photoperiod treatment. During that period the plant was well-watered and therefore, at night, a more sustained build-up of turgor could take place, potentially resulting in increased growth. Since this was not observed, the short photoperiod treatment probably led to a decreased availability in photo-assimilates and thus stem growth. While these observations could lead

one to speculate that a shortage in photo-assimilates has a greater effect on growth than mild drought, it should be noted that the fruits were removed before the drought. Had these strong sinks still been on the plant, drought might have had a more pronounced effect on the stem growth (De Swaef & Steppe, 2010). Likewise, if the plants were pruned before the short photoperiod, stem growth would probably have been hindered to a lesser extent due to less competition for photo-assimilates.

It has long been known that in tomato, continuous light has a damaging effect which is manifested for example by mottled leaf chlorosis and necrosis (Arthur *et al.*, 1930). In our experiment the plant experienced 72 hours of continuous light, but by the end of the experiment we had not observed any obvious visual damage. However, 72 hours was probably too short a period to observe any damage. During those 72 hours all normal physiological processes persisted (i.e., plant transpiration, photosynthesis and growth). The combination of relatively high light intensity and drought seemed to affect xylem flow and transpiration to a greater extent than phloem volume flow and net photosynthesis. During continuous light, both xylem and transpiration responded to irrigation events manifesting the effect of the drought. The photosynthesis and phloem volume flow persisted and the aggregated amount over 24 h was higher than during the normal diurnal period, consistent with the higher yields observed under such conditions in a continuous light-tolerant tomato line (Velez-Ramirez *et al.*, 2014).

Concluding remarks

Employing a unique combination of plant sensors and MRI flowmetry, we were able to quantify both xylem and phloem flow *in vivo*, as well as their main driving forces, being photosynthesis and transpiration. Through this setup, we discovered that basipetal phloem volume flow exhibits a diurnal pattern under normal conditions, i.e., with strong sinks (tomato fruits) still growing on the plant. This pattern was observed under both normal (16 h) as well as short (8 h) photoperiod and was likely achieved by (de)activating individual sieve tubes to maintain a constant phloem flow velocity. Therefore, we can conclude that a diurnal pattern in the basipetal phloem volume flow is normal behaviour for tomato plants growing under higher light conditions (at ca. $600 \mu\text{mol} \cdot \text{m}^{-2} \cdot \text{s}^{-1}$). Additionally, our combination of measurements shed light on simultaneous processes and revealed for the first time the correlation between dark respiration, night-time phloem volume flow and retardation of the stem growth during short photoperiods.

3.6. Acknowledgements

This research is financed in part by the BioSolar Cells open innovation consortium, supported by the Dutch Ministry of Economic Affairs, Agriculture and Innovations. The authors would also like to thank Flanders Innovation & Entrepreneurship (VLAIO) for the PhD grant for the second author. Ep Heuvelink and John Philippi are acknowledged for technical support.

3.7. References

- Arthur JM, Guthrie JD, Newell JM. 1930. Some effects of artificial climates on the growth and chemical composition of plants. *American Journal of Botany* **17**: 416–482.
- Borisjuk L, Rolletschek H, Neuberger T. 2012. Surveying the plant's world by magnetic resonance imaging. *The Plant Journal* **70**: 129–46.
- Damour G, Simonneau T, Cochard H, Urban L. 2010. An overview of models of stomatal conductance at the leaf level. *Plant, Cell & Environment* **33**: 1419–1438.
- De Schepper V, Steppe K. 2010. Development and verification of a water and sugar transport model using measured stem diameter variations. *Journal of Experimental Botany* **61**: 2083–99.
- De Schepper V, De Swaef T, Bauweraerts I, Steppe K. 2013. Phloem transport: a review of mechanisms and controls. *Journal of Experimental Botany* **64**: 4839–50.
- De Swaef T, Driever SM, Van Meulebroek L, Vanhaecke L, Marcelis LFM, Steppe K. 2013. Understanding the effect of carbon status on stem diameter variations. *Annals of Botany* **111**: 31–46.
- De Swaef T, Steppe K. 2010. Linking stem diameter variations to sap flow, turgor and water potential in tomato. *Functional Plant Biology* **37**: 429–438.
- De Swaef T, Verbist K, Cornelis W, Steppe K. 2012. Tomato sap flow, stem and fruit growth in relation to water availability in rockwool growing medium. *Plant and Soil* **350**: 237–252.
- FAOSAT. 2013. <http://faostat.fao.org/>
- Froelich DR, Mullendore DL, Jensen KH, Ross-Elliott TJ, Anstead JA, Thompson GA, Pélissier HC, Knoblauch M. 2011. Phloem ultrastructure and pressure flow: Sieve-Element-Occlusion-Related agglomerations do not affect translocation. *The Plant Cell* **23**: 4428–45.
- Gibon Y, Bläsing OE, Palacios-Rojas N, Pankovic D, Hendriks JHM, Fisahn J, Höhne M, Günther M, Stitt M. 2004. Adjustment of diurnal starch turnover to short days: depletion of sugar during the night leads to a temporary inhibition of carbohydrate utilization, accumulation of sugars and post-translational activation of ADP-glucose pyrophosphorylase in the followin. *The Plant Journal* **39**: 847–62.
- Hackel A, Schauer N, Carrari F, Fernie AR, Grimm B, Kühn C. 2006. Sucrose transporter LeSUT1 and LeSUT2 inhibition affects tomato fruit development in different ways. *The Plant Journal* **45**: 180–192.

- Hall AJ, Minchin PEH. 2013. A closed-form solution for steady-state coupled phloem/xylem flow using the Lambert-W function. *Plant, Cell & Environment* **36**: 2150–2162.
- Haydon MJ, Bell LJ, Webb A a R. 2011. Interactions between plant circadian clocks and solute transport. *Journal of Experimental Botany* **62**: 2333–48.
- Hölttä T, Vesala T, Sevanto S, Perämäki M, Nikinmaa E. 2006. Modeling xylem and phloem water flows in trees according to cohesion theory and Münch hypothesis. *Trees - Structure and Function* **20**: 67–78.
- Homan NM, Windt CW, Vergeldt FJ, Gerkema E, Van As H. 2007. 0.7 and 3 T MRI and Sap Flow in Intact Trees: Xylem and Phloem in Action. *Applied Magnetic Resonance* **32**: 157–170.
- Hubeau M, Steppe K. 2015. Plant-PET Scans: In Vivo Mapping of Xylem and Phloem Functioning. *Trends in Plant Science* **20**: 676–685.
- Jensen KH, Lee J, Bohr T, Bruus H, Holbrook NM, Zwieniecki MA. 2011. Optimality of the Münch mechanism for translocation of sugars in plants. *Journal of the Royal Society, Interface / the Royal Society* **8**: 1155–65.
- Kelly G, Moshelion M, David-Schwartz R, Halperin O, Wallach R, Attia Z, Belausov E, Granot D. 2013. Hexokinase mediates stomatal closure. *The Plant Journal* **75**: 977–88.
- Kockenberger W, Ki WI, Pope JM, Xia Y, Jeffrey KR, Komor E, Callaghan PT. 1997. Planta A non-invasive measurement of phloem and xylem water flow in castor. *Planta* **201**: 53–63.
- Lemoine R, La Camera S, Atanassova R, Dédaldéchamp F, Allario T, Pourtau N, Bonnemain J-L, Laloi M, Coutos-Thévenot P, Maurousset L, *et al.* 2013. Source-to-sink transport of sugar and regulation by environmental factors. *Frontiers in Plant Science* **4**: 272.
- McClung CR. 2006. Plant Circadian Rhythms. *The Plant Cell* **18**: 792–803.
- Minchin PEH, Thorpe MR. 2003. Using the short-lived isotope ^{11}C in mechanistic studies of photosynthate transport. *Functional Plant Biology* **30**: 831–841.
- Peuke AD, Rokitta M, Zimmermann U, Schreiber L, Haase A. 2001. Simultaneous measurement of water flow velocity and solute transport in xylem and phloem of adult plants of *Ricinus communis* over a daily time course by nuclear magnetic resonance spectrometry. *Plant, Cell & Environment* **24**: 491–503.
- Roessler PG, Monson RK. 1985. Midday depression in net photosynthesis and stomatal conductance in *Yucca glauca*. *Oecologia* **67**: 380–387.
- Scheenen TW, van Dusschoten D, de Jager PA, Van As H. 2000. Microscopic displacement imaging with pulsed field gradient turbo spin-echo NMR. *Journal of Magnetic Resonance* **142**: 207–15.
- Steinberg S, van Bavel C, McFarland M. 1989. A gauge to measure mass flow rate of sap in stems and trunks of woody plants. *Journal of the American Society for Horticultural Science* **114**: 466–472.
- Steppe K, Lemeur R. 2004. An experimental system for analysis of the dynamic sap-flow characteristics

in young trees: Results of a beech tree. *Functional Plant Biology* **31**: 83–92.

Steppe K, Sterck F, Deslauriers A. 2015. Diel growth dynamics in tree stems: Linking anatomy and ecophysiology. *Trends in Plant Science* **20**: 335–343.

Tardieu F, Simonneau T, Parent B. 2015. Modelling the coordination of the controls of stomatal aperture, transpiration, leaf growth, and abscisic acid: update and extension of the Tardieu–Davies model. *Journal of Experimental Botany* **66**: 2227–2237.

Thompson M V. 2006. Phloem: the long and the short of it. *Trends in Plant Science* **11**: 26–32.

Van As H. 2007. Intact plant MRI for the study of cell water relations, membrane permeability, cell-to-cell and long distance water transport. *Journal of Experimental Botany* **58**: 743–756.

Van As H, van Duynhoven J. 2013. MRI of plants and foods. *Journal of Magnetic Resonance* **229**: 25–34.

van Bavel MG, van Bavel CHM. 1990. *Dynagage installation and operational manual*. Houston: Dynamax Inc.

van Bel AJE. 2003a. The phloem, a miracle of ingenuity. *Plant, Cell and Environment* **26**: 125–149.

van Bel AJE. 2003b. Transport phloem: low profile, high impact. *Plant Physiology* **131**: 1509–10.

van Bel AJE, Ehlers K, Knoblauch M. 2002. Sieve elements caught in the act. *Trends in Plant Science* **7**: 126–32.

Vandegheuchte MW, Steppe K. 2013. Sap-flux density measurement methods: working principles and applicability. *Functional Plant Biology*: 213–223.

Velez-Ramirez AI, van Ieperen W, Vreugdenhil D, Poppel van MJA, Heuvelink E, Millenaar FF. 2014. A single locus confers tolerance to continuous light and allows substantial yield increase in tomato. *Nature Communications* **5**: 4549.

Wardlaw IF. 1993. Sink strength: Its expression in the plant. *Plant Cell & Environment* **16**: 1029–1031.

Windt CW, Vergeldt FJ, de Jager PA, van As H. 2006. MRI of long-distance water transport: a comparison of the phloem and xylem flow characteristics and dynamics in poplar, castor bean, tomato and tobacco. *Plant, Cell & Environment* **29**: 1715–29.

Zeeman SC, Smith SM, Smith AM. 2007. The diurnal metabolism of leaf starch. *The Biochemical Journal* **401**: 13–28.

Zgallai H, Steppe K, Lemeur R. 2006. Effects of different levels of water stress on leaf water potential, stomatal resistance, protein and chlorophyll content and certain anti-oxidative enzymes in tomato plants. *Journal of Integrative Plant Biology* **48**: 679–685.

3.8. Supporting information

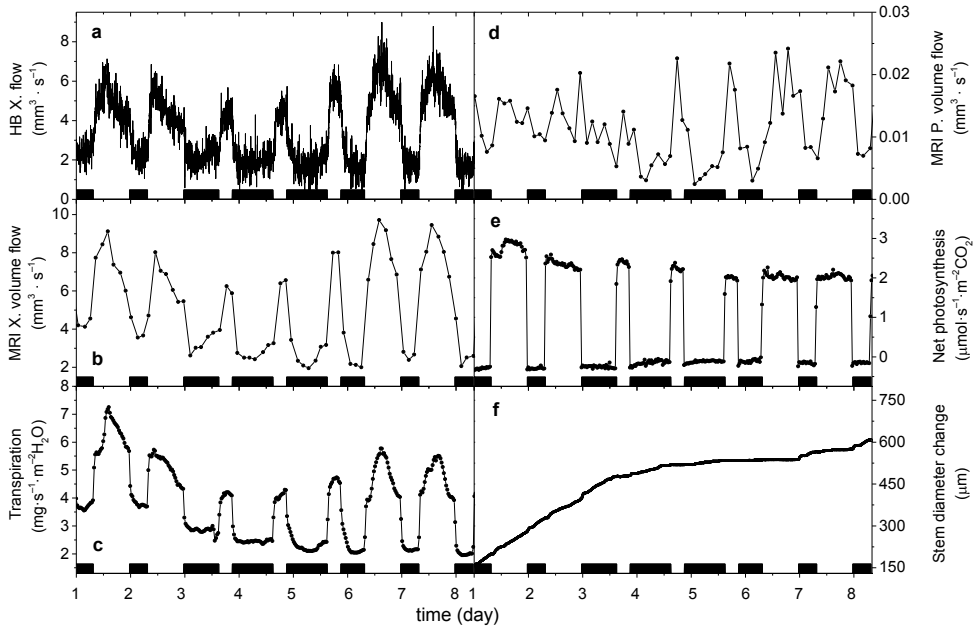


Figure S3.1: Replicate of the experiment - the effect of short photoperiod on (a) flow of xylem sap measured with HB, (b) and with MRI, (c) transpiration, (d) flow of phloem sap measured with MRI, (e) net photosynthesis, and (f) stem diameter change, all as a function of time in days. Black rectangles represent night-time.

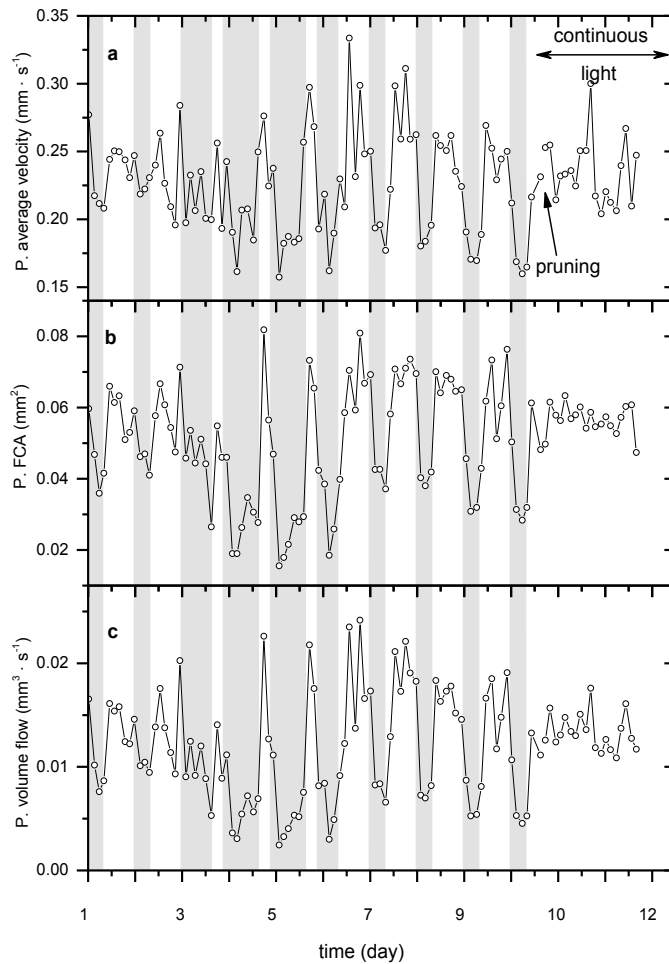


Figure S3.2: Replicate of the experiment - the effect of short photoperiod on (a) phloem velocity, (b) phloem flow conducting area (FCA), and (c) phloem flow. The short photoperiod treatment is followed by developed mild drought and further combined with simultaneous effect of fruit pruning and continuous light. All measured with MRI and all as a function of time in days. Grey stripes represent night-time.



Does the NMR transverse relaxation time in phloem region reflect phloem carbon status?

Alena Prusova, Frank J. Vergeldt, Edo Gerkema, Henk Van As

4.1. Summary

It has recently been shown that under lower sink strength not all sieve tubes are conducting phloem sap. To contribute to the debate about mechanisms driving phloem transport, it is of interest to know how the sucrose concentration in phloem sap relates to phloem flow. Sucrose concentration in phloem can be assessed by several techniques; however most of them are invasive. Here we explore whether the sucrose content in phloem sap can be assessed by the transverse relaxation time T_2 . Using MRI we studied the relation between the average T_2 relaxation time of the phloem and the phloem flow in the main stem of a three-month-old tomato plant (*Solanum lycopersicum* L.) while manipulating source strength either by means of light intensity or photoperiod length. We also measured stem diameter changes by a linear motion potentiometer. We hypothesised that T_2 relaxation time, when measured in parallel with phloem flow, can provide additional information about phloem carbon status. The combination of measurements presented here, i.e., the average T_2 relaxation time, phloem FCA and the stem diameter illustrate the complex process of a plant's adaptation to changes in source strength and phloem regulation.

4.2. Introduction

In higher plants, long-distance transport of photo-assimilates between source and sink(s) takes place in sieve tubes of phloem vascular tissue. Among the distributed photo-assimilates sucrose represents the largest fraction (van Bel & Hess, 2008). The phloem part of the vascular tissue is located in parallel with the xylem which in turn accommodates the long-distance transport of water and nutrients from roots to the aerial parts of the plant.

Using magnetic resonance imaging (MRI) flowmetry (Scheenen *et al.*, 2000), it has recently been shown that under higher source strength tomato plants transport higher amounts of phloem sap. This increased amount of phloem sap is transported in sieve tubes which do not conduct when not needed, i.e., under lower source strength (Chapter 2). Higher source strength was achieved by exposing the measured plant to higher light intensities. This activation of extra sieve tubes allowed for an increased amount of phloem sap to be transported while the phloem flow velocity to remain effectively constant. This observation confirms earlier suggestions about constant phloem flow velocity (Peuke *et al.*, 2001, 2015; Windt *et al.*, 2006). The signal detected by MRI flowmetry mainly originates from

protons of water molecules and therefore the measured parameter when measuring phloem flow (the volume flow) does not directly represent the amount of sucrose that is transported with the water in the phloem sap (Windt *et al.*, 2006; Van As, 2007; Borisjuk *et al.*, 2012). In other words, the observed increased phloem volume flow under higher source strength provides no information on the phloem sap sucrose concentration. Given that our understanding of the mechanisms driving phloem transport remain incomplete (Thompson, 2006), it is of interest to reveal whether the sucrose concentration in phloem sap increases or remains constant under higher source strength.

Sucrose concentration in phloem can be assessed with several techniques; however most of them are invasive like for example sap bleeding from severed phloem, in plants and trees which exude copiously like *Ricinus communis* (Peuke *et al.*, 2015), aphid stylectomy or EDTA-facilitated exudation (Turgeon & Wolf, 2009). MRI-based techniques are non-invasive techniques which allow the direct measurement of the sucrose concentration in transport phloem. The measured signal can be made selective for sucrose molecules. Among these quantitative techniques are for example chemical shift imaging, and volume or spectroscopic selective MRI (Tse *et al.*, 1996). However, both these approaches require relatively high signal intensities and therefore MR imagers at high magnetic field strengths, which in turn are not commonly built to accommodate samples as big as an adult tomato plant.

Another, albeit indirect, parameter to assess the sucrose content in phloem sap could be the transverse relaxation time T_2 . It is well-known that the T_2 relaxation time is sensitive to the physico-chemical environment in which the MRI active nuclei (protons of water molecules) find themselves and therefore can be used as a probe for studying this environment. Water protons in the vicinity of a semi-permeable membrane or in small organelles have shorter T_2 times compared to those in bulk water (van der Weerd *et al.*, 2002; Van As, 2007). T_2 is also influenced by chemical exchange between water protons and labile protons of some functional groups like carboxyl, amino or the abundant hydroxyl groups in sucrose (Hills & Duce, 1990; Perrin & Dwyer, 1990).

In this study we examined the effect of changed source strength on the T_2 relaxation time in the phloem region in the main stem of tomato plants measured at a magnetic field strength of 3T. T_2 relaxation time is sensitive to changes in sucrose concentrations at this field strength (Bottomley *et al.*, 1984; Hills & Duce,

1990; Bakhmutov, 2005). We hypothesised that the average T_2 in the phloem vascular tissue region reflects the phloem carbon status, i.e., the relative amount of sugars in the phloem vascular tissue.

4.3. Materials and Methods

Plant material and experimental setup

The results of two experiments (which we named I and II) are presented. For each experiment we used three-month-old tomato plants (*Solanum lycopersicum* cv. 'GT'). The plants were of comparable size; the plant used in experiment 'I' had a leaf area of 1.688 m² and the plant in the experiment 'II' had a leaf area of 1.422 m². Plants were grown in a greenhouse in 15 L pots under 16 h light / 8 h dark photoperiod. To allow imaging, the lower leaves on the main stem were removed two days before the start of the experiment to about 40 cm above the soil surface. All trusses with immature fruits and flowers were also removed two days before the experiment to remove strong sinks upstream from the MRI measurement site.

The plants were inserted into the MRI scanner one day prior to the experiment (to acclimatise) and remained inside the MRI scanner for the entire duration of the experiment. Inside the MRI scanner the temperature during the day was 24 °C and at night 20°C. Relative humidity fluctuated around 60%. In both experiments we manipulated the phloem flow by changing the source strength either by means of light intensity or length of the photoperiod. In experiment I, the photoperiod was 16 h day-time and 8 h night, however the photosynthetic active radiation (PAR) was decreased every three or more days from 780, to 600, 400, 230 and back to 600 $\mu\text{mol} \cdot \text{m}^{-2} \cdot \text{s}^{-1}$. In experiment II, the PAR was kept at 600 $\mu\text{mol} \cdot \text{m}^{-2} \cdot \text{s}^{-1}$ while the photoperiod was changed. For the first two days, the day-time was 16 h, thereafter for six days the day-time was 8 h and finally returned to 16 h day-time. During both experiments, the plants were well-watered (soil water potential was monitored and kept around -33 kPa).

MRI measurement

T_2 relaxation time and phloem flow measurements were conducted in a MRI scanner, consisting of a vertically-orientated superconducting magnet with a 50 cm vertical free bore (Magnex, Oxford, UK). For induction and detection of the signal, a bird cage RF coil of 4 cm diameter was used inside a 1 T/m gradient set (Bruker, Karlsruhe, Germany) controlled with the Avance console (Bruker, Karlsruhe,

Germany). The RF coil and the gradient system were specially designed to allow the insertion of intact plants (Homan *et al.*, 2007). The T_2 relaxation time measurement was carried out using a multi spin echo (MSE) pulse sequence resulting in T_2 map (Edzes *et al.*, 1998). For the phloem flow measurement the pulsed field gradient-turbo spin echo (PFG-TSE) sequence was used (Scheenen *et al.*, 2000) with the same experimental parameters as in Chapter 2. For the T_2 measurement in both experiments the following experimental parameters were used: imaging matrix = 128x128 pixels, field of view = 23x23 mm², slice thickness = 3 mm, echo time = 5 ms, number of echoes = 128, number of averages = 2, repetition time = 6000 ms and spectral width = 50 kHz. The T_2 measurement was recorded about every three hours of the experiment.

Data analysis

The MRI multi spin echo (MSE) measurement resulted in a cross-sectional image of the main stem where each pixel contains a spin echo train. The resulting decay curve is characterised by a single exponential decay or the sum of a number of exponential decays with decay times T_2 for each of the contributing components. A region of interest (ROI) was selected to be able to extract the relevant T_2 information only from the phloem tissue. The ROI selection was achieved using a phloem flow mask. The flow mask is a set of pixels which contains sieve tubes which conduct phloem sap and therefore exhibit net displacement in the MRI flow measurement. The flow masks for both experiments were obtained from MRI phloem flow measurements conducted on the same plant in the same cross-sectional position. The weighted average T_2 relaxation time in the ROI was estimated using the phasor approach (Digman *et al.*, 2008; Vergeldt *et al.*, 2016). The T_2 relaxation time(s) can be extracted from the signal decay curve. If such a signal decay curve would be obtained in a sample containing only bulk water, the signal would decay mono-exponentially with only one T_2 relaxation time constant of the bulk water. However, the pixels in the ROI contain different tissue types like sap-conducting sieve elements, companion cells and phloem parenchyma. In other words, water molecules within these regions may find themselves in compartments with different relaxation and diffusion properties (so-called partial-volume issue). Therefore, in pixels within the ROI a multi-exponential relaxation is expected. This complicates the interpretation of such data because a proper model containing the expected number of components should be known prior to fitting the data (the echo train). To overcome this issue, we used the phasor approach to extract the weighted average T_2 relaxation time in the ROI. This approach

overcomes the necessity of using a proper multi-exponential model and arguably performs better than a mono-exponential approach. The data analysis was performed with in-house functions and procedures written in IDL (ITT Visual Information Solutions, Boulder, Colorado, USA).

Sucrose phantom T_2 measurement

The dependency of the T_2 relaxation time of water protons on sucrose concentration was tested with a phantom consisting of ten sucrose-water solutions with different sucrose concentrations (0.1 – 1 mol L⁻¹). The T_2 relaxation time was measured using the same settings as for the actual plant experiments.

Independent of the tomato plant experiments, we measured T_2 relaxation times in a cross-section of the main stem of an adult *Ricinus communis* plant. This measurement was conducted continuously for five days. This plant is well known for easy sap collection (Turgeon & Wolf, 2009). At the end of the experiment we collected phloem sap exuded after a cutting and measured the sucrose concentration in the collected phloem sap with an optical refractometer.

4.4. Results

The data presented here were obtained during two experiments conducted on two different tomato plants. In both experiments the source strength was manipulated either with light intensity or photoperiodic length. In both experiments, besides the T_2 relaxation time, the phloem and xylem flow were measured. The phloem volume flow was correlated with the source strengths, i.e., under higher source strength (high light intensity or 16 h day-time) the phloem volume flow increased and vice versa. The increased volume flow was accompanied with constant phloem flow velocity and changing flow conducting area (FCA). Therefore under higher source strength, the increased amount of phloem sap was transported via sieve tubes which were not conducting under lower source strength. During both experiments the stem diameter was also measured to monitor stem water status and growth. The phloem and xylem flow data from experiment I were interpreted elsewhere (Chapter 2). Here we focus on the interpretation of T_2 relaxation times in the course of that source manipulation. A representative cross-sectional average T_2 relaxation time map of tomato main stem is depicted in figure 4.1. For every pixel, the average T_2 was obtained with the phasor approach. In the T_2 map, the phloem part of the vascular tissue can be clearly distinguished from the adjacent tissue types as it has lower average T_2 values. This cross-sectional image was measured

with a 256x256 imaging matrix, however the same field of view was used as is presented in the T_2 relaxation series below. Therefore stronger imaging gradients and a longer echo time had to be used which led to (in general) shorter average T_2 relaxation times (Edzes *et al.*, 1998).

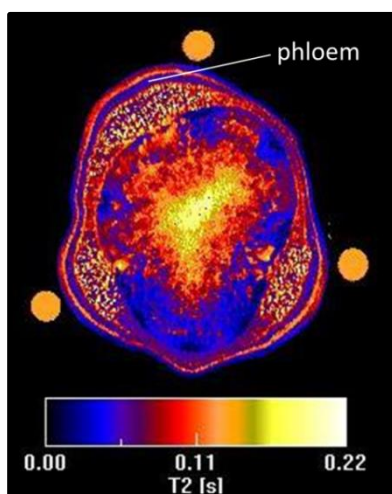


Figure 4.1: Representative cross-sectional T_2 map of the stem of a tomato. The dots around the stem represent reference tubes filled with stationary doped water, i.e., water with small amount of copper sulphate to decrease the relaxation time of the water. In common MRI practice, a linear colour scale is used, however, here the colour scale is non-linear to better differentiate between phloem and adjacent tissues, as well as emphasise that this image represents a parameter map, i.e., average T_2 relaxation time map.

Sucrose has a substantial effect on the T_2 relaxation time of water protons. Its concentration dependency is depicted in figure 4.2. As the sucrose concentration increases the T_2 relaxation time decreases in a non-linear manner. The sucrose concentration of phloem sap collected from *Ricinus communis* plant ($530 \text{ mol} \cdot \text{L}^{-1}$) is presented also in figure 4.2, and is correlated with the average T_2 relaxation time which was obtained as an average of three values of average T_2 relaxation time in the region of phloem measured in the morning hours on three consecutive days of measurement (standard deviation is smaller than the point size).

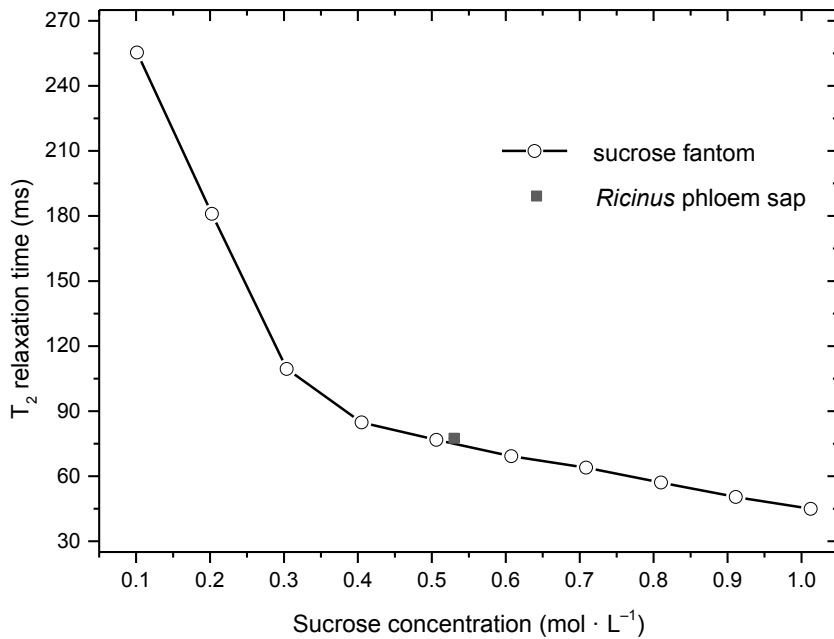


Figure 4.2: T_2 relaxation time of (phantom) sucrose solution (empty circles) as a function of the sucrose concentration measured in 3T MRI with comparable spatial resolution as in figure 4.3 and 4.4. The filled square represents average T_2 in the phloem region (obtained as an average T_2 value of three consecutive days in the morning hours, the error bar is smaller than the filled square) and phloem sap sucrose concentration measured with light refractometer.

An average T_2 relaxation time in phloem region

In both experiments the average T_2 in the phloem region exhibited a negative correlation with the phloem volume flow. At the beginning of experiment I, the plant experienced the highest light intensity and the phloem volume flow gradually increased while the average T_2 gradually decreased from 80 ms initially to 75 ms (Fig. 4.3, day 1–5). Furthermore, when the light intensity gradually decreased (three days for each light intensity), the phloem volume flow gradually decreased and the average T_2 gradually increased from 75 ms to 100 ms (Fig. 4.3, day 6–14). When the light intensity was increased again the phloem volume flow increased and the average T_2 decreased back to 83 ms. The stem growth rate was highest at the beginning of the experiment ($0.2 \text{ mm} \cdot \text{day}^{-1}$) when the plant experienced the highest light intensity; when the light intensity decreased the stem growth rate decreased as well (Fig. 4.3). Similar trends were observed in experiment II. Under short photoperiod, the phloem volume flow decreased while the average T_2 increased from an initial value of 83 ms (under normal 16 h day-length) to 104 ms (under short, 8 h day-length) (Fig. 4.4). The stem growth rate was lower during the short (8 h) days in comparison to normal (16 h) days. On top of these major changes, in both experiments the average T_2 in the phloem region tended to oscillate diurnally.

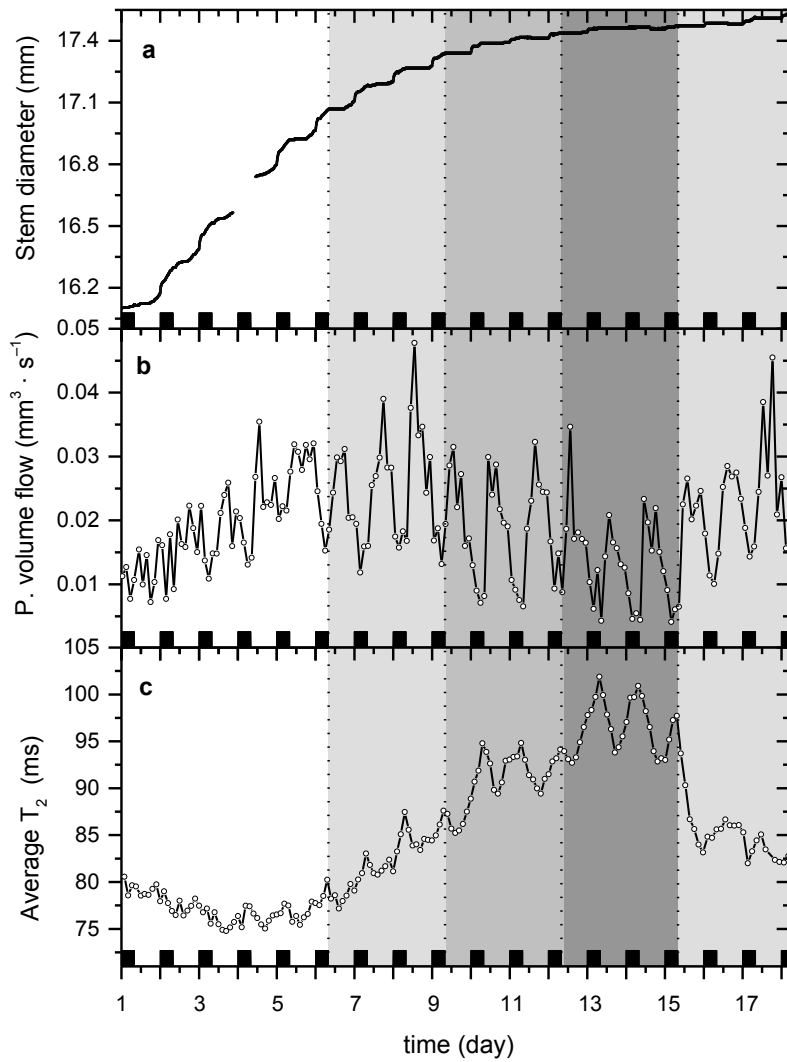


Figure 4.3: Experiment I. From the top of the plot: (a) stem diameter, (b) phloem volume flow, and (c) average T_2 relaxation time in the phloem region, all as a function of time. Black rectangles represent night-time. The different hues of grey correspond to different light intensities from the brightest to the darkest: 780, 600, 400, 230, and back to 600 $\mu\text{mol} \cdot \text{m}^{-2} \cdot \text{s}^{-1}$.

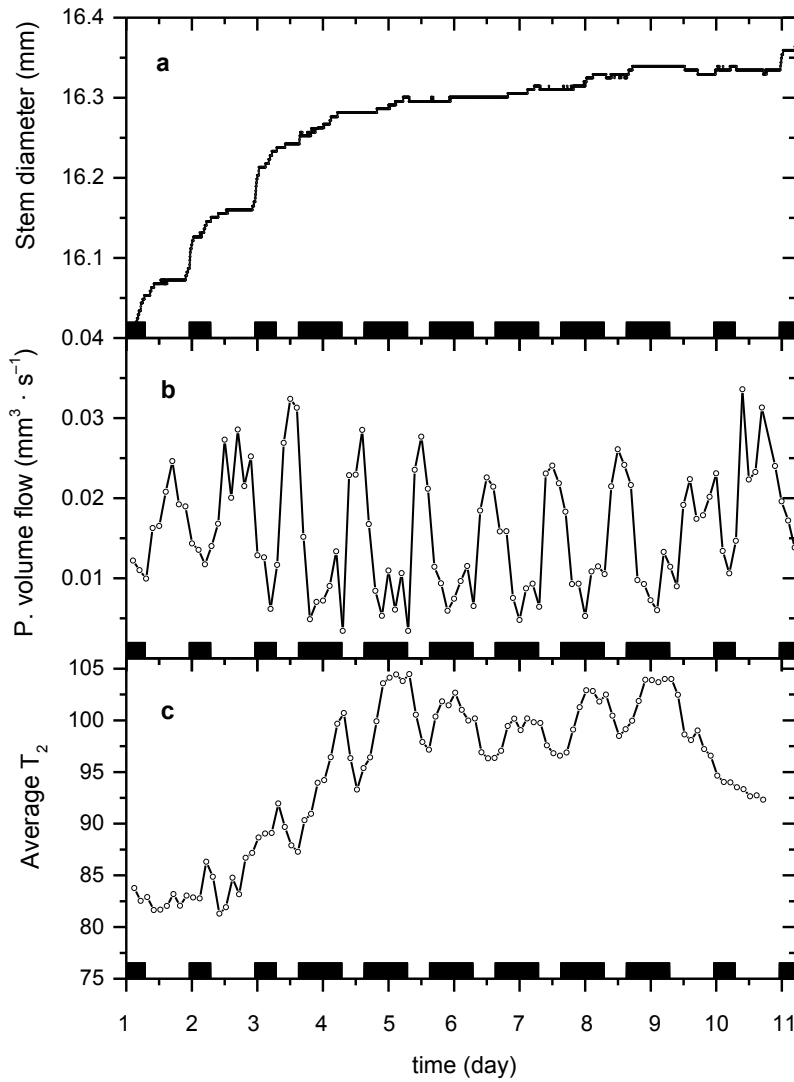


Figure 4.4: Experiment II. From the top of the plot: (a) stem diameter, (b) phloem volume flow, and (c) average T_2 relaxation time in the phloem region, all as a function of time. Black rectangles represent the night-time. The light intensity during the photoperiods was $600 \mu\text{mol} \cdot \text{m}^{-2} \cdot \text{s}^{-1}$.

4.5. Discussion

The most abundant solute in phloem sap (typically 80–90% of the total solute concentration) is sucrose (Vreugdenhil & Koot-Gronsveld, 1989) and in general among the distributed carbohydrates in phloem sap, sucrose represents the largest fraction across all herbaceous plants (van Bel & Hess, 2008). It has been shown that sucrose concentration in phloem varies significantly between different plant species (Ho *et al.*, 1987; Mitchell & Madore, 1992; Peuke *et al.*, 2001, 2015; Najla *et al.*, 2010). As we can see in figure 4.2, sucrose has a substantial effect on water T_2 relaxation time (Hills & Duce, 1990). Surprisingly, the observed sucrose concentration and the T_2 relaxation time in the phloem region in *Ricinus communis* correlated well. Therefore, we could speculate that the factor changing the T_2 relaxation time under different source strength is the sucrose and its concentration. The conducting sieve tubes (which accommodate the phloem sap flow) occupied only a fraction of the phloem part of the vascular tissue, which in both experiments was between 5–10%. Such a small fraction cannot explain the observed T_2 changes (Fig. 4.4 and 4.5). Therefore it is very likely that not only the conducting STs contribute to changes in the average T_2 relaxation time in the phloem region.

In plants in general, the water molecules can find themselves in variety of environments like for example vacuoles, cytoplasm, cell walls or extracellular spaces and therefore in plant tissue multi-exponential relaxation is normally observed (Belton & Ratcliffe, 1985). The sieve tubes (STs) contain several, mostly parietal organelles. When water molecules are in close proximity to organelles, those organelles can serve as relaxation sinks and therefore shorten the water relaxation time. However, the number of organelles is limited and their number is not expected to change in the course of several hours; therefore we do not expect that this is the cause of observed variations in T_2 relaxation time in the phloem region. When water molecules pass the semipermeable membrane (for example of those parietal organelles), the membrane can also serve as a relaxation sink, however no evidence has been found that membranes themselves act as a relaxation sink (van der Weerd *et al.*, 2002). Sieve elements (the building blocks of the sieve tubes) are symplasmically connected (via plasmodesmata) to adjacent companion cells (CC) and phloem sap is exchanged between these two compartments. This exchange can also influence the observed relaxation time of water and the resulting relaxation time depends on the difference in the relaxation times of water in the two exchanging water pools (van der Weerd *et al.*, 2001), i.e.,

in SE and CC. However, it is expected that this marginal lateral flux of phloem sap is in general out of phloem tissue (Turgeon & Wolf, 2009). This phloem sap lateral efflux is an essential part of the so-called leakage-retrieval mechanism (van Bel, 2003). Subsequently, after the phloem sap efflux, a part of the lost sucrose is actively transported (via sucrose transporters) back to the STs. Due to this active process of sucrose loading, we would expect that the sucrose concentration in CC and STs, and probably also in phloem PCs, is very comparable. This can explain the observed changes in the average T_2 relaxation time which most likely reflects changes in the sucrose concentration in the whole phloem region. When we examined the major T_2 relaxation time changes, we could conclude that under higher source strength (when we observed lower T_2 relaxation time), i.e., day 1–5 in figure 4.3, and day 1 and 2 in figure 4.4, the sucrose concentration in the phloem region was higher than under lower source strength (when we observed higher average T_2 relaxation time), i.e., day 6–15 in figure 4.3, and day 3–8 in figure 4.4. However, the absolute values of T_2 relaxation times should be interpreted with caution because the T_2 relaxation time can be affected by the measurement parameters. For example T_2 relaxation time can be affected by the strength of the imaging gradients and the echo time (Edzes *et al.*, 1998). A similar effect was also likely observed in the average T_2 relaxation time series which was acquired with a larger imaging matrix, i.e., 256x256 instead of 128x128 presented here (*cf.* Fig. 4.3 or Fig. 4.4 and S4.1). Although the absolute values of the average T_2 relaxation times were in general shorter, the trends were the same, i.e., under lower sink strength the average T_2 relaxation time increased and vice versa (Fig. S4.1 in supporting information). Therefore we can conclude that changes in the T_2 relaxation time, when acquired under the same conditions, correlates to changes in sucrose concentration.

On top of these major average T_2 relaxation time changes, we observed that the average T_2 relaxation time tended to oscillate on a diurnal basis. These diurnal oscillations could also be caused by changes in the sucrose concentration, however those changes are rather minor (< 10 ms) and could also be the result of opposing processes like water attraction by osmotically-active sucrose increases. The stem day/night shrinking/swelling pattern (De Swaef & Steppe, 2010) could also contribute to the average T_2 relaxation time diurnal oscillations.

The stem diameters grew the most at the beginning of both experiments, i.e., under the high source strength and high sucrose phloem sucrose concentration as

observed by T_2 , reflecting enough photo-assimilates for growth as well as sufficient water availability for growth. The combination of measurements presented here, i.e., the stem diameter, phloem flow characteristics and average T_2 illustrate the complex process of a plant's adaptation to changes in source strength by means of light intensity or photoperiod length.

4.6. Conclusion

We have demonstrated that T_2 relaxation time, when measured in parallel with phloem flow, can provide additional information about phloem region carbon status. The absolute values of T_2 relaxation times should be interpreted with caution because the T_2 relaxation time can be affected by both physiological processes as well as by the measurement parameters. However, if the T_2 is acquired in the same plants at similar developmental stage and under the same measurement settings (e.g. strength of the imaging gradients, echo time) changes in the T_2 relaxation time correlates to changes in sucrose concentration in the whole phloem region, including STs, CCs and PCs.

4.7. Acknowledgements

This research is financed in part by the BioSolar Cells open innovation consortium, supported by the Dutch Ministry of Economic Affairs, Agriculture and Innovations.

4.8. References

- Bakhtmutov VI. 2005.** *Practical NMR relaxation for chemists*. Chichester: Wiley & Sons Ltd.
- Belton PS, Ratcliffe FG. 1985.** NMR and compartmentation in biological tissues. *Progress in NMR Spectroscopy* **17**: 241–279.
- Borisjuk L, Rolletschek H, Neuberger T. 2012.** Surveying the plant's world by magnetic resonance imaging. *The Plant Journal* **70**: 129–46.
- Bottomley PA, Foster TH, Argersinger RE, Pfeifer LM. 1984.** A review of normal tissue hydrogen NMR relaxation times and relaxation mechanisms from 1–100 MHz: Dependence on tissue type, NMR frequency, temperature, species, excision, and age. *Medical Physics* **11**: 425–448.
- De Swaef T, Steppe K. 2010.** Linking stem diameter variations to sap flow, turgor and water potential in tomato. *Functional Plant Biology* **37**: 429–438.

- Edzes HT, van Dusschoten D, Van As H. 1998.** Quantitative T2 imaging of plant tissues by means of multi-echo MRI microscopy. *Magnetic Resonance Imaging* **16**: 185–196.
- Hills BP, Duce SL. 1990.** The influence of chemical and diffusive exchange on water proton transverse relaxation in plant tissues. *Magnetic Resonance Imaging* **8**: 321–331.
- Ho LC, Grange RI, Picken AJ. 1987.** An Analysis of the Accumulation of Water and Dry-Matter in Tomato Fruit. *Plant Cell & Environment* **10**: 157–162.
- Homan NM, Windt CW, Vergeldt FJ, Gerkema E, Van As H. 2007.** 0.7 and 3 T MRI and Sap Flow in Intact Trees: Xylem and Phloem in Action. *Applied Magnetic Resonance* **32**: 157–170.
- Mitchell DE, Madore MA. 1992.** Patterns of Assimilate Production and Translocation in Muskmelon (*Cucumis melo* L.): I. Diurnal Patterns. *Plant Physiology* **99**: 966–971.
- Najla S, Vercambre G, Génard M. 2010.** Improvement of the enhanced phloem exudation technique to estimate phloem concentration and turgor pressure in tomato. *Plant Science* **179**: 316–324.
- Perrin CL, Dwyer TJ. 1990.** Application of two-dimensional NMR to kinetics of chemical exchange. *Chemical Reviews* **90**: 935–967.
- Peuke AD, Gessler A, Trumbore S, Windt CW, Homan N, Gerkema E, Van As H. 2015.** Phloem flow and sugar transport in *Ricinus communis* L. is inhibited under anoxic conditions of shoot or roots. *Plant, Cell & Environment* **38**: 433–447.
- Peuke AD, Rokitta M, Zimmermann U, Schreiber L, Haase A. 2001.** Simultaneous measurement of water flow velocity and solute transport in xylem and phloem of adult plants of *Ricinus communis* over a daily time course by nuclear magnetic resonance spectrometry. *Plant, Cell & Environment* **24**: 491–503.
- Scheenen TW, van Dusschoten D, de Jager PA, Van As H. 2000.** Microscopic displacement imaging with pulsed field gradient turbo spin-echo NMR. *Journal of Magnetic Resonance* **142**: 207–15.
- Thompson M V. 2006.** Phloem: the long and the short of it. *Trends in Plant Science* **11**: 26–32.
- Tse TY, Spanswick RM, Jelinski LW. 1996.** Quantitative evaluation of NMR and MRI methods to measure sucrose concentrations in plants. *Protoplasma* **194**: 54–62.
- Turgeon R, Wolf S. 2009.** Phloem transport: cellular pathways and molecular trafficking. *Annual Review of Plant Biology* **60**: 207–21.
- Van As H. 2007.** Intact plant MRI for the study of cell water relations, membrane permeability, cell-to-cell and long distance water transport. *Journal of Experimental Botany* **58**: 743–756.
- van Bel AJE. 2003.** The phloem, a miracle of ingenuity. *Plant, Cell & Environment* **26**: 125–149.

- van Bel AJE, Hess PH. 2008.** Hexoses as phloem transport sugars: the end of a dogma? *Journal of Experimental Botany* **59**: 261–72.
- van der Weerd L, Claessens MMAE, Efdé C, Van As H. 2002.** Nuclear magnetic resonance imaging of membrane permeability changes in plants during osmotic stress. *Plant, Cell & Environment* **25**: 1539–1549.
- van der Weerd L, Claessens MM, Ruttink T, Vergeldt FJ, Schaafsma TJ, Van As H. 2001.** Quantitative NMR microscopy of osmotic stress responses in maize and pearl millet. *Journal of Experimental Botany* **52**: 2333–43.
- Vreugdenhil D, Koot-Gronsveld E a M. 1989.** Measurements of pH, sucrose and potassium ions in the phloem sap of castor bean (*Ricinus communis*) plants. *Physiologia Plantarum* **77**: 385–388.
- Windt CW, Vergeldt FJ, de Jager PA, Van As H. 2006.** MRI of long-distance water transport: a comparison of the phloem and xylem flow characteristics and dynamics in poplar, castor bean, tomato and tobacco. *Plant, Cell & Environment* **29**: 1715–29.

4.9. Supporting information

This experiment was conducted on a three-month-old tomato plant (*Solanum lycopersicum* cv. 'GT') bearing several fruit trusses (representing strong sinks). The tomato plant was grown in a greenhouse in 15 L pots under 16 h light / 8 h dark photoperiod. The lower leaves were removed two days before the start of the experiment to remove obstacles from the imaged part of the tomato plant stem (which was about 25 cm above the soil surface). The plant was inserted into the MRI scanner one day prior to the experiment (to acclimatise) and remained inside the MRI scanner for the entire duration of the experiment. Inside the MRI scanner the temperature during the day was 24 °C and at night 20 °C. Relative humidity fluctuated around 60%. The source strength was manipulated by means of the photoperiod. In the experiment the photosynthetic active radiation (PAR) was kept at $600 \mu\text{mol} \cdot \text{m}^{-2} \cdot \text{s}^{-1}$ while the photoperiod was changed. For the first two days, the day-time was 16 h, thereafter for three days day-time was 8 h and finally returned to 16 h day-time. During the experiments the plant was well-watered.

The T_2 relaxation time measurement was carried out using a multi spin echo (MSE) pulse sequence (Edzes *et al.*, 1998) with the following parameters: imaging matrix = 256x256 pixels, field of view = 22x22 mm², slice thickness = 1.5 mm, echo time = 7 ms, number of echoes = 128, number of averages = 2, repetition time = 6000 ms and spectral width = 50 kHz. The T_2 measurement was repeated about every five hours of the experiment while during the remaining time phloem and xylem flow was measured. The results are presented in figure S4.1. The average T_2 in the phloem region exhibited a negative correlation with the phloem volume flow as well as a negative correlation with stem growth.

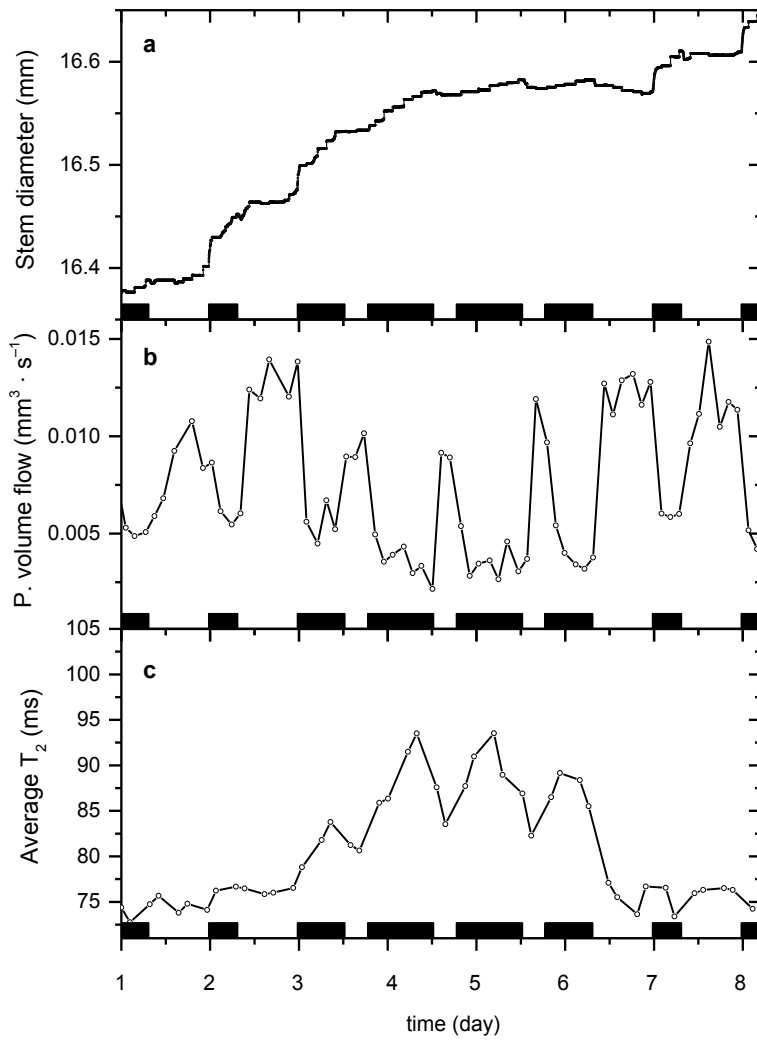


Figure S4.1: From the top of the plot: (a) stem diameter, (b) phloem volume flow, and (c) average T_2 relaxation time in the phloem region, all as a function of time. Black rectangles represent night-time. The light intensity during the day-time was $600 \mu\text{mol} \cdot \text{m}^{-2} \cdot \text{s}^{-1}$.



MRI characterisation of phloem transport in potato plant

Alena Prusova, Jose A. Abelenda

5.1. Summary

When studying phloem transport in plants with magnetic resonance imaging (MRI) flowmetry, plants with relatively low sink strength beneath the measurement site have so far been used. In order to study phloem transport dynamics, the source : sink ratio was manipulated by pruning or varying the environmental growth conditions. A potentially preferable approach is to work with plants which already possess strong sinks beneath the MRI measurement site, such as bulbs, tap roots or tubers. Potato (*Solanum tuberosum* L.) is an example of such a plant species. Therefore, in this study we measured phloem flow with MRI flowmetry in two potato plants (cv. Desiree). At the start of the MRI measurement both plants already possessed several developing tubers and therefore represented subjects with a strong sink below the MRI measurement site. One of the plants overexpressed the *StSWEET* gene (*35S:StSWEET*) which may have affected its source : sink ratio. The *35S:StSWEET* plant transported 60% higher amount of phloem sap than Desiree WT. Strikingly the average phloem flow velocity in both plants was the same ($0.35 \pm 0.05 \text{ mm} \cdot \text{s}^{-1}$). On the other hand, the phloem flow conducting area in *35S:StSWEET* plant was 90% larger than in Desiree WT. Hence the greater amount of transported phloem sap in *35S:StSWEET* plant was accommodated in more sieve tubes than in Desiree WT. This finding agrees with the hypothesis about the conserved nature of phloem flow velocity. Since both plants experienced the same microclimate and were of similar developmental stage and size, the greater amount of transported photo-assimilates in the *35S:StSWEET* plant was likely a result of an altered photo-assimilate partitioning between direct export and (either short or long term) storage in leaves and stem. Here we demonstrate that a potato plant with developing tubers represents a good subject to study phloem transport.

5.2. Introduction

In higher plants, water, nutrients and photo-assimilates are transported in vascular tissue. Water and nutrients are transported in the xylem part of the vascular tissue and photo-assimilates in the phloem part. When studying this so-called long distance transport, magnetic resonance imaging (MRI) flowmetry has been shown to be a uniquely-suited technique (Van As, 2007; Borisjuk *et al.*, 2012). The MRI signal originates from water molecules which naturally occur in plants. Therefore, MRI flowmetry is a truly non-invasive technique. MRI has been successfully used to study long-distance transport in both trees as well as herbaceous plants. In trees,

MRI flowmetry was used to study the long-distance transport in for example young *Populus tremula* (Windt *et al.*, 2006). In herbaceous plants, MRI flowmetry was used to study long-distance transport in for example *Ricinus communis* (Köckenberger *et al.*, 1997; Köckenberger, 2001; Peuke *et al.*, 2001, 2015; Mullendore *et al.*, 2010), *Cucumis sativus* (Scheenen *et al.*, 2002), *Solanum lycopersicum* (Windt *et al.*, 2006, 2009; Mullendore *et al.*, 2010), (Chapter 2), *Phaseolus vulgaris* or *Cucurbita maxima* (Mullendore *et al.*, 2010).

Xylem sap is transported from the roots to the aerial parts of the plant; therefore the direction of this transport is upwards. On the other hand, phloem sap is transported from source (the photosynthetically-active parts of the plant like leaves) to the sink(s) (i.e. area of growth or storage like for example terminal sinks like roots or shoot, or lateral sinks like for example cambium or fruits). Therefore this transport can occur in both directions with respect to the location of the sinks. The MRI measurement site is generally located on the main stem, somewhere between the roots and the rest of the plant. Therefore, in most cases the measured phloem transport is the one towards the roots (so-called basipetal phloem transport). However, in the majority of plants roots represent a sink with the lowest sink priority (Wardlaw, 1993), and therefore in most experiments fruit pruning or shoot manipulation are performed to alter the whole plant source : sink ratio and the phloem transport priorities. An ideal subject would be a plant with a strong sink below the MRI measurement site. Such a subject is for example *Solanum tuberosum* (potato), whose developing tubers represent a strong sink. It is also known that during tuber initiation at the stolon tips, sucrose unloading switches from apoplasmic to symplasmic, with a concomitant increase in sucrose synthase activity and a decrease in invertase activity in the cell wall (Struik *et al.*, 1999). Somewhat surprisingly, this plant species has not yet received much attention in the study of phloem and xylem flow dynamics, although this may have something to do with some of its inherent disadvantages like in general smaller leaf area as well as the plant stem size (Table 5.1).

Table 5.1 Overview of tomato and potato characteristic for MRI flowmetry measurements.

	<i>Solanum lycopersicum</i> (tomato)	<i>Solanum tuberosum</i> (potato)
Leaf area at adulthood*	large ($\leq 2 \text{ m}^2$)	medium/small ($\leq 0.2 \text{ m}^2$)
Stem diameter at the MRI measurement site	$\sim 16 \text{ mm}$	$\sim 7 \text{ mm}$
Absolute area of phloem part of vascular tissue	$\leq 2 \text{ mm}^2$	$\leq 0.8 \text{ mm}^2$
Amount of translocated phloem sap	$\leq 0.04 \text{ mm}^3 \cdot \text{s}^{-1}$	$\leq 0.01 \text{ mm}^3 \cdot \text{s}^{-1}$
Sink priority of the organ below the MRI measurement site	low (roots)	high (tubers)

*All presented figures are intended as guideline estimates only.

Using MRI flowmetry, it has recently been shown that not all phloem-transporting pathways (the sieve tubes, ST) act as conducting tissues when adult tomato plants are exposed to lower light intensities or shorter photoperiods, i.e., lower source strength. This regulation of the number of conducting ST resulted in a constant phloem flow velocity (albeit with diurnal pattern). A similar behaviour, i.e., the activation of sieve tubes which were not previously conducting was also observed after the pruning of tomato fruits (representing the removal of a strong sink) (Chapter 3). It has been hypothesised that phloem flow velocity across the species is conserved to be more or less constant and relatively slow; in this way, the plant is thought to maintain predictable signalling forces and prevent the potential dislocation of parietal ST organelles (Windt *et al.*, 2006; Turnbull & Lopez-Cobollo, 2013). However, to our knowledge, no data on phloem flow in potato have been reported.

Potato is closely-related to tomato and therefore, a similar behaviour, i.e., regulation of the number of conducting ST, could be expected. However alteration

of the source : sink ratio in potato is not as straightforward as in a tomato plant. Exposing potato plants to high light intensities could lead to unwanted stress, resulting in flowering (Luthra & Khan, 2000). Similarly, removing strong sinks (potato tubers) from a growing plant would be difficult without unduly disturbing the plant. An alternative means of altering the source : sink ratio is its manipulation through transgenesis. One possible target set of genes is the SWEET family of sucrose and glucose membrane transporters. SWEET proteins are thought to transport sugars across cell membranes and are expressed in a subset of the phloem parenchyma cells (Chen *et al.*, 2012). Therefore, plants with (artificially) higher levels of SWEET activity might be suitable test subjects as they might be expected to have an altered source : sink ratio. We were fortunate to have the possibility of including potato plants overexpressing the *StSWEET* gene in our experiment, enabling a comparison with wild-type potato for possible changes in phloem characteristics, i.e., phloem velocity, phloem volume flow or phloem flow conducting area.

5.3. Materials and Methods

Transgenic Desiree lines overexpressing the *StSWEET* gene under the regulatory control of the constitutive 35S promoter were developed as follows. The 35S:*StSWEET* construct was generated using the SWEET protein-coding region, after PCR amplification and cloning into the pENTR™/D-TOPO plasmid (Invitrogen) and further insertion by LR recombination into the pGWBΩ402 destination vector. Transgenic Desiree plants carrying the 35S:*StSWEET* were generated by *Agrobacterium*-mediated transformation of leaf explants as previously described (Martínez-García *et al.*, 2002). Desiree wild type (WT) and transgenic lines were grown in the greenhouse in long days. Both transgenic and WT potato plants had 14 leaves and were of the same age at the beginning of the MRI experiment, i.e., 9 weeks old. Both plants had already developed tubers before the start of the MRI experiment. Using magnetic resonance imaging (MRI) we measured phloem and xylem flow and T_2 relaxation time in the plant stem about 25 cm above the soil surface. Both plants were grown from *in vitro* plantlets and were therefore single stemmed plants, suitable for MRI measurement.

Plant material and microclimate conditions

Plants were grown in the greenhouse with 16 h light/8 h dark photoperiod. Inside the MRI scanner the following conditions were applied: day 24 °C, 16 h of 350

$\mu\text{mol} \cdot \text{m}^{-2} \cdot \text{s}^{-1}$ photosynthetically active radiation (PAR)/night 20°C, 8 h photoperiod. Relative humidity fluctuated around 60%. Plants were watered daily. The soil water potential was monitored with a tensiometer (CV5-U, Banbach Tensio-technique, Geisenheim, Germany), and was maintained at a value of around -33 kPa, i.e., the plants were well-watered. In the MRI scanner during the nights, the soil was water-cooled using pots with built-in tubing, to a temperature of around 18°C. The plants remained inside the MRI scanner for the entire duration of the experiment. Each experiment lasted six days. The first two days were used to allow the plants to acclimatise to the new microclimate.

MRI measurements

Phloem and xylem sap flow measurements were conducted in a MRI scanner, consisting of a vertically-orientated superconducting magnet with a 50 cm vertical free bore (Magnex, Oxford, UK). For induction and detection of the signal, a bird cage RF coil of 4 cm diameter was used inside a 1 T/m gradient set (Bruker, Karlsruhe, Germany) and controlled by the Avance console (Bruker, Karlsruhe, Germany) (Homan *et al.*, 2007).

Here we used a pulsed field gradient turbo spin echo (PFG-TSE) sequence (Scheenen *et al.*, 2000) for measurement of xylem or phloem sap displacement. For every pixel within an image we obtained a propagator (a displacement spectrum) (Scheenen *et al.*, 2000). This propagator was analysed with an approach described elsewhere (Scheenen *et al.*, 2000; Windt *et al.*, 2006; Van As, 2007) and resulted in the following parameters for each pixel: volume flow, amount of stationary water, flow conducting area (FCA) and average flow velocity. Flow measurements were carried out using the following imaging parameters: spectral width = 50 kHz, imaging matrix = 128x128 pixels, field of view = 17 x 17 mm², slice thickness = 3 mm, echo time = 5 ms. For the xylem measurements the specific parameters were: turbo factor = 8, number of averages = 2, repetition time = 2500 ms, displacement labelling time = 20 ms, gradient duration = 4 ms, 32 gradient steps, maximum gradient strengths = 400 mT · m⁻¹, and acquisition time = 42 min. For the phloem measurements the parameters were: turbo factor = 8, averages = 4, repetition time = 2000 ms, labelling time = 150 ms, gradient duration = 3 ms, 32 gradient steps, maximum gradient strengths = 200 mT · m⁻¹, and acquisition time = 68 min. The average T_2 relaxation time in the phloem region was obtained using a combination of phloem flow mask obtained from phloem flow measurement and the phasor approach as described in the Chapter 4. We alternated between xylem, phloem and

T_2 relaxation measurement. Data analysis was performed with IDL (ITT Visual Information Solutions, Boulder, Colorado, USA) using in-house processing, fitting, and quantification routines.

5.4. Results

We conducted two successive experiments, one using the *35S:StSWEET* potato plant and the other involving the Desiree WT potato plant. In both experiments we measured phloem and xylem flow, and average T_2 relaxation time in the potato plant stem.

Phloem flow characteristics

In figure 5.1 the recorded phloem flow parameters are presented, i.e., phloem volume flow, phloem flow average velocity and phloem flow conducting area for both plants. Unlike tomato, neither the *35S:StSWEET* potato plant nor the Desiree WT potato plant exhibited clear diurnal pattern in any of the basipetal phloem flow parameters. In both plants, the average phloem flow velocity was very comparable, i.e., $0.35 \pm 0.05 \text{ mm} \cdot \text{s}^{-1}$ for *35S:StSWEET* and $0.35 \pm 0.04 \text{ mm} \cdot \text{s}^{-1}$ for Desiree WT. Strikingly, the flow conducting area (FCA) for *35S:StSWEET* was almost twice as large as that of Desiree WT (0.036 ± 0.005 and 0.019 ± 0.003 respectively). This large difference in phloem FCA and comparable average phloem flow velocity resulted in a greater amount of transported phloem sap (volume flow) in *35S:StSWEET* than in Desiree WT. The average values of all three parameters are presented in Table 5.2. In the end of the experiment the *35S:StSWEET* plant had 11 tubers with a total fresh weight of 137 g. The Desiree WT plant had 8 tubers with a total fresh weight of 125g. There were no visual phenotype differences between the plants (WT and *35S:StSWEET*).

The remarkable differences in the phloem volume are visible in the respective phloem volume flow maps. Representative cross-sectional images of the potato stem overlaid with phloem volume flow maps of the *35S:StSWEET* plant and the Desiree WT plant are presented in figure 5.2. From the phloem flow maps, it can be seen that the maximal volume flows per pixels are comparable, however due to a larger phloem conducting area the *35S:StSWEET* plant transported a greater amount of phloem sap than the Desiree WT plant. The phloem volume flow maps of both potato plants presented in figure 5.2 were recorded at similar times in the light period of day 1 during both experiments.

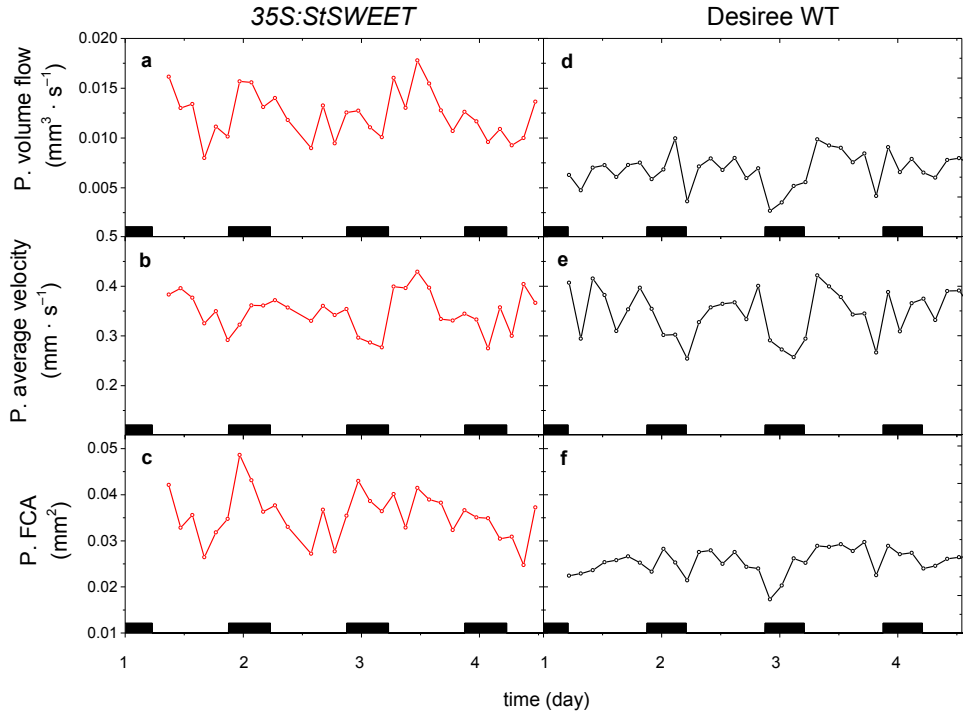


Figure 5.1: Comparison of phloem flow characteristics for *35S:StSWEET* plant (on the left) and *Desiree WT* (on the right). From the top of the plot: (a, d) volume flow of phloem sap, (b, e) average phloem flow velocity, and (c, f) phloem flow conducting area, all as a function of time. Black rectangles represent night-time.

Table 5.2 Phloem flow characteristics for *35S:StSWEET* and *Desiree WT* presented as an average for all days (D) and nights (N) as well as an average over the whole experiment (\bar{x}).

	<i>35S:StSWEET</i>			<i>Desiree</i>		
	D	N	\bar{x}	D	N	\bar{x}
Q	0.012±0.003	0.012±0.002	0.012±0.002	0.007±0.002	0.006±0.002	0.007±0.002
\bar{v}	0.36±0.04	0.32±0.04	0.35±0.04	0.36±0.05	0.32±0.04	0.35±0.05
FCA	0.034±0.005	0.038±0.005	0.036±0.005	0.019±0.003	0.018±0.004	0.019±0.003

(Q) phloem volume flow, (\bar{v}) average phloem flow velocity, (FCA) phloem flow conducting area

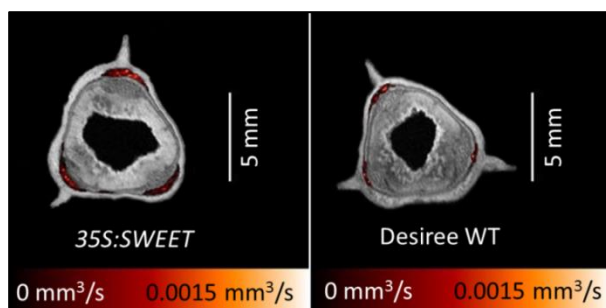


Figure 5.2: Representative cross-sectional images of potato stem with enhanced (T_2 based) contrast. On the left, an MRI image of *35S:StSWEET* potato plant and on the right an MRI image of Desiree WT potato plant.

Average T_2 relaxation time in phloem region

During both experiments, we also measured T_2 relaxation time in the same stem cross-section as phloem and xylem flow. The average T_2 relaxation times in the phloem region of both potato plants were very comparable (Fig. 5.3).

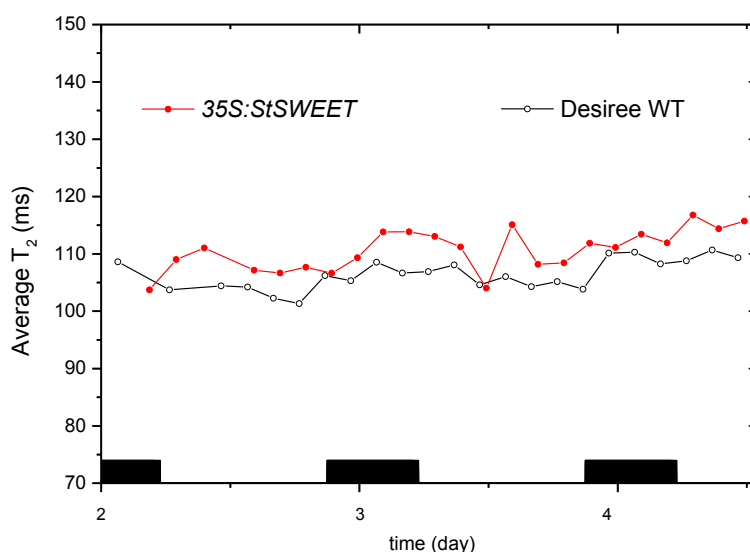


Figure 5.3: The average T_2 relaxation time in the phloem region as a function of time for *35S:StSWEET* (filled red circles) and Desiree WT plant (empty black circles). Black rectangles represent night-time.

Xylem flow characteristics & microclimate

The results from both experiments showed diurnal dynamics of xylem volume flow with the maximal values during the day and the minimum values at night (Fig. 5.4). The total leaf area of both plants was very comparable, i.e., 933 cm² for 35S:StSWEET and 850 cm² for Desiree WT. This was reflected in the fact that the maximal values of xylem volume flow were approximately the same for both experiments and both plants transpired about 120 mL · day⁻¹. In both experiments the xylem volume flow decreased towards the end of the light period which resulted in a shoulder like shape. We monitored the air temperature and the relative humidity inside the MRI scanner. From these data we calculated the vapour pressure deficit (VPD) which, unlike the xylem volume flow in both plants, had a rectangular shape towards the end of the light period (Fig. 5.4). The data on soil water potential ($\Psi_{w(soil)}$) show that both plants were well-watered.

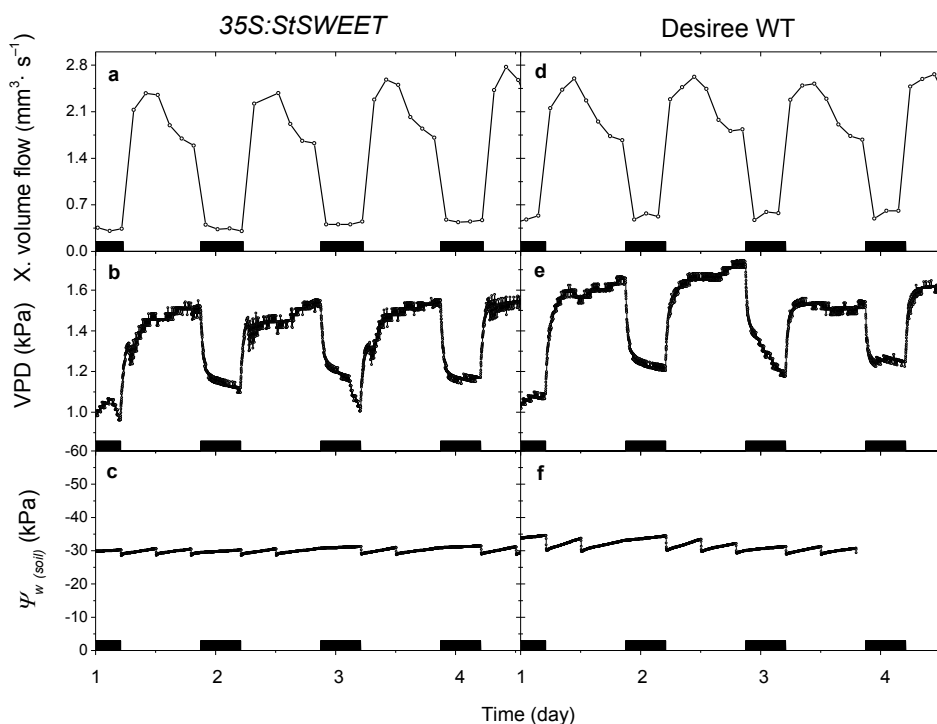


Figure 5.4: Xylem volume flow and the microclimate for both potato plants, for 35S:StSWEET plant (on the left) and Desiree WT (on the right). From the top of the plot: (a, d)

volume flow of xylem sap, (b, e) vapour pressure deficit (VPD), and (c, f) soil water potential, all as a function of time. Black rectangles represent night-time.

5.5. Discussion

Phloem flow velocity conserved

Our results showed that the *35S:StSWEET* plant transported a greater amount of phloem sap towards the roots and developing tubers than the Desiree WT plant. However in both plants, the phloem flow velocity was very comparable. The volume flow is a product of the flow velocity and the flow conducting area. Therefore, the greater amount of transported phloem sap in *35S:StSWEET* plant was associated with a larger flow conducting area (*35S:StSWEET* plant had 90% larger flow conducting area than Desiree WT). This observation agrees with a hypothesis that phloem flow velocity is conserved (Windt *et al.*, 2006), (Chapter 2 and 3). Manipulation via transgenesis has the potential to alter many physiological processes in the plant (though there was no obvious pleiotropic effects noted in the phenotype of the overexpression lines) and therefore it is even more striking that the phloem flow velocities were the same.

Altered photo-assimilates partitioning in 35S:StSWEET

Both plants were subjected to the same light intensity, similar VPD and sufficient irrigation. Therefore it is remarkable that the *35S:StSWEET* plant transported 60% more phloem sap than the Desiree WT plant. It is well known that the T_2 relaxation time is sensitive to the physical environment in which the MRI active nuclei (protons of water molecules) find themselves and therefore can be used as a probe for studying this environment (Van As, 2007). It has been shown that T_2 relaxation time in the phloem region reflects the phloem carbon status (Chapter 4). Although the average T_2 relaxation time in the phloem region of both plants was heterogeneous, the average values were very comparable. Therefore, we did not find any evidence to suggest that there were significant differences in the translocated phloem sap sugar concentration in both plants. As a result it seems that the *35S:StSWEET* plant had higher amounts of photo-assimilates available for transport than Desiree WT. This conclusion was supported by the difference between the plants in the so-called Munch's counter-flow. The water which is transported downwards in the phloem sap had to have first been transported upwards as part of the xylem sap. The phloem to xylem volume flow ratio then reflects the fraction of xylem water used to replenish the phloem water, which is in

turn exported from the source leaves as part of the phloem sap (Tanner & Beevers, 2001). The phloem to xylem volume flow ratio for the *35S:StSWEET* plant was 0.007 during the day and 0.03 at night, for the Desiree WT plant the ratio was 0.003 during the day and 0.01 at night. The higher phloem to xylem volume flow ratio for the *35S:StSWEET* plant indicates that a higher amount of xylem water was attracted to the phloem by means of osmosis which was likely caused by a higher absolute amount of photo-assimilates in the loading phloem. However, it is unclear how the *35S:StSWEET* plant might produce more photo-assimilates when it experienced the same microclimate as the Desiree WT plant. The most likely reason seems to be the effect of the overexpressed *SWEET* gene which altered partitioning of photo-assimilates between direct export and carbon reserves (i.e., transitory starch in chloroplasts and long-term starch reserves) (Boyer, 1996). Indeed, although we did not directly measure the starch content in the plants used in our experiments, it has been observed that on average the starch content in the leaves of *35S:StSWEET* plants was lower than in the Desiree WT (José Abelenda, personal communication).

Photosynthesis feedback regulation

In the xylem volume flow of both plants, we observed a decrease of the xylem flow towards the end of the light period, namely after 10 hours of light. The VPD is one of the major determinants of transpiration and thus the xylem volume flow (Damour *et al.*, 2010). The VPD day profile of both plants was practically rectangular and did not decrease towards the end of the light period. Therefore, the VPD was likely not the cause of the observed xylem volume flow decrease. A similar phenomenon of xylem volume flow decrease has also been observed in tomato plants exposed to 16 h long days (Chapter 2 and 3). That phenomenon was explained by the filling up of short-term carbon storage pools, resulting in photosynthesis feedback regulation (Kelly *et al.*, 2013). Although we did not measure photosynthesis in this experiment, we expect that the xylem volume flow decrease in both potato plants was also caused by photosynthesis feedback inhibition. This might be expected behaviour in the Desiree WT growing under long (16h light) days. Observing this phenomenon in the *35S:StSWEET* plant was somewhat surprising given that, as earlier speculated, the overexpression of *SWEET* may alter the photo-assimilates partitioning to favour their direct export.

Conclusion

In conclusion, our results demonstrate that potato plants are an interesting subject to study phloem transport given the location of strong sinks below the MRI measurement. Furthermore, our results showed that the 35S:*StSWEET* plant transported a greater amount of phloem sap than Desiree WT, however the phloem flow velocities in both plants were the same. This agrees with the hypothesis that the phloem flow velocity is conserved.

5.6. References

- Borisjuk L, Rolletschek H, Neuberger T. 2012.** Surveying the plant's world by magnetic resonance imaging. *The Plant Journal* **70**: 129–46.
- Boyer C. 1996.** *Photoassimilate distribution in plants and crops: source-sink relationships* (E Zamski and AA Schaffer, Eds.). New York: Dekker.
- Chen L-Q, Qu X-Q, Hou B-H, Sosso D, Osorio S, Fernie AR, Frommer WB, Zhu XG, Long SP, Ort DR, et al. 2012.** Sucrose efflux mediated by SWEET proteins as a key step for phloem transport. *Science* **335**: 207–11.
- Damour G, Simonneau T, Cochard H, Urban L. 2010.** An overview of models of stomatal conductance at the leaf level. *Plant, Cell & Environment* **33**: 1419–1438.
- Homan NM, Windt CW, Vergeldt FJ, Gerkema E, Van As H. 2007.** 0.7 and 3 T MRI and Sap Flow in Intact Trees: Xylem and Phloem in Action. *Applied Magnetic Resonance* **32**: 157–170.
- Kelly G, Moshelion M, David-Schwartz R, Halperin O, Wallach R, Attia Z, Belausov E, Granot D. 2013.** Hexokinase mediates stomatal closure. *The Plant Journal* **75**: 977–88.
- Köckenberger W. 2001.** Functional imaging of plants by magnetic resonance. *Trends in Plant Science* **6**: 286–292.
- Köckenberger W, Ki WI, Pope JM, Xia Y, Jeffrey KR, Komor E, Callaghan PT. 1997.** Plant A non-invasive measurement of phloem and xylem water flow in castor. *Planta* **201**: 53–63.
- Luthra SK, Khan IA. 2000.** Induction of flowering in potato under short day conditions. In: Khurana PSM, ed. *Potato, Global Research & Development*. Shimla: Indian Potato Association, 150–152.
- Martínez-García JF, Virgós-Soler A, Prat S. 2002.** Control of photoperiod-regulated tuberization in potato by the Arabidopsis flowering-time gene CONSTANS. *Proceedings of the National Academy of Sciences of the United States of America* **99**: 15211–15216.
- Mullendore DL, Windt CW, Van As H, Knoblauch M. 2010.** Sieve tube geometry in relation to phloem flow. *The Plant Cell* **22**: 579–93.
- Peuke AD, Gessler A, Trumbore S, Windt CW, Homan N, Gerkema E, Van As H. 2015.** Phloem flow and sugar transport in *Ricinus communis* L. is inhibited under anoxic conditions of shoot or roots. *Plant, Cell & Environment* **38**: 433–447.

- Peuke AD, Rokitta M, Zimmermann U, Schreiber L, Haase A. 2001.** Simultaneous measurement of water flow velocity and solute transport in xylem and phloem of adult plants of *Ricinus communis* over a daily time course by nuclear magnetic resonance spectrometry. *Plant, Cell & Environment* **24**: 491–503.
- Scheenen TW, van Dusschoten D, de Jager PA, Van As H. 2000.** Microscopic displacement imaging with pulsed field gradient turbo spin-echo NMR. *Journal of Magnetic Resonance* **142**: 207–15.
- Scheenen T, Heemskerk A, de Jager A, Vergeldt F, Van As H. 2002.** Functional imaging of plants: a nuclear magnetic resonance study of a cucumber plant. *Biophysical Journal* **82**: 481–492.
- Struik PC, Vreugdenhil D, van Eck HJ, Bachem CW, Visser RGF. 1999.** Physiological and genetic control of tuber formation. *Potato Research* **42**: 313–331.
- Tanner W, Beevers H. 2001.** Transpiration, a prerequisite for long-distance transport of minerals in plants? *Proceedings of the National Academy of Sciences of the United States of America* **98**: 9443–9447.
- Turnbull CGN, Lopez-Cobollo RM. 2013.** Heavy traffic in the fast lane: long-distance signalling by macromolecules. *New Phytologist* **198**: 33–51.
- Van As H. 2007.** Intact plant MRI for the study of cell water relations, membrane permeability, cell-to-cell and long distance water transport. *Journal of Experimental Botany* **58**: 743–756.
- Wardlaw IF. 1993.** Sink strength: Its expression in the plant. *Plant Cell & Environment* **16**: 1029–1031.
- Windt CW, Gerkema E, Van As H. 2009.** Most water in the tomato truss is imported through the xylem, not the phloem: a nuclear magnetic resonance flow imaging study. *Plant Physiology* **151**: 830–42.
- Windt CW, Vergeldt FJ, de Jager PA, van As H. 2006.** MRI of long-distance water transport: a comparison of the phloem and xylem flow characteristics and dynamics in poplar, castor bean, tomato and tobacco. *Plant, Cell & Environment* **29**: 1715–29.



General Discussion

Throughout the previous chapters we have explored phloem flow characteristics in tomato and potato plants with MRI flowmetry. We observed a variety of phloem flow behaviour like for example a diurnal pattern of phloem volume flow and virtually constant phloem flow velocity with a simultaneous change in flow conducting area (FCA). When we examined the T_2 relaxation time in the phloem region, we observed an increase in T_2 under low source strength and vice versa. This last chapter aims to summarise the presented work and weigh up the possible consequences of the presented findings.

6.1. Conserved phloem flow velocity

In Chapter 2, we saw a diurnal pattern in the phloem flow velocity in tomato with higher values during the day and lower values at night. However, the velocity remained within well-defined boundaries during these different periods, namely between $0.24 \pm 0.03 \text{ mm} \cdot \text{s}^{-1}$ during the day and $0.20 \pm 0.01 \text{ mm} \cdot \text{s}^{-1}$ at night. In chapter 3 we observed a very similar trend, when the values for velocity remained between $0.26 \pm 0.03 \text{ mm} \cdot \text{s}^{-1}$ and $0.21 \pm 0.01 \text{ mm} \cdot \text{s}^{-1}$. In potato plants (Chapter 5) the phloem flow velocity was found to be $0.35 \pm 0.05 \text{ mm} \cdot \text{s}^{-1}$ with no diurnal pattern. Therefore, the measured values of phloem flow velocities are not identical across the measured plants, but in individual plants the phloem flow velocities tend to remain constant and are well in the range between 0.25 and 0.4 as reported earlier for a number of plants of different size (Windt *et al.*, 2006). We have also observed that when the plants were manipulated in terms of source strength (either by means of light intensity or photoperiod length) or in terms of their source : sink ratio (fruit pruning), the phloem flow velocity (unlike FCA) was unaffected. During these manipulations it appeared that the phloem flow was regulated by the number of actively conducting sieve tubes (Chapter 2, 3 and 5). This led us to conclude that phloem sap flow velocity is indeed regulated to remain within well-defined boundaries on a per-plant basis, and thus displays a constancy of both pattern and range. Such a constant and relatively slow phloem flow velocity may help the plant in maintaining predictable signalling.

6.2. Phloem transport at maximum capacity

One of the common assumptions is that all sieve tubes are actively and continuously conducting the phloem sap. However, in Chapter 2 and 3, it has been demonstrated that not all sieve tubes are active all of the time and that plants can (de)activate sieve tubes when needed. In tomato, this (de)activation occurs

diurnally as well as under changing source strength. This observation suggests that phloem sap flow (volume flow) is indeed regulated locally (on a per sieve tube basis) as has previously been suggested (Thompson & Holbrook, 2003b; Thompson, 2006).

The finding that phloem flow velocity is conserved, and that volume flow is regulated by the number of active sieve tubes can have profound implications. Let's consider the hypothetical case when all crucial parameters of photosynthesis, e.g. photosynthetic capacity, stomatal conductance and CO₂ diffusion towards chloroplasts in the mesophyll, would all increase, while simultaneously experiencing optimal water, nutrient and light availability. In such a scenario, phloem transport would be at its maximum capacity. If these conditions could be realised in practice, it is likely that photosynthesis would become limited by the transport of photo-assimilates because of the finite number of sieve tubes and constant flow velocity.

Our attempts to drive phloem flow to its maximum capacity are presented in figures 6.1, 6.2 and 6.3 (additional to Fig. 2.2 and 2.3). In figure 6.1 we see the phloem flow characteristics measured in a well-watered adult potato plant with developing tubers, exposed to moderately-high light intensity (450 $\mu\text{mol} \cdot \text{m}^{-2} \cdot \text{s}^{-1}$). The phloem velocity exhibited a diurnal pattern with higher velocities during the day than at night; however the phloem FCA did not exhibit any significant pattern (Fig. 6.1). One possible explanation for these results is that the plant was at its maximum capacity for phloem transport.

Elevated atmospheric CO₂ concentrations increase source strength and could provide another means of observing phloem transport at its maximum capacity. We measured under such conditions, where a tomato plant was exposed to normal and (after 34 hours) an elevated atmospheric CO₂ concentration (900 ppm), higher light intensity and was well-watered (Fig. 6.2). Surprisingly, none of the phloem parameters exhibited a clear diurnal pattern. We also did not observe any significant differences in phloem characteristics between normal and elevated CO₂ concentrations. However, the plant's behaviour was likely affected by the very high relative humidity (close to 100 %) due to the experimental setup. Repeating this experiment (including measuring at even higher CO₂ concentrations) but with a stricter control of micro-climate conditions would no doubt yield interesting results.

The maximum capacity of the phloem transport could also be reached by exposing a plant to continuous light. Although continuous-light-tolerant tomato lines exist (Velez-Ramirez *et al.*, 2014), we did not have the opportunity to measure them and therefore performed a continuous-light experiment using a standard tomato line (cv. GT). After just one day of exposure to continuous light, we observed a striking change in the phloem flow characteristics (Fig. 6.3). At continuous light, neither phloem flow velocity nor FCA exhibited a diurnal pattern and both remained at the higher daytime values which were observed in the previous days. We observed a decrease in the xylem flow profile during normal day-lengths (Fig. 6.3 day 1 and 2) towards the end of the light period. We named this phenomenon 'feedback inhibition' (Chapter 2 and 3), and attributed it to the filling up of short-term carbon storage pools. To verify this, we would need data on the starch content of the leaves as well as information on stomatal conductance. We found that when a plant experiences continuous light (Fig. 6.3 day 3 on), its xylem volume flow profile levels off at a very comparable value to that which follows feedback inhibition - an observation which agrees with our hypothesis.

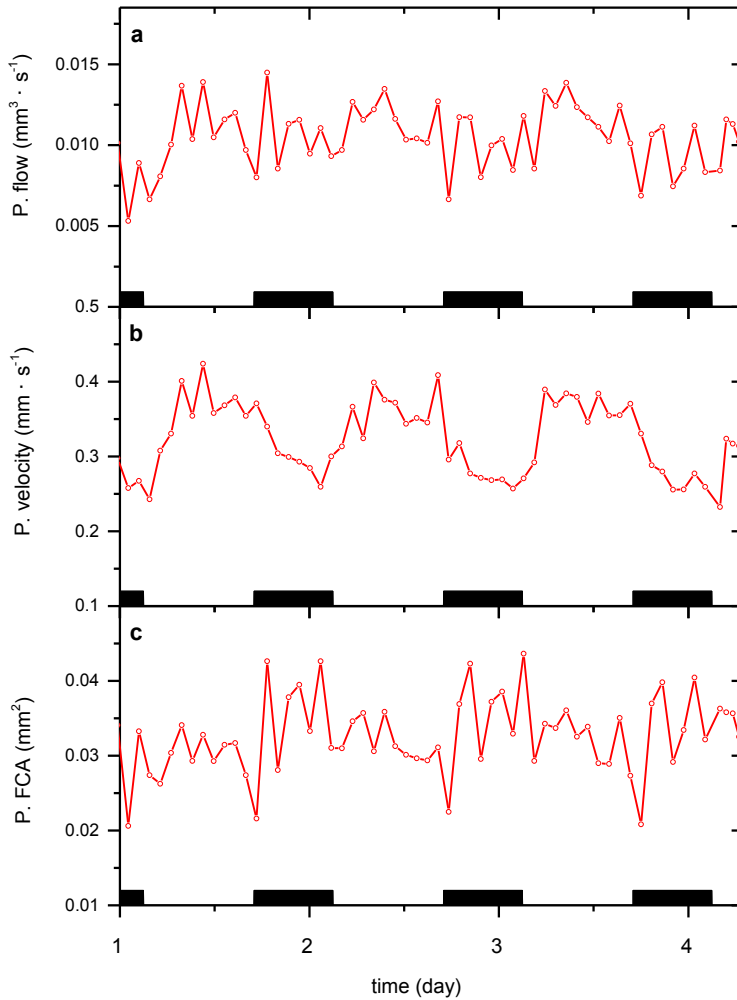


Figure 6.1: Phloem flow characteristics of an adult potato plant (cv. Karnico) with several developing tubers exposed to light intensity of $450 \mu\text{mol} \cdot \text{m}^{-2} \cdot \text{s}^{-1}$. From the top of the plot: (a) volume flow of phloem flow sap, (b) diurnal pattern exhibiting average phloem flow velocity, and (c) phloem flow conducting area, all as a function of time; black rectangles represent night-time.

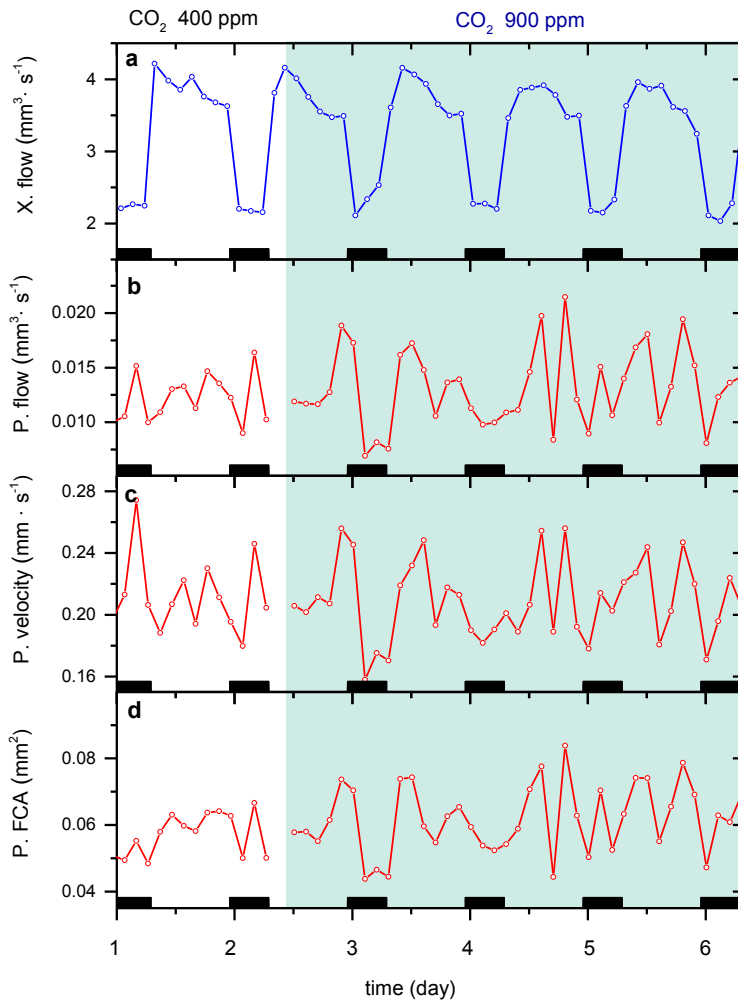


Figure 6.2: Xylem and phloem flow characteristics of an adult three-month-old tomato plant (cv. GT) acquired under normal (white part of the plot) and elevated (blue part of the plot) CO_2 concentration in the plant's atmosphere and exposed to a light intensity of $600 \mu\text{mol} \cdot \text{m}^{-2} \cdot \text{s}^{-1}$. From the top of the plot: (a) volume flow of xylem sap, (b) volume flow of phloem sap, (c) average phloem flow velocity, and (d) phloem flow conducting area, all as a function of time; black rectangles represent night-time. The increased CO_2 concentration was achieved by enclosing the plant in an impermeable plastic membrane and recirculating the air while monitoring the CO_2 concentration with Infra-Red Gas Analyser and regulating it with a PID CO_2 injector.

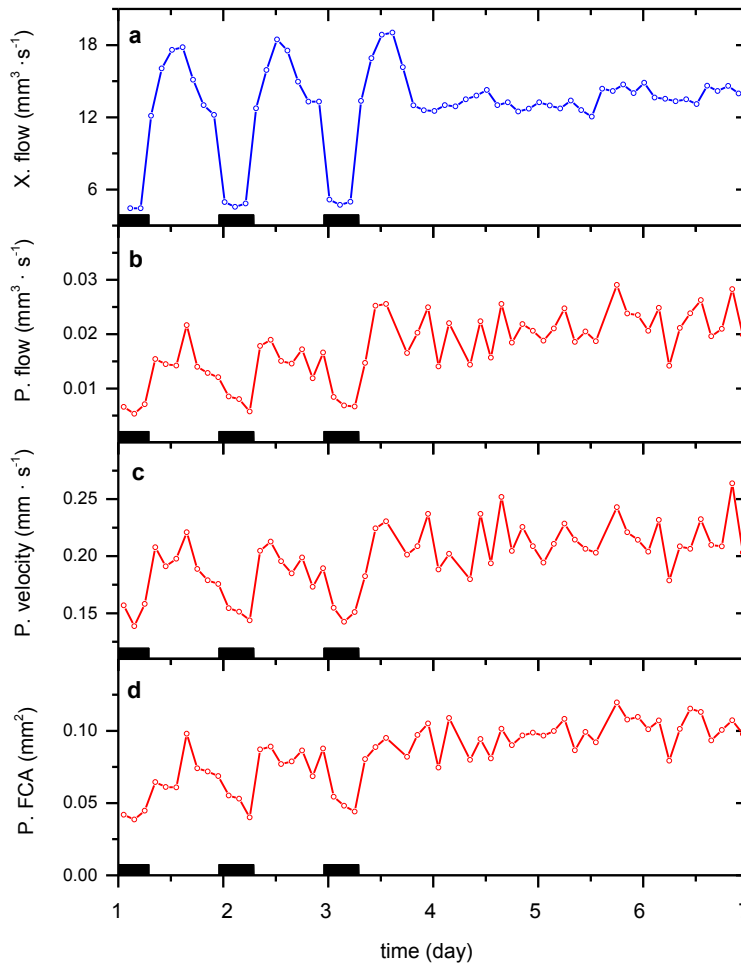


Figure 6.3: Xylem and phloem flow characteristics of an adult three-month-old tomato plant (cv. GT) with pruned fruit trusses and flowers. After four days of 16 h day-time (two days for acclimation) the plant was exposed to continuous light. From the top of the plot: (a) volume flow of xylem sap, (b) volume flow of phloem sap, (c) average phloem flow velocity, and (d) phloem flow conducting area, all as a function of time; black rectangles represent night-time. The light intensity during the day-periods was $600 \mu\text{mol} \cdot \text{m}^{-2} \cdot \text{s}^{-1}$.

6.3. Is phloem transport a limiting factor for photosynthesis (and ultimately for yield)?

In the context of current efforts to improve plant photosynthetic efficiency (Zhu *et al.*, 2010; Kramer & Evans, 2011), and ultimately crop yield to provide greater food security in the face of an increasing worldwide population, limitation by phloem transport should be taken into account. Current intensive horticulture commonly boosts production through a CO₂-enriched atmosphere (up to 2000 ppm), high light intensities and long photoperiods, optimal nutrient availability and regular irrigation. Under such conditions, it could already be the case that the limiting factor for photosynthesis is phloem transport (Adams III *et al.*, 2013, 2014), (as we attempted to demonstrate in figures 6.1, 6.2 and 6.3). A plant's history may also have an effect on leaf vasculature anatomy and ultimately on the photosynthetic rate (Adams III *et al.*, 2013). The improvement of phloem loading as well as transport could be a novel target of research that should be pursued in parallel to other efforts at improving photosynthetic efficiency.

It is well-known that yield is a complex trait with many components (Shi *et al.*, 2009). From a breeding perspective, it is desirable to understand these component traits, particularly in selecting for particular environments. Assuming phloem transport 'efficiency' were one of these components (e.g. through increased fructokianase activity in vascular tissue (Granot *et al.*, 2014)), it should in theory be possible to select for plants with higher phloem efficiencies. However, the traditional approach in breeding is to generate large segregating populations from which to select superior lines. This would no doubt necessitate high-throughput phenotyping, for which MRI is not particularly suited. It would also require some prior knowledge about variation of this trait within a species, knowledge which is not currently available, although anatomical, biochemical and gene expression data suggest large heterogeneity in sieve element – companion cell complexes of loading as well as transport phloem within and between species (Slewiniski *et al.*, 2013). The use of non-conventional breeding techniques such as transgenesis may circumvent these issues (Chapter 5), although in practice they are currently, at least from a societal perspective, an unacceptable method of crop improvement. One possible solution could be the calibration of phloem transport models (derived from current models (Thompson & Holbrook, 2003a; Minchin & Lacomte, 2005; Hölttä *et al.*, 2006; Pickard & Abraham-Shrauner, 2009; De Schepper & Steppe, 2010; De Swaef *et al.*, 2013)) with in-depth phenotyping data. Such data could be

generated using an integrated approach combining several independent plant sensors (as demonstrated in Chapter 3). The data could be extended using a combination of such MRI assessed phloem flow characteristics and SEM-based measurements of the geometry of microfluidic sieve tube system (sieve tubes, sieve plates and sieve plate pores *etc.* (Mullendore *et al.*, 2010)). Further key input parameters might be phloem sap sucrose concentrations (ideally assessed with a non-invasive method such as localised magnetic resonance spectroscopy), and leaf starch content (ideally obtained with a non-destructive method). Another vital parameter could be obtained with (in plant MRI a relatively new approach) MRI combined with positron emission tomography (PET) for photo-assimilated carbon allocation (Jahnke *et al.*, 2009; De Schepper *et al.*, 2013; Hubeau & Steppe, 2015). Once calibrated, such a model could be fed with more easily obtained (and hence, high throughput) parameters in order to gain an approximate phloem phenotype for use in both trait discovery and breeding programs.

Current models e.g. (Thompson & Holbrook, 2003a,b, 2004) should be revised as the possible (de)activation of sieve tubes (Chapter 2) is not considered. Our findings also have implications in terms of increased sucrose concentration (Chapter 4). Under the current hypothesis that all sieve tubes remain active continuously, an increase in sucrose concentration would lead to an increase in the sap viscosity which would ultimately hinder phloem transport (Hölttä *et al.*, 2006). Under our proposed model of phloem regulation, previously non-conducting sieve tube activation would reduce the resistance (Hall & Minchin, 2013) and may allow phloem transport to be maintained for higher sucrose concentrations.

6.4. Further prospects of plant MRI

MRI flowmetry is a promising tool for studying long-distance transport in plants. As we demonstrated (Chapter 3), the use of independent plant sensors together with MRI flowmetry is the ideal approach to understand the interplay between diverse processes and long-distance transport in plants. Eventually, such data could be used for the validation of long-distance transport models. However, one of the essential parameters, sap sucrose concentration, which determines sap viscosity and therefore phloem resistance (Hall & Minchin, 2013), is still missing. Existing techniques for sucrose concentration assessment are invasive and therefore the results could be biased. The ideal way to assess the phloem sap sucrose concentration non-invasively involves MRI-based techniques like chemical shift imaging or volume/spectroscopy selective MRI. These techniques require

relatively high sensitivity and therefore MR imagers at high magnetic field strengths, which in turn are not commonly built to accommodate samples as big as an adult tomato plant or the like (e.g., potato plant, Chapter 5). Therefore, measuring the T_2 relaxation time seems to be an attractive (although indirect) alternative method of exploring phloem carbon status because it is relatively easy and fast (e.g. 20 min). The T_2 relaxation time values are, however, not uniquely related to the concentration of a certain compound (like sucrose). Nevertheless, if the T_2 relaxation time data are treated with caution, and especially when recorded during experiments where the test plant is in one way or the other manipulated, these data can provide insight into transport phloem carbon status (then the T_2 relaxation time correlates to changes in sucrose concentration in the whole phloem region). An ideal step forward in this field would be to measure phloem sucrose transport directly using the propagator approach (the approach which is used in this thesis to assess the phloem water transport) by combining the PFG-STE with a preceding ‘sucrose selection’ (Van As & van Duynhoven, 2013). However, we should not forget to mention that the measurement of water flowing in phloem sieve tubes is already a tremendous challenge. The flowing phloem water per pixel is as small as ~5 % of the flow mask (in tomato) and therefore is already near the lower detection threshold. Measuring xylem water transport is much ‘easier’. Therefore, routinely implementing a protocol to measure sucrose transport using MRI will, no doubt, be very challenging.

MRI, in general, is scarcely used in the field of plant research (Borisjuk *et al.*, 2012). One of the reasons could be its low throughput and relatively high cost as well as its complicated operation. MRI has great potential to be used for in-depth phenotyping, ideally integrating its measurement with those of other plant sensors. However, although it might sound trivial, operating a system as easy as a LED (the source of light) inside the strong magnetic field of an MRI scanner is in itself challenging. For similar reasons, the use of diverse plant sensors within an MRI scanner is not straightforward (all parts have to be non-magnetic, ideally operating under direct current or well shielded). Also, microclimate control inside an MRI scanner is hard to control. The MRI scanner using a closed bore (as the one used in this thesis) consists of a super-conducting magnet and provides a high magnetic field with very good homogeneity. This, however, comes with a price of limited accessibility to the plant. Once it is inserted in the scanner, something as straightforward as collecting leaf samples becomes an issue.

An attractive alternative would be the use of portable MRI scanners with an open access design such a C-shape (Windt & Blumler, 2015) or openable Halbach (Windt *et al.*, 2011) permanent magnets. Such portable scanners could be used directly in greenhouses. Ideally, several of these ‘MRI-modules’ could be applied simultaneously at different positions of a plant. Several types of ‘portable’ (up to several tens of kg) NMR/MRI modules have been recently developed (Kimura *et al.*, 2011; Windt *et al.*, 2011; Jones *et al.*, 2012; Windt & Blumler, 2015). However, their increased mobility comes with certain trade-offs, such as low magnetic field strength with lower field homogeneity and therefore compromised sensitivity. In the coming decades, novel cryogen-free magnets, providing better homogeneity and higher magnetic fields, may well help bring MRI flowmetry to the plant, rather than bringing the plant to MRI.

6.5. References

- Adams III WW, Cohu CM, Amiard V, Demmig-Adams B. 2014. Associations between the acclimation of phloem-cell wall ingrowths in minor veins and maximal photosynthesis rate. *Frontiers in Plant Science* 5: 24.
- Adams III WW, Cohu CM, Muller O, Demmig-Adams B. 2013. Foliar phloem infrastructure in support of photosynthesis. *Frontiers in plant science* 4: 194.
- Borisjuk L, Rolletschek H, Neuberger T. 2012. Surveying the plant's world by magnetic resonance imaging. *The Plant Journal* 70: 129–46.
- De Schepper V, Bühler J, Thorpe M, Roeb G, Huber G, van Dusschoten D, Jahnke S, Steppe K. 2013. (11)C-PET imaging reveals transport dynamics and sectorial plasticity of oak phloem after girdling. *Frontiers in Plant Science* 4: 1–9.
- De Schepper V, Steppe K. 2010. Development and verification of a water and sugar transport model using measured stem diameter variations. *Journal of Experimental Botany* 61: 2083–99.
- De Swaef T, Driever SM, Van Meulebroek L, Vanhaecke L, Marcelis LFM, Steppe K. 2013. Understanding the effect of carbon status on stem diameter variations. *Annals of Botany* 111: 31–46.
- Granot D, Kelly G, Stein O, David-Schwartz R. 2014. Substantial roles of hexokinase and fructokinase in the effects of sugars on plant physiology and development. *Journal of Experimental Botany* 65: 809–819.
- Hall AJ, Minchin PEH. 2013. A closed-form solution for steady-state coupled phloem/xylem flow using the Lambert-W function. *Plant, Cell & Environment* 36: 2150–2162.
- Hölttä T, Vesala T, Sevanto S, Perämäki M, Nikinmaa E. 2006. Modeling xylem and phloem water flows in trees according to cohesion theory and Münch hypothesis. *Trees* 20: 67–78.
- Hubeau M, Steppe K. 2015. Plant-PET Scans: In Vivo Mapping of Xylem and Phloem Functioning. *Trends in Plant Science* 20: 676–685.
- Jahnke S, Menzel MI, van Dusschoten D, Roeb GW, Bühler J, Minwuyelet S, Blümmler P, Temperton VM, Hombach T, Streun M, et al. 2009. Combined MRI-PET dissects dynamic changes in plant structures and functions. *The Plant Journal* 59: 634–44.
- Jones M, Aptaker PS, Cox J, Gardiner B a, McDonald PJ. 2012. A transportable magnetic resonance imaging system for in situ measurements of living trees: the Tree Hugger. *Journal of Magnetic Resonance* 218: 133–40.
- Kimura T, Geya Y, Terada Y, Kose K, Haishi T, Gemma H, Sekozawa Y. 2011. Development of a mobile magnetic resonance imaging system for outdoor tree measurements. *Review of Scientific Instruments* 82: 53704.
- Kramer DM, Evans JR. 2011. The importance of energy balance in improving photosynthetic productivity. *Plant Physiology* 155: 70–8.
- Minchin PEH, Lacointe A. 2005. New understanding on phloem physiology and possible consequences for modelling long-distance carbon transport. *New Phytologist* 166: 771–9.

- Mullendore DL, Windt CW, Van As H, Knoblauch M. 2010.** Sieve tube geometry in relation to phloem flow. *The Plant Cell* **22**: 579–93.
- Pickard WE, Abraham-Shrauner B. 2009.** A ‘simplest’ steady-state Munch-like model of phloem translocation, with source and pathway and sink. *Functional Plant Biology* **36**: 629–644.
- Shi J, Li R, Qiu D, Jiang C, Yan L, Morgan C, Bancroft I, Zhao J, Meng J. 2009.** Unraveling the complex trait of crop yield with quantitative trait loci mapping in *Brassica napus*. *Genetics* **182**: 851–861.
- Slewiniski TL, Zhang C, Turgeon R. 2013.** Structural and functional heterogeneity in phloem loading and transport. *Frontiers in Plant Science* **4**: 244.
- Thompson MV. 2006.** Phloem: the long and the short of it. *Trends in Plant Science* **11**: 26–32.
- Thompson MV, Holbrook NM. 2003a.** Application of a Single-solute Non-steady-state Phloem Model to the Study of Long-distance Assimilate Transport. *Journal of Theoretical Biology* **220**: 419–455.
- Thompson MV, Holbrook NM. 2003b.** Scaling phloem transport: water potential equilibrium and osmoregulatory flow. *Plant, Cell & Environment* **26**: 1561–1577.
- Thompson MV, Holbrook NM. 2004.** Scaling phloem transport: information transmission. *Plant, Cell & Environment* **27**: 509–519.
- Van As H, van Duynhoven J. 2013.** MRI of plants and foods. *Journal of Magnetic Resonance* **229**: 25–34.
- Velez-Ramirez AI, van Ieperen W, Vreugdenhil D, Poppel van MJA, Heuvelink E, Millenaar FF. 2014.** A single locus confers tolerance to continuous light and allows substantial yield increase in tomato. *Nature Communications* **5**: 4549.
- Windt CW, Blumler P. 2015.** A portable NMR sensor to measure dynamic changes in the amount of water in living stems or fruit and its potential to measure sap flow. *Tree Physiology*: 366–375.
- Windt CW, Soltner H, van Dusschoten D, Blümle P. 2011.** A portable Halbach magnet that can be opened and closed without force: the NMR-CUFF. *Journal of Magnetic Resonance* **208**: 27–33.
- Windt CW, Vergeldt FJ, de Jager PA, van As H. 2006.** MRI of long-distance water transport: a comparison of the phloem and xylem flow characteristics and dynamics in poplar, castor bean, tomato and tobacco. *Plant, Cell & Environment* **29**: 1715–29.
- Zhu XG, Long SP, Ort DR. 2010.** Improving photosynthetic efficiency for greater yield. *Annual Review in Plant Biology* **61**: 235–261.

This thesis aims to answer the question whether phloem transport can be a limiting factor for photosynthesis efficiency (and ultimately causing a bottleneck towards achieving higher yields). To answer this key question, we manipulated the source:sink ratio within tomato (*Solanum lycopersicum* L.) while measuring phloem transport with magnetic resonance imaging (MRI) flowmetry. Additionally we compared phloem flow characteristics of two potato plants (*Solanum tuberosum* L.) which differed in source : sink ratio. In **Chapter 2**, the source strength was manipulated by varying the light intensity. An increase in phloem sap volume flow under higher light intensities was observed. However, under all light intensities applied, the phloem flow velocity was found to be constant (as has previously been suggested in other studies) although a clear diurnal pattern was observed. This finding does not fit in current models to describe the mechanism of phloem transport and a different mechanism must be at play. The results of this chapter demonstrate that increased levels of photo-assimilates are transported in sieve tubes, which are activated when needed by the plant. This is the first study which shows that plants activate individual sieve tubes when more photo-assimilates are available, yet maintain constant velocity. Those observations were in a tomato plant with pruned fruit trusses (i.e., in a simplified system). In **Chapter 3**, we investigated whether tomato plants still exhibit constant phloem flow velocity (with a diurnal pattern) under normal conditions, i.e., with strong sinks (tomato fruits) still attached. This was tested for both a long and short photoperiod by measuring flow characteristics with MRI flowmetry. We simultaneously monitored other plant processes like xylem flow rates with a heat balance sensor, net photosynthesis with gas exchange and stem diameter changes with a linear motion potentiometer. With this integrated approach, we revealed a correlation between night phloem volume flow, dark respiration and stem growth. We also conclusively showed that phloem volume flow performs a diurnal pattern under a variety of source-sink ratios which appears to be a normal behaviour for tomato plants growing under moderately-high light conditions. In chapters 2 and 3 we learned that under higher source strength a greater amount of phloem sap is transported, but the changes in flow were not accompanied by changes in velocity. To further our understanding of the mechanisms driving phloem transport, it is of interest to know how the sucrose concentration in phloem sap relates to phloem flow. In **Chapter 4** we used an average T_2 relaxation time in the phloem vascular tissue region to reveal the plant's phloem carbon status under source manipulation. In this chapter we demonstrated that T_2 relaxation time, when measured in parallel with phloem flow, can provide additional information about

phloem region carbon status, i.e., changes in the T_2 relaxation time are correlated with changes in sucrose concentration in the whole phloem region.

When studying phloem transport in plants with magnetic resonance imaging (MRI) flowmetry, plants which are relatively easy to manipulate (e.g. fruit pruning) like tomato have so far been used. However, tomato plants (used in all three previous chapters) have relatively low sink strength beneath the MRI measurement site. A potentially preferable approach is to work with plants with strong sinks beneath the measurement site. In **Chapter 5** we studied potato as a potentially better test subject for MRI flowmetry as it possesses strong sink below the MRI measurement site (i.e., developing tubers). For that purpose we used two potato plants (cv. Desiree) both with several developing tubers. One of the plants overexpressed the *StSWEET* gene (*35S:StSWEET*) which appears to have altered its source : sink ratio. As a result, the *35S:StSWEET* plant transported 60% more phloem sap than Desiree WT. Strikingly, the average phloem flow velocity in both plants was the same and the greater amount of transported phloem sap in the *35S:StSWEET* plant was accommodated by more sieve tubes than in Desiree WT. This finding agrees with the hypothesis about the conserved nature of phloem flow velocity, where volume flow is regulated by the number of active sieve tubes (Chapter 2 and 3). In this chapter we also demonstrate that a potato plant with developing tubers represents a good subject to study phloem transport with MRI flowmetry. We concluded that under optimal conditions (which are commonly met in greenhouses) phloem transport is likely to reach its maximum capacity and therefore photosynthesis could be limited by the export and transport of photo-assimilates because of the finite number of sieve tubes and constant flow velocity.

All who were involved in one way or another with the work presented in this thesis deserve my thanks. First of all, I would like to thank my co-promotor and daily supervisor Henk Van As for giving me the opportunity to work at the Laboratory of Biophysics. Henk was always open and enthusiastic towards discussions over our data. My thanks go also to my promotor Herbert van Amerongen. My sincere thanks go to Frank Vergeldt who introduced me to MRI (which was for me - as a physical chemist specialised in calorimetry - an absolutely new subject), programming and MRI data analysis. To become proficient in plant MRI would have been impossible without the invaluable advice and help of Carel Windt. The data presented in this thesis (and much more besides) would not exist without the help of Edo Gerkema. Thanks to Edo, I could conduct my experiments over weekends, changing parameters at crazy hours and several times measuring over the Christmas holidays. All this 'outside-regular-hours' work, Edo did with a smile and good humour. My thanks go also to John Philippi who built several (and for my experiments essential) devices (e.g., LED light source, data logger for plants sensors etc.) and once even rescued my laptop! I am very grateful to Rob Koehorst, Anna Kortstee, Ernest Aliche, Jose Abelenda, Kathy Steppe, Bart Van de Waal, Veerle De Schepper, Jeremmy Harnbinson, Graham Taylor, Gerard van der Linden, Christian Bachem, Aldrik Velders, Junyou Wang, Silvia Lechthaler, and Andre Maassen. I would like to thank my office-mate Daan de Kort for his moral support and for being my paranymp. Other colleagues helped with many different issues and contributed to the special atmosphere in the Biophysics lab. My thanks go to: Netty Hoefakker, Olga Chukutsina, Shazia Farouq, Julia Krug (special thanks for being my paranymp), Carel Fijen, Evgenia Iermak, Shanthi Pagadala, Tünde Tóth, Tatiana Nikolaieva, Yashar Ranjbar, Fugui Xiao, Caner Ünlü, Lijin Tian, John van Duynhoven, Arjen Bader, Emilie Wientjes, Johannes Hohelbein, Pieter de Waard, Cor Wolfs, Elena Golovina and Jacques Vervoort. And finally, my heart-felt thanks go to my father and Milena for their support, and to Peter for his support, patience and help.

Alena Prusova was born on June 9, 1984 in Ceske Budejovice, The Czech Republic. Alena graduated from Chemistry Secondary School in Ceske Budejovice in 2003 and began a degree in Applied Physical Chemistry at Brno University of Technology where, in 2008, she graduated with a title Ing. (Czech equivalent of BSc. together with MSc.). Being interested in biopolymers, Alena began a Ph.D. study at Brno University of Technology (Czech Republic)/Koblenz-Landau University (Germany). During her Ph.D. she studied peculiar properties of water interacting with biopolymers using diverse techniques (DSC, TGA, TGA-MS, HRUS, CP-MAS-NMR spectroscopy, time domain NMR and FFC-NMR relaxometry). She graduated her PhD in 2013 in Landau obtaining a title of Dr. rer. nat. (Doctor rerum naturalium, German equivalent of Ph.D.). During her Ph.D. she was fascinated by NMR and therefore she took an opportunity to learn more of this phenomenon during another Ph.D. in Wageningen.

- **Prusova A.**, Vergeldt F. J., Windt C. W., Gerkema E., Koehorst R. B. M, Philippi J. G. M., Van As H. Source strength manipulation in tomato changes phloem flow, but not its velocity. (*submitted*)

- **Prusova, A.**, Van de Wal, B. A. E., De Schepper V., Vergeldt F. J., Gerkema E., Steppe K., Van As H. Effect of photoperiod on xylem and phloem sap transport in tomato. (*submitted*)

- Vergeldt F. J., **Prusova A.**, Fereidouni F., van Amerongen H., Van As H., Scheenen T. W. J., Bader A. N. Multi-component quantitative MRI by phasor representation. (*in preparation*)

- Wang J., Groeneveld A., Oikonomou M., **Prusova A.**, Van As H., van Lent J. W. M., Velders A. H. Revealing and tuning the core, structure, properties and function of polymer micelles with lanthanide-coordination complexes. *Soft Matter*, 2016, vol.12, 99–105.

- Lechthaler S., Robert E., Tonné N., **Prusova A.**, Gerkema E., Van As H., Koedam N. and Windt C. W. Rhizophoraceae mangrove saplings use water stored in their enlarged hypocotyl and thickened leaves to surmount sudden changes in soil water salinity. *Frontiers in Plant Science*, 2016, vol. 7, 895.

- **Prusova A.**, Vergeldt F. J., Kučerík J. Influence of water content and drying on the physical structure of native hyaluronan. *Carbohydrate polymers*, 2013, vol. 95, 515–521.

- Šmejkalová D., Hermannová M., Šulánková R., **Prusova A.**, Kučerík J., Velebný V. Structural and conformation differences of acylated hyaluronan modified in protic and aprotic solvent system. *Carbohydrate Polymers*, 2012, vol. 87, 1460–1466.

- Kučerík J., Bursáková P., **Prusova A.**, Grebíková L., Schaumann G.E. Hydration of humic and fulvic acids studied by DSC. *Journal of Thermal Analysis and Calorimetry*, 2012, vol. 110, 451–459.

- Špěrová M., Nasadil P., **Prusova A.**, Kučerík J.: A hint on the correlation between cellulose fibers polymerization degree and their thermal and thermo-oxidative degradation. *Journal of Thermal Analysis and Calorimetry*, 2012, vol. 110, 71–76.

- Kučerík J., **Prusova A.**, Rotaru A., Flimel K., Janeček J., Conte P. DSC study on hyaluronan hydration and dehydration, *Thermochimica acta*, 2011, vol. 523 , 245–249.

- **Prusova A.**, Šmejkalová D., Chytil M., Velebný V., Kučerík J. An alternative DSC approach to study hydration of hyaluronan. *Carbohydrate Polymers*, 2010, vol. 82, 498–503.

- **Prusova A.**, Conte P., Kučerík J., Alonyo G. Dynamics of hyaluronan aqueous solutions as assessed by fast field cycling NMR relaxometry. *Analytical and Bioanalytical Chemistry*, 2010, vol. 397, 3023–3028.

Education Statement of the Graduate School The Graduate School

**EXPERIMENTAL
PLANT
SCIENCES**

Experimental Plant Sciences

Issued to: Alena Prusova
Date: 20 October 2016
Group: Laboratory of Biophysics
University: Wageningen University & Research

1) Start-up phase

date

► **First presentation of your project**

Title: Phloem transport capacity
and water limitation

Jun 07, 2012

► **Writing or rewriting a project proposal**

► **Writing a review or book chapter**

► **MSc courses**

Advances in Magnetic resonance
(BIP - 31806)

Apr 2013

Programing in Python (INF-22306)

Sep-Oct 2013

► **Laboratory use of isotopes**

Subtotal Start-up Phase

*7.5 credits**

2) Scientific Exposure

date

► **EPS PhD student days**

EPS PhD student day, Leiden University

Nov 29, 2013

EPS PhD student day, Soest, NL

Jan 29-30, 2015

► **EPS theme symposia**

EPS Theme 1 Symposium 'Developmental
Biology of
Plants', Plants', University of Amsterdam

Jan 17, 2013

EPS Theme 3 Symposium 'Metabolism and
adaptation', University of Amsterdam

Mar 22, 2013

EPS Theme 3 Symposium 'Metabolism and
adaptation', Wageningen University

Feb 08, 2015

► **Lunteren days and other National Platforms**

BioSolar Cells annual meeting	Jun 10-11, 2012
BioSolar Cells cluster 3	Nov 23, 2012
BioSolar Cells valorization day	Jun 15, 2013
BioSolar Cells annual meeting	Jun 13-14, 2013
BioSolar Cells cluster 3	Nov 28, 2013
BioSolar Cells annual meeting	Jun 23-24, 2014
BioSolar Cells cluster 3	Dec 12, 2014
BioSolar Cells annual meeting	Jun 17-18, 2015
Annual Meeting 'Experimental Plant Sciences', Lunteren, NL	Apr 25-26, 2013
Annual Meeting 'Experimental Plant Sciences', Lunteren, NL	Apr 14-15, 2014
Annual Meeting 'Experimental Plant Sciences', Lunteren, NL	Apr 13-14, 2015
Dutch NMR discussion group - Eindhoven University	Nov 08, 2013
Dutch NMR discussion group - Oss	Oct 31, 2014
Dutch NMR discussion group - Utrecht University	Nov 05-06, 2015
► Seminars (series), workshops and symposia	
Cost STRESS - workshop on modeling, Gent, Belgium	Jun 04-07, 2014
Measuring the Photosynthetic phenome, Wageningen University, NL	Jul 07-09, 2014
Preclinical Imaging User' s Meeting, Etlingen, Germany	Oct 13-14, 2015
Seminar plus	
► International symposia and congresses	
Magnetic resonance in food, Wageningen, NL	Jun 26-29, 2012
9th international workskop on sap flow, Gent, Belgium	Jun 04-07, 2013
EUROMAR 2015, Prague, Czech Republic	Jul 05-10, 2015
International Conference on Magnetic Resonance Microscopy, Munich, Germany	Aug 02-06, 2015
Internarional Congress on Photosynthesis Research, Maastricht, NL	Aug 07-12, 2016
► Presentations	
<i>Talk:</i> BioSolar Cells cluster 3	Nov 23, 2012
<i>Poster:</i> Lunteren annual EPS meeting	Apr 25-26, 2013
<i>Poster:</i> 9th international workskop on sap flow (poster prize)	Jun 04-07, 2013
<i>Talk and Poster:</i> BioSolar Cells annual meeting	Jun 13-14, 2013

<i>Talk:</i> BioSolar Cells cluster 3	Nov 28, 2013
<i>Poster:</i> Lunteren annual EPS meeting	Apr 14-15, 2014
<i>Talk and Poster:</i> BioSolar Cells annual meeting (poster prize)	Jun 23-24, 2014
<i>Talk:</i> BioSolar Cells cluster 3	Dec 12, 2014
<i>Talk:</i> BioSolar Cells annual meeting	Jun 17-18, 2015
<i>Talk:</i> EPS PhD student day, Soest, NL	Jan 29-30, 2015
<i>Poster:</i> Lunteren annual EPS meeting	Apr 13-14, 2015
<i>Talk:</i> Measuring the Photosynthetic phenome	Jul 07-09, 2014
<i>Talk:</i> EPS Theme 3 'Metabolism and adaptation'	Feb 08, 2015
<i>Talk:</i> EUROMAR 2015	Jul 05-10, 2015
<i>Poster:</i> International Conference on Magnetic Resonance Microscopy (poster prize)	Aug 02-06, 2015
<i>Talk:</i> Internarional Congress on Photosynthesis Research	Aug 07-12, 2016
► IAB interview	
Excursions	
<hr/>	
<i>Subtotal Scientific Exposure</i>	<i>33.4 credits*</i>
<hr/>	
3) In-Depth Studies	<u><i>date</i></u>
► EPS courses or other PhD courses	
Course 'In Vivo MRI'	Dec 03-14, 2012
Course 'Basic Statistics'	Dec 08-16, 2014
► Journal club	
PhD NMR group journal club	2013-2014
► Individual research training	
<hr/>	
<i>Subtotal In-Depth Studies</i>	<i>5.5 credits*</i>
<hr/>	
4) Personal development	<u><i>date</i></u>
► Skill training courses	
Competence Assessment	Aug 28, 2012
Social Dutch for Employees, Wageningen in'to Languages	Oct-Dec 2013
Techniques for writing and presenting scientific paper	Dec 03-06, 2013
Scientific Writing	Dec 12-Feb 18, 2014
Project and Time Management (P&TM)	Jan 28-Mar 11, 2014
Effective behaviour in professional surroundings	Apr 15&May 13, 2014
Reviewing a scientific paper	Mar 05, 2015
Writing grant proposals	Apr-May 2015

► **Organisation of PhD students day, course or conference**

► **Membership of Board, Committee or PhD council**

Subtotal Personal Development

*10.2 credits**

TOTAL NUMBER OF CREDIT POINTS*

56,6

Herewith the Graduate School declares that the PhD candidate has complied with the educational requirements set by the Educational Committee of EPS which comprises of a minimum total of 30 ECTS credits

** A credit represents a normative study load of 28 hours of study.*

Research presented in this thesis was performed at the Laboratory of Biophysics, Wageningen University, The Netherlands.

This project was conducted within the research programme of BioSolar Cells, cofinanced by the Dutch Ministry of Economic Affairs, Agriculture and Innovation.

Financial support from the Laboratory of Biophysics for printing this thesis is gratefully acknowledged.

Printed by GVO drukkers & vormgevers B.V., The Netherlands.